Aus dem Max-Delbrück-Centrum für Molekulare Medizin (MDC) und
der Medizinischen Fakultät Charité – Universitätsmedizin Berlin

DISSERTATION

Functional analysis of components of the kallikrein-kinin system in genetically altered rat models

Funktionsanalyse von Komponenten des Kallikrein-Kinin-Systems in genetisch veränderten Rattenmodellen

zur Erlangung des akademischen Grades
Doctor rerum medicinalium (Dr. rer. medic.)

vorgelegt der Medizinischen Fakultät
Charité – Universitätsmedizin Berlin

Von

Sara Maghsodi

Datum der Promotion:
25. November 2022

Table of Contents

List of Figures

List of Tables

Abbreviations

AAE	Acquired angioedema
ACE	Angiotensin converting enzyme
ACh	Acetylcholine
ANG II	Angiotensin II
ANOVA	Analysis of variance
BK	Bradykinin
$BKCa^{2+}$	Big conductance calcium sensitive potassium channel
B1R	B1 receptor
B2R	B2 receptor
B1R-TGR	B1 receptor transgenic rat
B2R-TGR	B2 receptor transgenic rat
BM	Bone Marrow
Cas9	Crispr-associated
C1-INH	C1 inhibitor
cIMP	Cyclic inosine monophosphate
CPM	Carboxypeptidase M
CPN	Carboxypeptidase N
cDNA	Complementary DNA
cGMP	Cyclic guanosine monophosphate
COX	Cyclooxygenase
Crispr	Clustered regularly interspaced short palindromic repeats
CYP450	Cytochrome P450
DAG	Diacylglycerol
DAPI	4, 6-diamidino-2-phenylindole
ddH_2O	Double-distilled water
$Des\text{-}Arg^9\text{-}BK$	$Des\text{-}Arg^9\text{-}Bradykinin$
DMEM	Dulbecco's modified Eagle's medium
DMSO	Dimethyl sulfoxide
DNA	Deoxyribonucleic acid
DNase	Deoxyribonuclease
dNTPs	Deoxyribonucleotides
ENA	Enalapril
EDHF	Endothelial derived hyperpolarising factor
EDRF	Endothelial derived relaxing factor
EETs	Epoxyeicosatrienoic acids
eNOS	Endothelial nitric oxide (NO) synthase
FACS	Flow cytometry
Gapdh	Glyceraldehyde-3-phosphate dehydrogenase
G-CSF	Granulocyte-colony-stimulating factor
GPI	Glycosylphosphatidylinositol
H&E	Hematoxylin and eosin
HK	High molecular-weight kininogen
HSPC	Hematopoietic stem/progenitor cell
iNOS	Nitric oxide synthase, inducible
JNK	NH_2-terminal kinase
KKS	Kallikrein-kinin system

K_{ATP}	ATP-dependent K^+ channels
K_{IR}	Inward rectifying potassium channels
LaGeSo	Landesamt for Gesundheit und Soziales
LK	Low molecular-weight kininogen
LVH	Ventricular hypertrophy
MAPK	Mitogen-activated protein kinase
MCPs	Metallo-type carboxypeptidases
MDC	Max Delbrück Centrum for Molecular Medicine in the Helmholtz Association
MEK	Mitogen-activated protein kinase kinase
MERGETPA	2-[2-(diaminomethylideneamino) ethylsulfanylmethyl]-3-sulfanylpropanoic acid
$MgCl_2$	Magnesium chloride
M-MLV	Moloney Murine Leukemia Virus
MNC	Mononuclear cells
MLCK	Myosin light chain kinase
MLCP	Myosin light chain phosphatase
mRNA	Messenger ribonucleic acid
n	Number of animals/independent experiments
NF-κB	Nuclear factor-κB
NO	Nitric oxide
PGE2	Prostaglandin E_2
PMN	Polymorphonuclear cells
PKC	Protein kinase C
PLA2	Phospholipase A2
PLC	Phospholipase C
RAS	Renin angiotensin aldosterone system
RNA	Ribonucleic acid
RNase	Ribonuclease
ROCK	Rho-associated protein kinase
ROS	Reactive oxygen species
RT	Reverse transcription
SDF-1α	Stromal cell-derived factor
SDS	Sodium dodecylsulfate
SDS-PAGE	SDS-Polyacrylamide gel electrophoresis
SECA	Sarco/ endoplasmic reticulum calcium ATPase
SR	Sarcoplasmic reticulum
gRNA	guide RNA
TAE	Tris-acetate-EDTA
Tbp	TATA box-binding protein-like protein 1 (Tbpl1)
TBST	Tris-buffered saline containing 0.5% Tween
TK	T-kininogen
TLR	Toll-like receptors
Tris	Tris(hydroxymethyl)aminomethane
TRPC	Transient receptor potential channels
TRPM	Transient receptor potential melastatin
TRPML	Transient receptor potential cation channel, mucolipin
TRPV	Transient receptor potential vanilloid channel
u-PA	Urinary type plasminogen activator
PR3	Proteinase 3
VDCC	Voltage-dependent calcium channel
WB	Western blot

Symbols and Units

%	Percent
*g	Relative centrifugal force
°C	Degree Celsius
A	Ampère
AU	Arbitrary units
bp	Base pair
FI	Fluorescence intensity
g	Gramm
h	Hour
kb	Kilobase
kDa	Kilodalton
kg	Kilogramm
M	Molar
mA	Milliampère
min	Minute
mL	Milliliter
mM	Millimolar
mV	Millivolt
ng	Nanogramm
nm	Nanometer
pmol	Picomole
rpm	Rotations per minute
sec	Second
U	Unit
V	Volt
µL	Microliter
µm	Micrometer
µM	Micromolar

Summary

The kallikrein-kinin system (KKS) in mammals consists of kininogens, kallikreins, kininases and kinins. One of the main products of this cascade is bradykinin (BK). The physiological activity of BK is multidirectional and, besides its cardioprotective functions, it has multiple pathophysiologic functions such as: induction of vasodilation, increase in vascular permeability and the consequent induction of angioedema. Two kinin receptors have been described; the inducible B1 receptor (B1R) and the constitutive B2 receptor (B2R). To clarify their vascular function, we generated transgenic rats overexpressing either B1R (B1R-TGR) or B2R (B2R-TGR) exclusively on the endothelium. We observed spontaneous edema formation together with a severe pancreatitis in about 10% of B2R-TGR. To clarify the contribution of second messenger systems as well as K^+ and Ca^{2+} channels to the signaling mechanisms involved in B1R and B2R mediated vasorelaxation, the reactivity of aorta rings was first investigated. Our data suggest that prostaglandins are not involved in the B1R and B2R agonist-induced vasorelaxation. However, the present data provide strong evidence that NO-mediated stimulation of K^+ channels is involved both in B1R- and B2R-induced vasorelaxation. It is evident that, in particular, the large conductance Ca^{2+} sensitive K^+ channels are involved. In addition, we also found the involvement of transient receptor potential channels, specifically TRPC4, in vasorelaxation induced by kinins in both B1R and B2R transgenic aorta. Since it has been shown that ACE-inhibitors such as enalapril (ENA) induce edema in patients, we tested the chronic treatment of ENA in B2R-TGR animals, which may be a model for spontaneous angioedema. In addition, the acute effect of the B2R antagonist Hoe140 was tested in B2R-TGR with spontaneous edema. Our data revealed that ENA significantly increased extravasations in some tissues like testis, stomach, heart, lung and kidney compared to the control group. Furthermore, we observed that acute treatment of edemic B2R-TGR with the B2R antagonist Hoe140 significantly decreased extravasations in the heart.
Since carboxypeptidase M (CPM) generates the agonists of B1R, we generated CPM knock-out rats (CPM-KO). Besides kinins, CPM also metabolizes other proteins, peptides and several chemokines, in particular CXCL12. In the bone marrow, CXCL12 affects the development and regulation of hematopoietic stem cells and their mobilization. Using FACS, we observed a significant reduction of B-cells in CPM-KO blood compared to controls, and the percentage of non-classical monocytes decreased and $CD8^+$ T cells increased in CPM-KO spleen. In CPM-KO bone marrow, the percentage of T cells, $CD8^+$ T cells and classical monocytes increased.

Zusammenfassung

Das Kallikrein-Kinin-System (KKS) besteht aus Kininogenen, Kallikreinen, Kininasen und Kininen. Eines der Hauptprodukte dieser Kaskade ist Bradykinin (BK). BK hat neben seinen kardioprotektiven Funktionen mehrere pathophysiologische Funktionen wie: Induktion der Vasodilatation, Erhöhung der Gefäßpermeabilität und folglich Induktion von Angioödemen. Zwei Kinin-Rezeptoren wurden beschrieben; der induzierbare B1-Rezeptor (B1R) und der konstitutive B2-Rezeptor (B2R). Um ihre vaskuläre Funktion zu klären, haben wir transgene Ratten erzeugt, die entweder den B1R (B1R-TGR) oder B2R (B2R-TGR) ausschließlich auf dem Endothel überexprimieren. Bei etwa 10% der B2R-TGR beobachteten wir eine spontane Ödem Bildung zusammen mit einer schweren Pankreatitis. Zur Klärung der Beteiligung von Second-Messenger-Systemen, K+- und Ca2+-Kanälen an den Signalmechanismen der B1R- und B2R-vermittelten Vasorelaxation, wurde zunächst die Reaktivität von Aortenringen untersucht. Unsere Daten legen nahe, dass Prostaglandine nicht an der durch B1R- und B2R-Agonisten induzierten Gefäßrelaxation beteiligt sind. Unsere Daten liefern jedoch starke Beweise dafür, dass die NO-vermittelte Stimulation von K+-Kanälen sowohl an der B1R- als auch an der B2R-induzierten Vasorelaxation beteiligt ist. Es ist offensichtlich, dass besonders Ca2+-regulierte K+-Kanäle beteiligt sind. Darüber hinaus fanden wir auch die Beteiligung von *transient receptor potential channels*, insbesondere TRPC4, an der durch Kinine induzierten Vasorelaxation sowohl in der transgenen B1R- als auch in der B2R-transgenen Aorta. Da gezeigt wurde, dass ACE-Hemmer wie Enalapril (ENA) bei Patienten Ödeme induzieren, wurde die chronische Behandlung von ENA an B2R-TGR-Tieren getestet, die ein Modell für spontane Angioödeme sein können. Außerdem wurde die akute Wirkung des B2R-Antagonisten Hoe140 in B2R-TGR mit Spontanödem getestet. Unsere Daten zeigten, dass ENA die Permeabilität in einigen Geweben wie Hoden, Magen, Herz, Lunge und Niere im Vergleich zur Kontrollgruppe signifikant erhöhte. Weiter beobachteten wir, dass die akute Behandlung von ödemischem B2R-TGR mit dem B2R-Antagonisten Hoe140 die Extravasation im Herzen signifikant verringerte. Da Carboxypeptidase M (CPM) die Agonisten für B1R generiert, haben wir CPM Knockout Ratten (CPM-KO) generiert. Neben Kininen metabolisiert CPM weitere Proteine, Peptide und verschiedene Chemokine, insbesondere CXCL12. Im Knochenmark beeinflusst CXCL12 die Entwicklung und Regulation von hämatopoetischen Stammzellen und deren Mobilisierung. Mit FACS beobachteten wir eine signifikante Reduktion von B-Zellen im CPM-KO Blut im Vergleich zu Kontrollen und der Anteil nicht-klassischer Monozyten nahm ab und CD8+ T-Zellen stiegen an in der CPM-KO Milz. Im CPM-KO Knochenmark stieg der Prozentsatz an T-Zellen, CD8+ T-Zellen und klassischen Monozyten.

1 Introduction

1.1 The Kallikrein kinin system

Coordinated action of several systems is essential for cardiovascular regulation. The renin-angiotensin system (RAS) and the kallikrein-kinin system (KKS) are two such systems that regulate cardiovascular mechanisms through their interactive responses. The KKS in mammals is a well characterized biological pathway which, upon activation, releases vasoactive peptides such as kinins [1]. Kinins comprise a set of blood and tissue peptides that play a key role in the trigger of inflammation, blood pressure control and coagulation processes [2]. The KKS is initiated by the serine protease tissue and plasma kallikreins, which produce kinins from high- and low-molecular-weight kininogen (HK and LK), respectively (Figure 1). Different biological actions of kinins are mediated by acting on their specific receptors, B1 and B2.

1.1.1 Kininogens

Kininogens are glycoproteins generated/synthetized in the liver and are mainly found in the plasma, but also in organs like kidney. HK and LK are formed by alternative splicing of the *Kng1*-primary transcript composed of eleven exons and ten introns. Both kininogens contain an identical N-terminal heavy chain, which consists of domains D1, D2, D3 and D4, including bradykinin (BK) and two different C-terminal light chains (consisting of D5 and D6 domains). The LK C-terminus consists of a D5 domain, whereas the HK C-terminus possesses D5 and D6 (which binds to prekallikrein and factor XI) domains [3]. There is also a T-kininogen (TK) encoded by a separate gene, but it has only been identified in the rat [4]. The human kininogen gene is a single copy gene, whereas the mouse genome contains 2 homologous kininogen genes, *Kng1* and *Kng2*. These two kininogens have different expression profiles in tissues [5]. Plasma HK, LK, and also Delta-HK-D5, another kininogen isoform, do not exist in the plasma of mice with *Kng1* deletion, as Merkulov et al. reported in 2008 [6].

1.1.2 The kinin-forming enzymes

Classically, kinins are generated by two main pathways of the KKS. They are termed as tissue and plasma systems depending on the location of kininogen and kallikrein [7, 8] (Figure 1). The plasma KKS starts with the induction of the intrinsic coagulation pathway and was initially considered as a surface-activated coagulation system. Tissue KKS, the second pathway of kinin generation, includes tissue kallikrein and its substrate, LK. Each of these enzyme systems is involved in different pathophysiological conditions [9]. Tissue kallikrein mainly forms kallidin (lysyl-bradykinin, KD) from LK, and plasma kallikrein forms BK from HK [10]. Plasma kallikrein and tissue

kallikrein are different in terms of their gene structure, specificity toward substrates, immunological features, type of kinin generated and their molecular weight [11, 12].

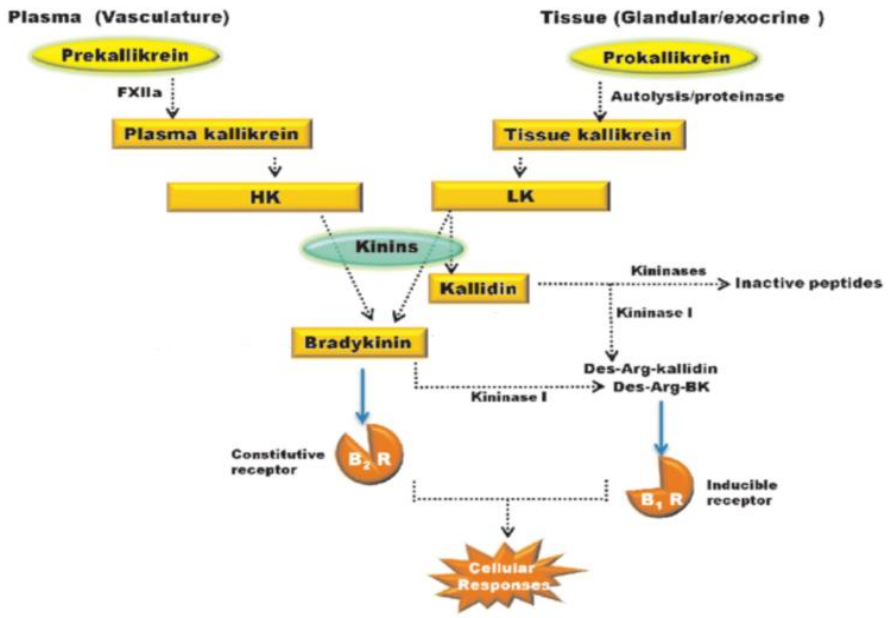

Figure 1: Schematic diagram of the KKS. Plasma and tissue kallikrein are secreted in a zymogen form and activated by proteolytic cleavage. They generate bradykinin (BK) and kallidin from HK and LK kininogens, which act through the B2 receptor (B2R). BK is converted by carboxypeptidases (kininases I) to des-Arg^{9}-BK, which acts through the B1 receptor (B1R). Different biological actions of kinins, such as control of blood pressure, electrolyte balance and inflammation, are mediated by their action on B1R and B2R [2].

1.1.2.1 Plasma kallikrein

Plasma kallikrein (*KLKB1*), or Fletcher factor, is encoded by the *KLKB1* gene, a single gene located on human chromosome 4q35. Plasma kallikrein has no known paralogue. This gene possesses 15 exons and encodes an inactive precursor, prekallikrein, which must undergo proteolytic processing to become activated [13, 14]. Prekallikrein is exclusively expressed by the liver. Coagulation factor XII converts plasma prekallikrein to the active enzyme. Factor XII is also present as a proenzyme and is activated by exposure to an anionic surface, which leads to conformational alterations as well as auto-activation and conversion of prekallikrein to activate plasma kallikrein. Plasma kallikrein is able to reciprocally activate factor XII to activated factor XIIa and cleaves HK to BK [15] (Figure 2). Overall, two distinct pathways can be started by activated factor XII. The first pathway triggered is the intrinsic coagulation pathway through FXI activation, and the second pathway is the KKS by plasma kallikrein activation [16].

1.1.2.2 Tissue kallikrein

The recently revised nomenclature of the human kallikrein gene family identified 15 different genes (*KLK1* to *KLK15*) localized on human chromosome 19q13.3-q13.4. All the genes code for serine proteases, consist of five coding exons, and exhibit significant structural similarities [17]. All proteins encoded by these genes are initially synthesized as preproenzymes, and they are converted to active enzymes undergoing different processes. The *KLK1* gene is mainly expressed in the pancreas, kidney and salivary glands [18]. The *KLK2* and *KLK3* genes are mainly expressed in prostatic tissues, and also to a lesser extent in other different tissues [19]. All of the remaining kallikreins are expressed in different tissues and are not tissue-specific. *KLK1*, among all the human kallikreins is the only enzyme that efficiently exerts kininogenase activity. *KLK1* is considered as tissue kallikrein, which play an important role in the release of kinins, mainly KD, from LK. It has been shown that *KLK1* is also involved in the processing of growth factors and peptide hormones [8]. In addition to the kininogenase activity, *KLK1* is capable of binding and activating the B2R directly and it induces smooth muscle contraction [20, 21]. Recent investigations have demonstrated the importance of *KLK1* in the regulation of microcirculation and cardiovascular system health [22, 23]. In human tissue, kallikrein liberates KD and plasma kallikrein liberates BK, whereas in the rat both tissue and plasma kallikrein only generate BK [24, 25] (Figure 2).

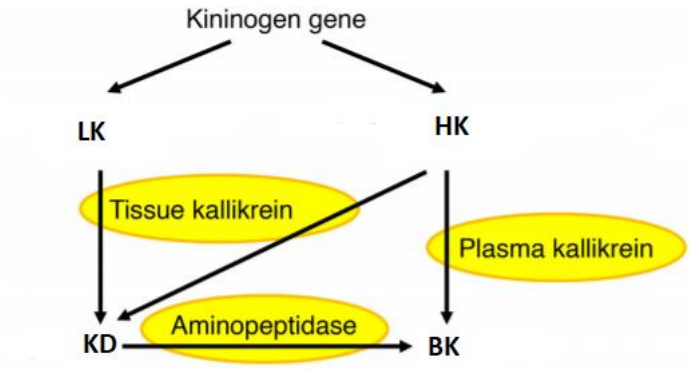

Figure 2: Plasma kallikrein cleaves HK to produce BK, whereas tissue kallikrein cleaves both LK and HK to produce KD. BK can also be generated by aminopeptidase-mediated cleavage of KD [26].

1.1.2.3 Other kinin forming enzymes

In addition to tissue and plasma kallikrein, there are serum and tissue proteases which also form kinins [27]. Plasmin is a serine protease which degrades many blood plasma proteins, including fibrin clots, being essential for fibrinolysis, the breakdown of fibrin polymers in blood clots. Apart from this function, plasmin is involved in the release of BK and des-Arg^{9}-BK from HK. Numerous studies indicate the existence of an axis between the plasminogen (plasmin precursor) activation system and the contact system [16, 28]. The major activator of plasminogen is tissue plasminogen activator (t-PA), a serine protease from endothelial cells. Urokinase or urinary type plasminogen activator (u-PA) can also activate plasminogen [29]. There is also clinical evidence supporting the role of FXIIa as plasminogen activator [30]. Studies have shown that proteinase 3 (PR3) cleaves HK and forms another type of BK, with two additional amino acids on both the C and N termini [31].

1.1.3 Kinin metabolizing enzymes

Kinins have a very short half-life (< 1 minute) in tissues and blood since they are quickly metabolized/inactivated by different proteases. Five metallopeptidases, including aminopeptidase P (APP), angiotensin I-converting enzyme (ACE), neutral endo-peptidase 24.11 (NEP) and carboxy-peptidases M and N (CPM, CPN), are primarily Kinin metabolizing enzymes. The CPM and N (kininase I) metabolites of BK and KD, which are agonists for the B2R, are bradykinin-(1-8) or des-Arg^{9}-BK and des-Arg^{10}-KD, respectively, which are also active, but more potent on B1R [15]. Therefore, these carboxypeptidases are very important enzymes in the regulation of the KKS.

1.1.3.1 Carboxypeptidases

A protease is an enzyme that catalyzes the hydrolysis of proteins into smaller polypeptides or single amino acids. Recently it has been recognized that proteases can react as precise modulators of diverse proteins and play a key role in cellular processes in all living organisms [32]. Based on the structure of their catalytic site or catalytic mechanism that they use [33] proteases are grouped into six catalytic groups including serine, threonine, cysteine, aspartic, glutamic and metallo proteases. Some proteases particularly cleave amino acids from the N- or C-termini like aminopeptidases and carboxypeptidases, which are called exopeptidases. Other proteases cleave proteins and peptides in the middle, which are called endopeptidases (Figure 3).

As mentioned above carboxypeptidases (CPs) are specified as proteases that catalyse the hydrolysis of peptides and proteins at their C-terminus. The carboxypeptidases are classified into three major groups: serine, cysteine or metallo-carboxypeptidases (Table1). They can be found in all living organisms and accomplish great variety of biological functions such as: food digestion and cell signalling regulating.

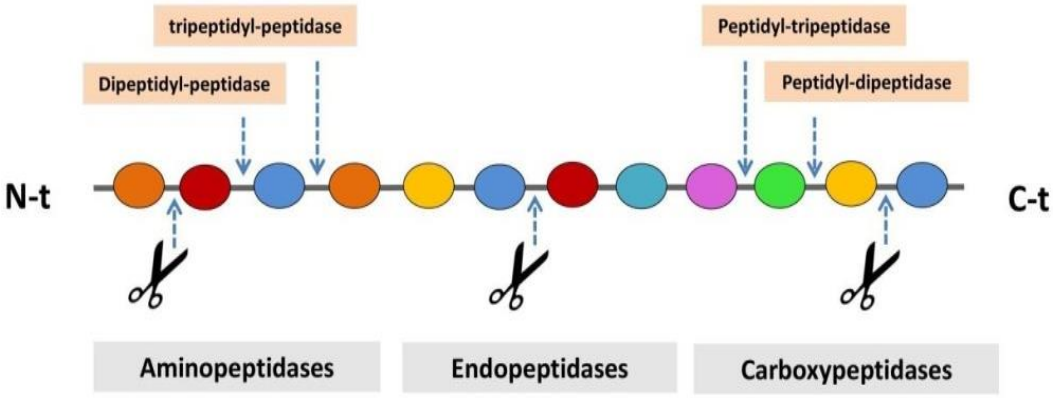

Figure 3: Scheme of the concept of endo-and exopeptidases according to the position of the cleavage of the peptide bond. Endopeptidases cleave peptide bonds in the middle of protein or peptide. Exopeptidases cleave N or C termini. They can be subdivided into amino-and carboxypeptidases. [34].

Table1: carboxypeptidase subfamilies [34]

Catalytic type	MEROPS family	Name
Metallo	M2	ACE2
	M14 subfamily A	CPA1 CPA2 CPA3 CPA4 CPA5 CPA6 CPB CPU or TAFI CPO
	M14 subfamily B	CPE CPD CPM CPN CPZ CPX1 CPX2 AEBP1
	M14 subfamily C	Gamma-D-glutamyl-(L)-meso-diaminopimelate peptidase I
	M14 subfamily D	CCP1 CCP2 CCP3 CCP4 CCP5 CCP6
	M15	Zinc D-Ala-D-Alacarboxypeptidase
	M20 subfamily A	Glutamate carboxypeptidase
	M20 subfamily D	Carboxypeptidase Ss1
	M28 subfamily B	Glutamate carboxypeptidase II NAALADASE L peptidase
	M32	CarboxypeptidasetaqT cCP1 TcCP2
Serine	S10	Serine carboxypeptidase A Vitellogenic carboxypeptidase-like RISC peptidase
	S28	Lysosomal Pro-X carboxypeptidase
Cysteine	C1 subfamily A	Cathepsin X

1.1.3.2 Metallo-carboxypeptidases

The M14 family, also named the N/E subfamily or regulatory carboxypeptidases from metallo-type carboxypeptidases (MCPs) group, is the family of carboxypeptidases with the most members [33]. MCPs are again classified into six different families of proteases based on their zinc binding site according to the MEROPS database (Table1). The subfamily M14B of MCPs is composed of CPN, CPM, CPE, CPZ, CPX1, CPX2, AEBP1 and CPD (Figure 4).

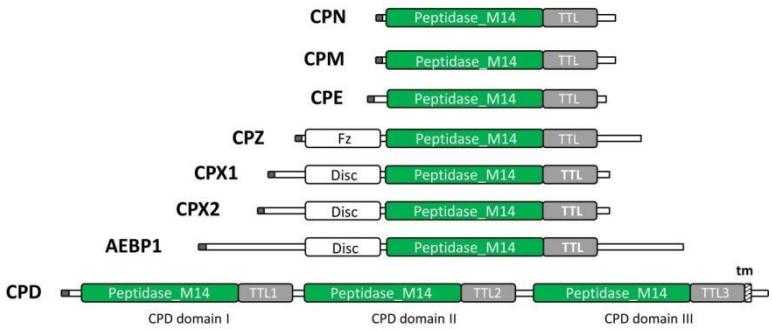

Figure 4: Members of M14B subfamily with their domain structures

CPE, CPN, CPM, CPD and CPZ are produced and secreted as active enzymes and do not have any pro-domain to regulate their activity. However, other members of the M14B subfamily are produced as inactive enzymes, including AEBP1, CPX1 and CPX2. The function of these inactive members is unknown [35, 36].

1.1.3.2.1 Carboxypeptidase M and N

CPM has been proposed to regulate peptide hormone activity and processing. CPM is a membrane-bound enzyme and most abundant in lung and placenta [37]. It is also present in blood vessels and on myeloid cells where it was discovered as a differentiation-dependent cell surface antigen. Moreover, soluble forms of CPM are found in urine, seminal plasma and amniotic fluid [37]. The primary and the most important function of CPM is to inactivate or change the specificity of vasoactive peptides including kinins and the anaphylatoxins, C3a, C4a and C5a. Furthermore, these enzymes also process peptide hormones that are not fully processed by other CPs within the secretory pathway. A unique feature of CPM is its binding via a glycosylphosphatidylinositol (GPI) glycan anchor [38] to the plasma membranes of various cell types like lung endothelial cells, alveolar macrophages, ovarian follicles, trophoblasts, placental and kidney microvilli, blood vessels, and nerves. Stromal cells in bone marrow (BM) also express CPM. It mobilizes progenitor cells of myeloid, erythroid, and megakaryocytic cells, as well as polymorphonuclear (PMN) and mononuclear cells (MNC). Some factors, such as Granulocyte-colony-stimulating factor (G-CSF),

are able to increase the expression of CPM in the above mentioned cells [39]. Recent studies have shown that the chemokine stromal cell-derived factor (SDF)-1α (CXCL12), with a lysine at the C terminus, is a CPM substrate. In the bone marrow (BM) microenvironment, SDF-1α is produced by different cell types including fibroblastic cells, endothelial cells, and osteoblasts. CXCL12, via binding to its receptor CXCR4 expressed on hematopoietic stem/progenitor cells (HSPC), produces a strong retention signal for these cells [40]. CPN is another member of subfamily M14B, or regulatory carboxypeptidases. CPN is a zinc metallo protease consisting of two small and two large subunits which form a tetramer. The small subunits are responsible for the enzymatic activity, and the large subunits protect the enzyme against degradation in the blood stream [41]. The cDNA encoding the human CPN have been cloned, and the genes for the large and small subunits were localized to human chromosomes 8p22–23 and 10, respectively [42, 43]. CPN is generated by liver cells and secreted into the blood, and is not present in tissues, differing from the CPM, which is mainly found on the cell membranes of various tissues, including blood vessels. CPN, similarly to CPM, is capable of cleaving carboxyl-terminal arginine or lysine residues of peptides, such as BK, KD, complement anaphylatoxins, fibrinopeptides and other substrates [44, 45, 46].

1.1.3.3 Other kinin metabolizing enzymes

Aminopeptidase P can transform KD to BK by removing the N-terminal Lys. Both KD and BK activate B2R. Neutral endopeptidase 24.11 (NEP, also called neprilysin) and ACE, also called kininase II, both liberate dipeptides from the C-terminus of KD and BK, thereby inactivating the peptides.

1.1.4 Kinin receptors

Kinin receptors have been characterized through studies on isolated organs in vitro and have been named B1 and B2 [47, 48, 49]. Both receptors belong to the family of G-protein coupled receptors with seven-transmembrane domains. A gene analysis of human, rabbit and rat genomes has shown that a single-copy gene encodes B1R and B2R in both cases [50, 51, 47]. The human kinin receptor genes are located in the same locus of chromosome 14 (14q32.1 – q32.2), with less than 20 kb of genomic DNA separating them. The degree of amino acid identity is 36% between the human B1R and B2R sequences, and most of the homology is located in the seven transmembrane regions [47]. The intracellular loops of both BK receptors only exhibit low homologies [52].

1.1.4.1 Kinin B1 receptor

The product of the human B1R gene (*BDKRB1*) consists of 353 amino acids and is 70% homologous to the mouse and the rat *Bdkbr1* genes [51]. It has been shown that B1R genes contain three exons separated by two introns and an intronless coding region located on the third exon [53,

[54, 55] (Figure 5). B1R is less responsive to BK and KD than to its carboxypeptidase metabolites, des-Arg[9]-BK and des-Arg[10]-BK [48, 56]. B1R receptors are normally not expressed under physiological conditions, but induced after tissue injury or during certain inflammatory processes and pathological conditions such as: exposure to bacterial endotoxins or cytokines, Interleukin 1 beta (IL-1β) and tumour necrosis factor alpha (TNFα) inflammation, and myocardial infarction [57, 58, 59, 60]. This is an unusual characteristic for a G-protein-coupled receptor which is very similar to the tyrosine-kinase-linked receptors. Nevertheless, the constitutive expression of B1R in some cell types such as sensory neurons has also been reported [61]. The induction of B1R has been linked to mediators produced in inflammation. B1R expression is regulated by signalling pathways including mitogen-activated protein kinase (MAPKs), protein kinase C (PKC) and phosphatidylinositol-3 kinase (PI3-K), that are activated by stimuli such as infection and inflammation, and which are able to modulate transcription factors like nuclear factor-κB (NF-*κ*B), activating protein-1 (AP-1) and cAMP response element-binding protein (CREB) [58]. Gene analysis of B1R has revealed that the receptor promoter possesses different sequence-specific regions for different DNA binding proteins, which shows that B1R expression could be regulated by several transcription factors [62, 63]. Recent studies have demonstrated that p38 MAPK and c-Jun NH_2-terminal kinase (JNK) are basically involved in the regulation of B1R mRNA expression induced by vascular tissue trauma [64]. Moreover, PKC is also associated with the B1R upregulation in various isolated tissue preparations [65] (Figure 6). B1R and B2R often exert similar effects after stimulation, but the signalling pattern is different. In contrast to most other G-protein-coupled receptors, B1R is not internalized following binding of its ligand, des-Arg[9]-BK, resulting in prolonged activation of signal transduction. Moreover, it has been shown to exert constitutive, ligand-independent activity. Thus, all responses of the B1R to agonist stimulation favour persistent signalling, which contributes to the switch from an acute to a chronic phase of inflammation and/or tissue repair in KKS [57].

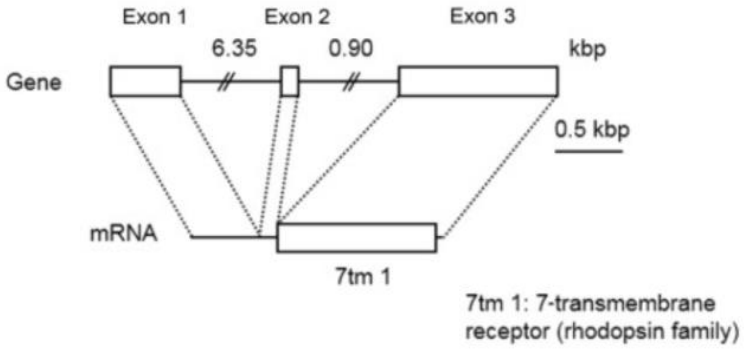

Figure 5: Gene and mRNA of the human B1R receptor: BDKRB1, location 14q32.1–q32.2 [67].

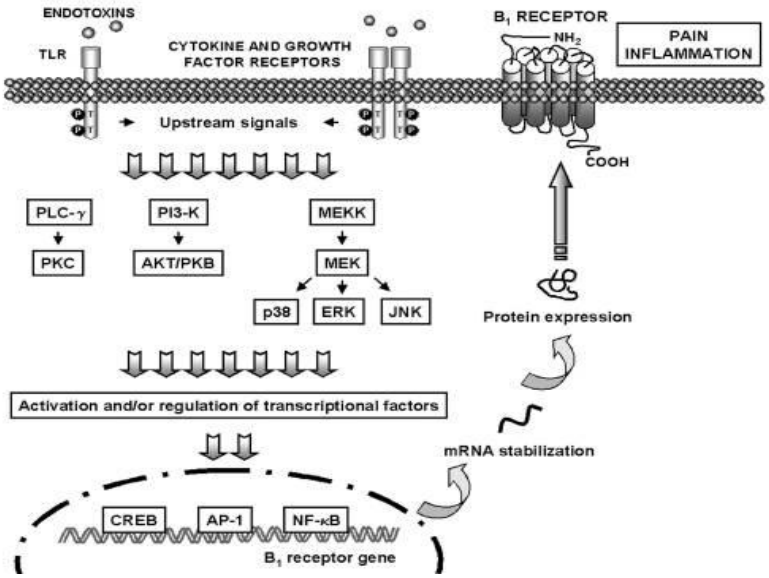

Figure 6: Possible mechanisms underlying B1R upregulation. AP-1, activating protein-1; AKT/PKB, protein kinase B; CREB, c-AMP response element-binding; ERK, c-junNH2-terminal kinase; MAPK, extracellular signal-regulated kinase; JNK, mitogen-activated protein kinase; MEKK, mitogen-activated protein kinase; NF-κB, nuclear factor-κB; PI3-K, phosphatidylinositol-3 kinase; PLC, mitogen-activated protein kinase kinase; MEK, phospholipase C; PKC, protein kinase C; TLR, Toll-like receptors [59].

1.1.4.2 Kinin B2 receptor

The human B2R (*BDKRB2)* gene product consists of 391 amino acids, is about 80% homologous to the mouse and rat *Bdkrb2* gene, and consists of three exons separated by two introns and an intronless coding region located on the third exon [50, 66, 53, 54, 55] (Figure 7). However, Pesquero et al. (1994), based on the findings of others [67], demonstrated an additional exon in the rat gene, revealing a four exon-three intron gene. The B2R has been found in the majority of tissues and is particularly located on endothelial cells, smooth muscle cells, fibroblasts, mesangial cells, some neurons and neutrophils astrocytes. Since B1R is constitutively expressed under normal conditions, most biological functions of kinins are dependent on the presence of B2R on these cell types [68]. B2R are activated by BK and KD, generated by either plasma or tissue kallikreins, and removal of the C-terminal arginine from BK and KD via CPN strongly reduces their affinity toward B2R [69, 15]. The B2R populations are not static, and some studies show that the B2R is regulated; however, this subtype is expressed in many cell types and its expression does not undergo rapid modulation [47]. B2R is a so-called recycling receptor and exerts a strong but short response to stimulation, due to a rapid receptor internalization and sequestration. Under long duration stimulation, its mRNA is down regulated [70, 71].

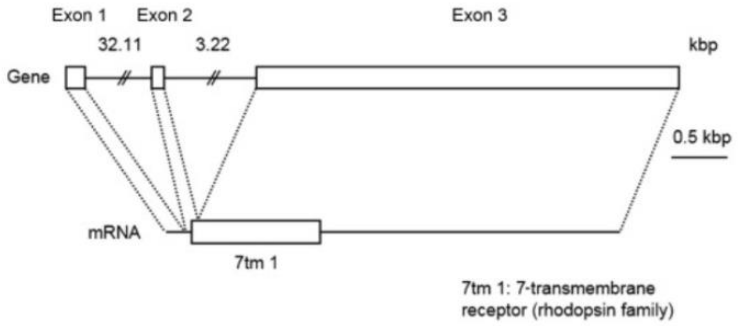

Figure 7: Gene and mRNA of the human B2R: BDKRB2, location 14q32.1-q32.2 [67].

1.2 Kinin receptor signalling in the vascular wall

Stimulation of both kinin receptors - B1 and B2 - starts an almost similar pathway of intra and intercellular responses, and several second messenger systems are activated which change with cell and tissue type. Kinin peptides induce excitability, cell division, contraction, permeability, and the release of a diversity of biologically active factors. Studies have demonstrated that both B1R and B2R link to $G\alpha_{q/11}$ and $G\alpha_{i/o}$ [52, 72]. Stimulation of B1R and B2R leads to the initiation of PKC and tyrosine kinase pathways, correlated with the activation of MAPK and NF-κB. The interaction of Kinins with B1R and B2R induces PLC activation, and subsequently hydrolysis of phosphatidylinositol to inositol 1,4,5-triphosphate (IP3) and diacylglycerol (DAG), followed by increases in intracellular Ca^{2+}. It also leads to the mobilization of phospholipase A (PLA) and the biosynthesis and release of prostaglandins and eicosanoids [47]. Other signal transductions promoted by kinin receptors are the mobilization of phospholipase A and the biosynthesis and release of prostaglandins and eicosanoids. Furthermore, B1R and B2R activation leads to the translocation of PKC from the cytosol to the plasma membrane. Ca^{2+} mediates the activation of endothelial nitric oxide synthase (eNOS) and ultimately the production of NO in endothelial cells as well as the stimulation of PLA2. Arachidonic acid can also be liberated from cellular membrane phospholipids by the action of PLA2 and lead to prostaglandin production [73, 74]. In spite of the fact that the B1R and B2R seem to start similar signal transduction pathways, the patterns of signalling are distinctive in terms of the variation of Ca^{2+} concentration in duration and in intensity. While the intracellular Ca^{2+} increase mediated by B2R is transient and independent of extracellular Ca^{2+}, B1R induces a more sustained signal depending on extracellular Ca^{2+} [48] (Figure 8).

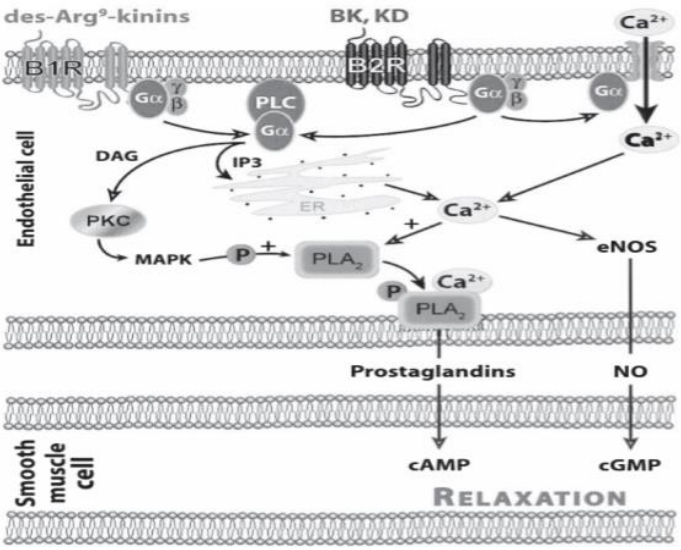

Figure 8: Kinin receptors and their signalling pathways in the vascular wall. Kinin interaction with B1R and B2R starts PLC activation and the hydrolysis of IP to IP3 and DAG. Stimulation of B1R and B2R leads to the initiation of PKC and tyrosine kinase pathways, correlated with the activation of MAPK. ER: endoplasmic reticulum [9].

In the first reference to the KKS in 1909, Abelous and Bardier described the hypotensive impact of tissue kallikrein in dogs. Tissue kallikrein as well as LK are expressed in the vascular wall; PPK and HK circulate and can bind to endothelial cells. Furthermore, B2R is expressed in endothelial and smooth muscle cells constitutively and B1R can also be induced in these cell types [75]. The kinin generating enzymes as well as the kinin degrading enzymes, particularly ACE, are also localised in vascular tissue [76]. One important biological function of BK is the regulation of vascular tone. It is very important to comprehend the interaction between kinin peptides and endothelial cells and their influence on the physiology of the vascular system. Kinins can both contract or dilate vascular smooth muscle depending on: (a) the kinin receptor present on the cell; (b) the sort and intensity of kininases present on endothelial cells [56]. It has been indicated that BK is able to induce both endothelium-dependent and endothelium-independent relaxation in a variety of vessels [77, 78]. It has been demonstrated in the porcine iliac artery that BK-induced endothelium-dependent relaxation by activating B2R at low concentration, whereas it induced an endothelium-independent contraction by activating B1R at higher concentrations [79]. Another biological effect of BK in vessels alongside vasodilatation is the ability to increase in vascular permeability. Cytosolic Ca^{2+} increase as a result of the kinin binding receptor leads to the shortening of contractile proteins present in the endothelial cells, resulting in the formation of fenestrations in the walls of microvascular tissue and the extravasation of plasma constituents as well as of leukocytes [80, 81]. In the vasculature, both B1R and B2R activate a wide spectrum of vasoactive pathways, including NO release, prostaglandins formation and endothelium derived relaxation factors [82, 83].

1.2.1 Bradykinin-induced Nitric Oxide release

The major mechanism responsible for BK-stimulated NO production at least partly involves eNOS phosphorylation [84]. Several studies indicated that inhibition of NO synthesis significantly decreases the BK-induced relaxation of coronary arteries of dogs and also less pronounced relaxation of porcine coronary arteries [85]. The classical G (q)-protein-coupled receptor activation of phospholipase C-β (PLC-β) after stimulation of B2R by BK initiates the formation of IP3 and DAG, driving a biphasic increment in intracellular free Ca^{2+}. The PLC-β is thought to be involved in the activation of transient receptor potential (TRPC) channels, and in some endothelial cells, BK stimulates TRPC6 to induce increases in intracellular Ca^{2+}. Another important mechanism, by which BK induces the activation of eNOS, is the phosphorylation of PKA [86].

1.2.1.1 Vascular physiological and pathophysiological actions of NO

In *Table 2* some physiological and pathophysiological functions of NO in vasculature are shown.

Table 2: Vascular physiological and pathophysiological actions of NO [87]

Direct vasodilation	receptor mediated and flow dependent
Indirect vasodilation by inhibiting vasoconstrictors	inhibits angiotensin II and sympathetic vasoconstriction
Anti-thrombotic effect	blocked platelet adhesion to the vascular endothelium
Anti-inflammatory effect	inhibits leukocyte adhesion to vascular endothelium; scavenges superoxide anion
Anti-proliferative effect	inhibits smooth muscle hyperplasia
Vasoconstriction	coronary vasospasm, elevated systemic vascular resistance, hypertension
Thrombosis	as a result of platelet aggregation and adhesion to vascular endothelium
Inflammation	is able to regulate the release of several inflammatory mediators from different cells participating in inflammatory responses, including leukocytes, macrophages, mast cells, endothelial cells, and platelets

1.2.1.2 Signaling pathways of vascular tone regulation by NO

NO is a membrane-permeable gas that reacts with a variety of biomolecules to evoke cellular responses, particularly the activation of soluble guanylylcyclase (sGC) in vascular smooth muscle cells, and it produces the cyclic guanosine monophosphate (cGMP). Vascular endothelial cells synthesize NO in response to a variety of stimuli, including shear stress, bradykinin, acetylcholine, histamine, serotonin, substance P, and ATP (Figure 9). These factors increase intracellular Ca^{2+} and thereby stimulate the Ca^{2+}/CaM-activated eNOS. Endothelial eNOS produces NO from arginine, and NO subsequently diffuses to the vascular smooth muscle cell to initiate downstream signalling events and vasorelaxation [88]. NO induces the formation of cGMP by activating sGC in the vascular smooth muscle cells. Cyclic GMP inhibits calcium influx by protein kinase G (PKG) activation through the voltage-dependent calcium channel (VDCC) and calcium release mediated by IP3 receptor (IP3R) [89]. PKG also acts on sarco/endoplasmic reticulum calcium ATPase (SERCA) to promote the reuptake of cytosolic calcium into the sarcoplasmic reticulum (SR). The decreased intracellular calcium concentration and inactive calmodulin avoid the activation of myosin light chain kinase (MLCK). The activity of myosin light chain phosphatase (MLCP) increases due to the decreased calcium and the actin-myosin link is destroyed, which results in smooth muscle relaxation. NO also is able to induce the production of inosine cyclic 3,5'-monophosphate (cIMP) instead of cGMP by GC, which activates Rho-associated protein kinase (ROCK) and inhibits MLCP, resulting in contraction under hypoxic condition [90].

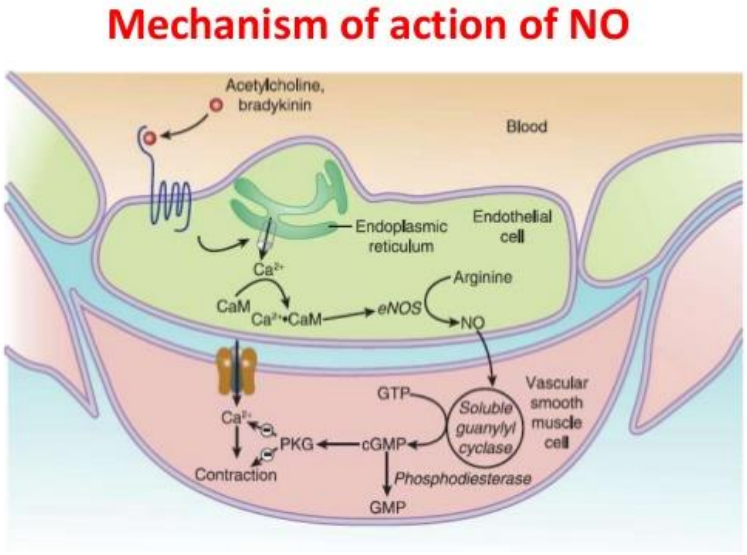

Figure 9: Regulation of vascular tone by NO. Acetylcholine or BK binding to its receptor B1 or B2 on endothelial cells activates eNOS to produce the diffusible signalling molecule NO. NO induces the formation of cGMP in the vascular smooth muscle cells. cGMP, by the activation of PKG, inhibits calcium influx, causing arterial vessels to relax and increase blood flow [91].

1.2.2 Prostaglandins

In addition to NO, endothelial cells also produce and release prostacyclin (PGI2) from cyclooxygenase-derived metabolites in response to shear stress and agonists. Bradykinin increases the production of prostaglandins (PGs) in different ways mediated through its receptors. It leads to the phosphorylation and translocation of cytosolic phospholipase A2 in a Ca^{2+} dependent manner [91, 92]. Bradykinin also stimulates membrane-associated Ca^{2+}-independent phospholipase A2 [93]. Both the Ca^{2+}-dependent and -independent A2 phospholipase stimulation lead to the liberation of arachidonic acid from membrane phospholipids. Bradykinin also induces cyclooxygenase-2, which forms PGs from arachidonic acid [94]. The bradykinin-stimulated formation of prostaglandin E_2 (PGE2) is mediated by the Gi protein connected to B1R and B2R. Eventually PGs mediate some of the effects of the kinins on vascular tone [95, 96] (Figure 10).

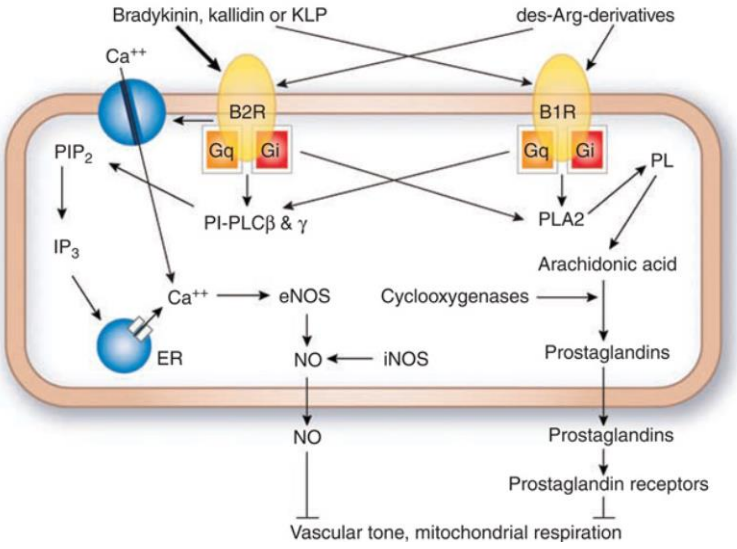

Figure 10: Prostaglandin generation by binding of kinins to B1 and B2 receptors. PIP_2, phosphatidylinositol-4,5-bisphosphate; PI-PLC, phosphatidylinositol-specific phospholipase C; IP_3, 1,4,5-inositol triphosphate; ER, endoplasmic reticulum; PL, phospholipids; PLA2, phospholipase A [98].

1.2.3 Endothelium-Derived Hyperpolarizing Factor (EDHF)

In contrast to the well-defined NO and PGI_2 pathways, the molecular constituents and mechanism of EDHF-mediated relaxation remain controversial. In Endothelium-Derived Hyperpolarizing Factor, or EDHF, there is a substance and/or electrical signal generated in endothelial cells and acting by increasing potassium (K^+) conductance, resulting in vascular smooth muscle cell hyperpolarization, causing these cells to relax [97, 98]. NO released from endothelial cells to a great extent mediates relaxation in the large conduit artery, but it has been shown that EDHF modulates vascular tone in small resistance arteries [99]. The contribution of EDHFs increases as the vessel size decreases, with the predominant EDHF activity in the resistance vessels [100, 101]. EDHFs vary in different vascular beds, but always increase K^+ conductance and lead to vascular smooth muscle cell hyperpolarization and relaxation [98, 102] (Figure 11). This EDHF-induced membrane hyperpolarization is mediated by the opening of smooth muscle cell K^+ channels and K^+ efflux along its chemical gradient. Therefore, EDHF activity is defined as agonist-induced, endothelium-dependent relaxation that is not inhibited by cyclooxygenase or NO synthase inhibitors, but rather by K^+ channel blockers [103].

1.2.3.1 Potassium (K_{Ca}^+) Channels

Agonists such as BK stimulate endothelial GPCR, provoking an increase in intracellular calcium in the endothelial cell [104]. Agonists that produce hyperpolarization also stimulate the efflux of K^+ [105]. However, there are several smooth muscle K^+ channels; endothelium-dependent hyperpolarization is not inhibited by glibenclamide, an inhibitor of ATP-dependent K^+ channels (K_{ATP}^+), or by inhibition of inward rectifying potassium channels (K_{IR}^+) [106]. Signalling mediated by EDHF is abolished by applying a combination of inhibitors including apamin (a specific inhibitor of K_{Ca}^+ channels of small conductance (SK_{Ca}^+ channels)), charybdotoxin (a nonselective inhibitor of large-conductance channels (BK_{Ca}^+)), and TRAM-34 (an inhibitor of intermediate-conductance (IK_{Ca}^+) channels). These inhibitors act on K_{Ca}^+ channels on endothelial cells, rather than K^+ channels on smooth muscle cells [107, 108]. An increased level of intracellular calcium in endothelial cells opens K_{Ca}^+ channels and causes efflux of K^+ into the myoendothelial space that initiates the following signalling pathways. The first is the synthesis of cytochrome P450 (CYP450) metabolites (see below). The second is the transferring of endothelial cell hyperpolarization to the vascular smooth muscle via gap junctions, and the third is that the release of K^+ via K_{Ca}^+ channels located in the endothelial cells induces smooth muscle hyperpolarization by activating K_{Ca}^+ channels and/or Na^+-K^+-ATPase on vascular smooth muscle cells [103].

1.2.3.2 Epoxyeicosatrienoicacids (EETs)

EETs are generated from arachidonic acid by cytochrome P450 (CYP450) epoxygenases [102]. EETs induce activation of K_{Ca}^+ channels, which apparently is mediated by a series of intracellular pathways and finally results in the hyperpolarization of smooth muscle cells by increasing the efflux of K^+ through K_{Ca}^+ channels [109, 110]. Studies have shown that 11, 12-EET activates large-conductance K_{Ca}^+ channel current and hyperpolarizes arterial smooth muscle. Large-conductance K_{Ca}^+ channels are largely located in vascular smooth muscle, whereas the CYP450-2C enzyme is located in both the endothelium and smooth muscle cells [111]. The role of EETs as potential EDHFs can be assessed using azoles such as miconazole to selectively inhibit arachidonic acid oxidation, and they have been made partially responsible for endothelium-dependent vasodilation in the human microcirculation [112] (Figure 11).

1.2.3.3 Hydrogen peroxide involved in EDHF responses

Hydrogen peroxide is one of the activators of calcium-dependent potassium channels and remains a contender as an EDHF [113] (Figure 11). It has been suggested that reactive oxygen species are able to increase K^+ efflux by activating K^+ channels and hyperpolarize smooth muscle cells, and that hydrogen peroxide may be considered as an EDHF [114]. Vascular endothelial cells have the ability to create superoxide and hydrogen peroxide from a few intracellular sources, including endothelial NO synthase, cyclooxygenases, lipoxygenases, cytochrome P-450 epoxygenases, nicotinamide adenine dinucleotide phosphate (NAD(P)H) oxidases, and xanthine oxidase [115]. Hydrogen peroxide, like EDHF, is able to stimulate endothelial K^+ channels and cause hyperpolarization. The type of K^+ channels activated may vary in different species [116].

1.2.3.4 Gap junctions

The EDHF phenomenon may possibly be described by the passive electrotonic spread of hyperpolarization from the endothelium to smooth muscle cells via gap junctions [117, 118]. These connect endothelial cells to other endothelial cells and to smooth muscle cells, preparing a passage with a low electrical resistance between the cells. Gap junctions are formed by the attachment of two connexons present in neighbor cells forming an aqueous pore, allowing the transfer of ions and electrical continuity in membrane potential between cells [119]. The number of gap junctions increases with the decreasing size of the artery [120], indicating a higher importance of EDHF in the resistance than in the conductance vessels [121].

1.2.3.5 Potassium (K^+)

It has been shown that a medium elevation in the myo-endothelial K^+ concentration is able to induce hyperpolarization in vascular smooth muscle cells by activating the inwardly rectifying K^+ channels and the Na^+/ K^+ ATPase [106,122,123]. However, it is unlikely that K^+ *per se* is EDHF.

1.2.4 Interactions between Nitric Oxide, Prostacyclin, and EDHF

NO, prostacyclin and EDHF are principle mediators of the vasodilatory effect of the endothelium. These three factors apparently act synergistically to regulate the vascular tone in a complex manner. In conduit arteries like the aorta, NO is the prevailing endothelium-derived vasodilator, but it has a relatively lower contribution in the resistance vessels of the microcirculation, where EDHF plays a more important role [121].

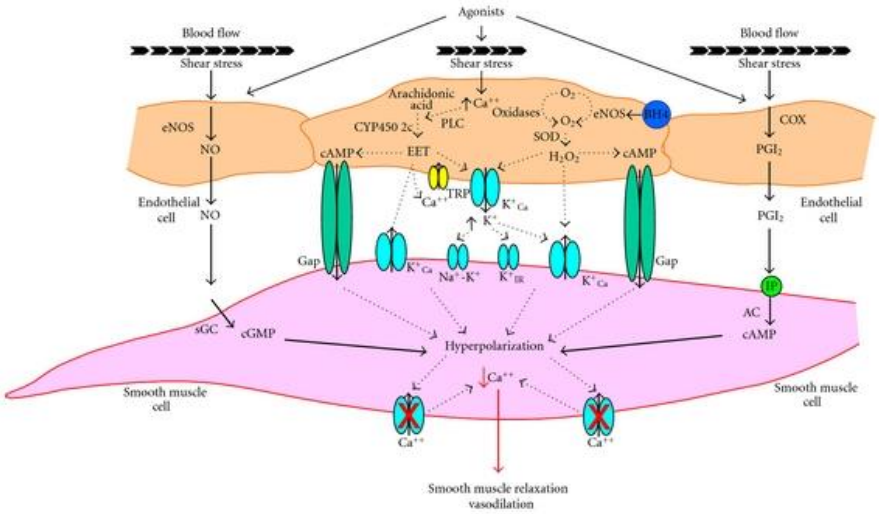

Figure 11: Pathways of endothelium-derived vasodilation. Bradykinin, acetylcholine, substance P or shear stress stimulate the activation of eNOS and cyclooxygenase (COX), providing NO-, PGI2- and EDHF-mediated dilation in the endothelial cells [124].

1.2.5 Transient Receptor Potential Channels (TRPC)

1.2.5.1 Molecular biology of TRP channels

There are three endothelium dependent relaxation pathways: NO, PGI2 and EDHF. As described above, triggering of all these pathways requires the Ca^{2+} ion and the intracellular Ca^{2+} should be increased. There are different Ca^{2+} channels on the cell membrane. But among them, transient receptor potential channels (TRPs) are the most important Ca^{2+} channels (Figure 12).

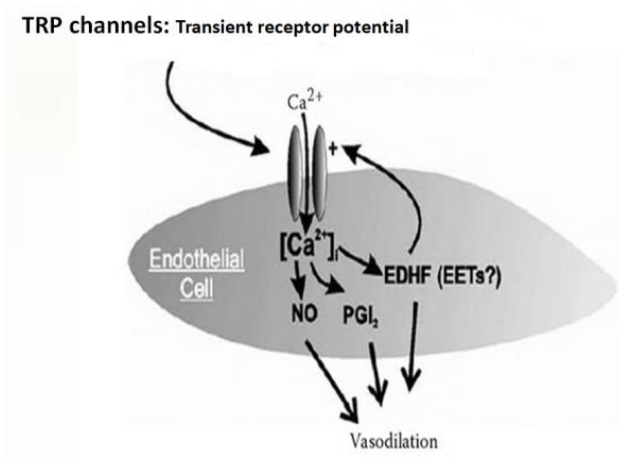

Figure 12: Endothelium-dependent vasorelaxation pathway. TRP channels are the most important Ca^{2+} channels, which provide the required amount of Ca^{2+} for the endothelium dependent relaxation pathways NO, PGI2 and EDHF [125].

TRP channels are conserved integral membrane tetramer proteins formed by subunits with six transmembrane domains, and containing cation-selective pores. These ion channels exhibit non-selective permeability to cations, including sodium, calcium and magnesium. In several cases they show high calcium permeability. In particular TRPV5 and TRPV6 show significant specificity for Ca^{2+} ions [124] . The TRP superfamily of ion channels comprises seven subfamilies [125] (Figure 13), namely: TRPC (canonical); TRPM (melastatin or long TRPs); TRPV (vanilloid); TRPA (ankyrin), whose only member is the transmembrane protein 1; TRPP (polycystin); TRPML (mucolipin); and TRPN (Nomp-C homologues), which has a single member. Primarily, TRPs are classified by relying on their amino acid sequence and less on their ion or ligand selectivity. TRP channels play an important role in the function of diverse physiological processes, including homeostatic functions (Ca^{2+} and Mg^{2+} reabsorption and osmoregulation), sensory functions (temperature sensation, taste transduction, nociception), and some other functions like muscle contraction and relaxation [125]. There are different stimuli that are able to activate TRPs and temperature is one of the most remarkable of them. Several natural products (capsaicin, menthol, or carvacrol) have been shown to activate TRP channel gating [126]. All TRPCs are linked to G protein-coupled receptors and receptor tyrosine kinases, but some TRPs have also been described that are activated by PLC and production of DAG and IP_3 [126].

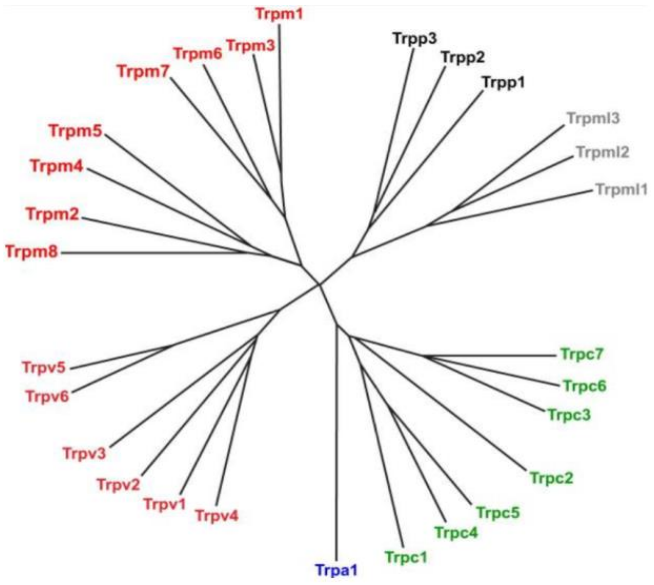

Figure 13: The TRP superfamily of ion channels comprises seven subfamilies [127].

1.2.5.2 Physiological functions of TRP channels in the vasculature

The main function of the vasculature is to ensure efficient oxygenation and nutrition of tissues by the regulation of blood flow and vascular permeability. The vasculature is also pivotal for other homeostatic functions, such as: haemostasis, lipid transport, and immune surveillance [127]. Acute regulation of vascular diameter, blood flow and consequently vascular resistance relies on the activation of the contractile machinery in vascular smooth muscle cells [128]. Changes in cytosolic Ca^{2+}, ion fluxes, and membrane potential are important factors in the regulation of smooth muscle's contractile machinery [129]. Endothelial cells play a pivotal role on vascular tone and permeability, and endothelial dysfunction may lead to the pathogenesis of cardiovascular diseases [130, 131]. Studies confirmed that many TRP channels are highly expressed in endothelial and vascular smooth muscle cells and play an essential role in the modulation and integration of regulatory pathways within the vascular wall to control vasomotor tone [132, 133, 134, 135, 136]. These studies showed the importance of TRP channels in the regulation of vascular smooth muscle tone and tissue blood flow [137].

1.2.5.2.1 The role of TRP channels in vascular smooth muscle cells

Vascular resistance is regulated by the activation of the contractile machinery in vascular smooth muscle cells, which contract when exposed to a variety of excitatory neurotransmitters and hormones. Many of these constrictors act through the activation of PLC, which converts phosphatidylinositol-4,5-bisphosphate into IP_3 and DAG [138, 128]. IP_3 mediates the Ca^{2+} release from the sarcoplasmic reticulum, leading to the transient increase in cytosolic Ca^{2+} level, which primarily is not sufficient for vasoconstriction [139, 140]. Extracellular Ca^{2+} influx, in part through voltage-gated Ca^{2+} channels, increases the cytosolic Ca^{2+} level required for a maintained vasoconstriction [141, 142]. The L-type voltage-dependent Ca^{2+} channel (VDCC) is activated by membrane depolarization. Accumulating evidence supports the idea that cation influx through TRP channels depolarizes the plasma membrane, which subsequently leads to the activation of VDCC channels [137]. The resultant increase in Ca^{2+} results in a formation of calmodulin-Ca^{2+} (Cd-Ca^{2+}) complexes. An important Cd-Ca^{2+} target is the enzyme MLCK which phosphorylates the light chain of myosin, enabling the molecular interaction of myosin with actin for contraction [137]. On the other hand, dephosphorylation of myosin by MLCP is associated with muscle relaxation. Thus, membrane depolarization and the subsequent influx of Ca^{2+} through the TRP channel is a primary mechanism of vascular smooth muscle cell contraction. Several recent studies have shown the important functional roles for TRP channels expressed by vascular smooth muscle cells [137] (Table 3).

Table 3: Types of TRP channels in vascular smooth muscle and their function [137]

TRP	Function	Tissue
TRPC1	ROCE (receptor-operated Ca2+ entry) (ET-1 constriction), SOCE (store-operated Ca2+ entry)	Brain, aorta, lung
TRPC3	GPCR-mediated vasoconstriction	Brain, aorta, heart, kidney, lung
TRPC4	SOCE	Aorta, mesentery
TRPC5	SOCE	Brain
TRPC6	GPCR-mediated vasoconstriction, myogenic tone	Portal vein, aorta, brain
TRPV1	Vasoconstriction	Aorta, skeletal muscle, mesentery, cephalic circulation
TRPV2	Mechanosensitive Ca^{2+} influx	Aorta
TRPV3	mRNA present in VSM but no known function	Aorta, lung
TRPV4	Ca^{2+} influx, vasodilation	Brain, mesentery

1.2.5.2.2 The role of TRP channels in the vascular endothelium

The vascular endothelium is a highly differentiated cellular monolayer of metabolically dynamic endothelial cells that line the entire circulatory system, from the heart to the smallest capillaries in the body, and is strategically located at the interface between the vascular lumen and the underlying smooth muscle cells. Endothelial cells are involved in a variety of physiological and pathophysiological processes. The main functions of the endothelium are: regulation of vascular tone, control of vascular permeability, coagulation, fibrinolysis, vascular inflammatory reactions, angiogenesis, and blood vessel formation [143]. Endothelial cells express a great variety of membrane-bound ion channels. The most important functions of the endothelial ion channels are to regulate the influx of Ca^{2+} and to modulate endothelial cell membrane potential [144]. The evidence available suggests that TRP channels are the most important cation channels in vascular endothelial cells and function as intracellular [Ca^{2+}] regulators, which are important for endothelial cell function. Around 20 diverse TRP channel family members are expressed in endothelial cells [135], and the following channels are functional in endothelial cells: TRPC1, TRPC3 [145], TRPC4, TRPC5, TRPC6 [146], TRPV1, TRPV3 [147], TRPV4 [148] and TRPA1 [149] (Table 4).

Table 4: Types of TRP channels in vascular endothelium and their function [137]

TRP	Function	Tissue
TRPC1	Angiogenesis, permeability	Embryonic tissue, lung
TRPC3	Angiogenesis, endothelium-dependent relaxation	Mesenteric arteries
TRPC4	Angiogenesis, endothelium-dependent relaxation, permeability	Aorta, lung
TRPC5	Angiogenesis	Umbilical vein
TRPC6	Angiogenesis, permeability	Umbilical vein, epidermis
TRPV1	Endothelium-dependent relaxation	Mesenteric arteries, heart
TRPV3	Endothelium-dependent relaxation	Brain
TRPV4	Angiogenesis, endothelium-dependent relaxation, permeability	Aorta, mesenteric arteries, skeletal muscle, heart, lung, brain
TRPA1	Endothelium-dependent relaxation	Brain

1.2.5.2.2.1 TRP channels and endothelium-dependent vasodilation

The endothelium exerts important effects on vascular tone by balancing constrictor and dilator actions. It has been investigated whether endothelium-dependent vasodilation is stimulated by Ca^{2+} influx pathways via TRP channels [144] such as TRPV1, TRPV3, TRPV4, TRPA1, TRPC3 and TRPC4 [149].

TRPV1 channels (Vanilloid Receptor 1) are stimulated by capsaicin, a small lipophilic molecule in chili peppers that induces sensations of heat [150]. TRPV1 plays a role in endothelium-dependent relaxation. Poblete et al. demonstrated that Ca^{2+} influx through TRPV1 channel activation with anandamide increased the release of endothelium-derived NO and caused vasodilation [151].

TRPV3 channel is a sensitizing receptor [152] and is stimulated by harmless heat and dietary monoterpenes [153]. Earley et al. found that TRPV3 channels are present in the endothelium of rat cerebral arteries. Administration of Carvacrol (TRPV3 activator) induced an endothelium-dependent dilation of isolated cerebral arteries that was not prevented by NOS or COX inhibitors [147].

TRPV4 channels are present in endothelial cells of aorta and are activated by heat (25–43°C) [154] and cell swelling [155]. Recent studies suggest that arachidonic acid metabolites like 5,6-epoxyeicosatrienoic acid (5,6 EET) and 8,9 epoxyeicosatrienoicacid (8,9 EET) generated by cytochrome P450 epoxygenases lead to channel activation [154,156]. These compounds are generated by endothelial cells and may act as EDHFs in some vascular beds [137]. Exogenous administration of EETs leads to the vasodilation of isolated mesenteric arteries from wild-type, but not $TRPV4^{-/-}$, mice [149].

TRPA1 channels respond to a wide range of agonists, including: the dietary molecules allicin [157] (found in garlic) and allylisothiocyanate (AITC [158], extracted from mustard oil); ambient toxins, such as acrolein and nicotine [159, 160]; and anesthetic agents, such as propofol and lidocaine [161, 162]. TRPA1 channels are highly permeable to Ca^{2+} [163]. Recent studies have demonstrated the involvement of TRPA1 channels in vascular regulation [137]. Other studies demonstrated that the TRPA1 channel causes an endothelium-dependent vasodilation through Ca^{2+} influx in arterial endothelial cells. In a study done by Earley and colleagues, they showed that TRPA1 channels exist in arterial endothelial cells, and that the compound AITC induced relaxation in cerebral arteries, which was inhibited by TRPA1 inhibitors and endothelium denudation. They also demonstrated that the AITC induced relaxation response was not blocked by NOS and COX blockade, whereas the response was inhibited by SK, IK, or K_{IR} channel blockers [149].

TRPC3 channels are permeable to Ca^{2+}, Na^{+} and K^{+} [164]. The channel is activated by GPCR pathways and its mediated Ca^{2+} signalling is based on a direct interaction with diacylglycerol [165]. Several investigations implicated the involvement of TRPC3 in endothelium-mediated vasodilatation. Recent studies have suggested the contribution of endothelial TRPC3 channels in the vasorelaxation response induced by luminal flow and bradykinin [166, 167]. Senadheera et al. showed the important role of TRPC3 in endothelium-dependent hyperpolarization-mediated dilation by increasing the intracellular Ca^{2+} that activates SK and IK channels and induces endothelial cell hyperpolarization in mesenteric arteries [168].

TRPC4 channels are Ca^{2+}/Na^{+} -permeable cation channels that are expressed in many cell types and tissues like endothelial cells, and they play a determinant role in endothelial Ca^{2+} signalling and functions [169]. In 2001, Freichel et al. showed an impaired relaxation, ACh-induced Ca^{2+} influx and SOCE in aortic endothelial cells of TRPC4 knockout mice [170].

1.3 Physiological and pathophysiological roles of the KKS

The physiological activity of BK is multidirectional and it may play a major role in cardiovascular function and in the pathogenesis of cardiovascular disease [171]. Besides its cardioprotective functions, BK has multiple pathophysiological functions, such as: induction of vasodilation, increase in vascular permeability and induction of angioedema as a consequence of vascular leakage [172] (Figure 14). KKS functions as a regulator of the cardiovascular system in physiological and pathophysiological conditions [173].

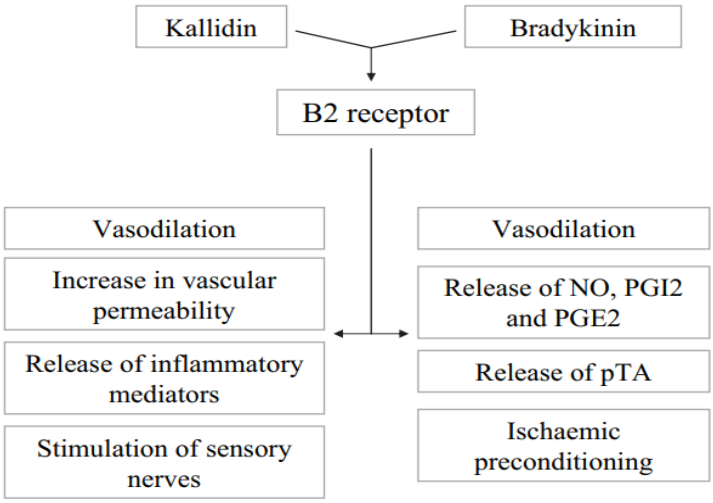

Figure 14: Clinical implications of bradykinin. BK exerts multidirectional activities and plays an important role in cardiovascular function and in the pathogenesis of cardiovascular and other disease [168].

1.3.1 Role of bradykinin in pain

A growing body of studies suggest kinins - through binding the B2R function - as modulatory transmitters that play a role in the physiological control of spinal- and supra-spinal-nociceptive neurotransmission [68]. All components of the KKS have been localised in the brain and spinal cord, including kininogens, kallikreins, B2R and kinin-degrading enzymes. It has been demonstrated that the administration of BK into the cerebral ventricles causes an anti-nociceptive effect through a noradrenergic mechanism in rabbits [174, 175]. This anti-nociceptive response is mediated by B2R due to the release of noradrenaline from descending inhibitory neurons [176]. It has been shown that BK exerts its nociceptive effect greatly in a direct action on B2R located on sensory terminals projecting to the superficial laminae of the spinal cord. The specific role of B1R and B2R in inflammatory pain perception is associated with the pattern of their expression. Primary non-myelinated sensory neurons constitutively express B2R and BK, contributing to the acute pain response [177] mediated by the release of DAG [178] and protein kinase C activation [178]. Kinin receptor antagonists appear to be potential therapeutics for analgesia, since animal models of inflammatory pain have been used to show that B1R or B2R antagonists exert analgesia [179].

1.3.2 Bradykinin and inflammation

BK is a mediator of inflammation, and its release is associated to the severity of the acute inflammation which is inhibited by a B2R antagonist. However frequent stimulation by an irritant induces a reaction that is inhibited by a B1R antagonist [180]. Applying BK through the activation of B2R reproduces rubor and calor, which are two important signs of inflammation mediated by the vasodilatation which is induced by the release of NO and PGI2 in vascular endothelial cells [9]. It has been suggested that B1R plays an important role in neutrophil accumulation in inflammatory conditions, as the functional ablation of the *Bdkrb1* gene in mice is correlated with a dramatic defect of this process [181]. Experimental studies have indicated that B2Rs are involved in the acute phase of the inflammatory response, but B1Rs participate in the chronic phase of the response [182]. This probably happens in light of the fact that the B2R function is short-term because of fast ligand dissociation, receptor desensitization and internalization. In contrast, B1Rs produce long-lasting responses and signalling due to limited desensitization and internalization [183, 184, 185, 186, 187].

1.3.3 Cardiovascular disorders and the KKS

1.3.3.1 Ischemia

A large number of studies have indicated that kinins are highly important mediators of cardiovascular protective mechanisms. This protective effect is because of the localization of KKS components in the heart and vascular tissues [188, 189]. Kinins are released during ischemia [190] and cause beneficial cardiac effects [191]. BK infusion into coronary arteries significantly reduces the

severity of ischemia-induced arrhythmia [192]. Kinins interact with endothelial B2Rs leading to the liberation of NO and PGI2, exerting vasodilator, ischemic, and anti-proliferative effects, as well as preserving myocardial stores of energy-rich phosphates and glycogen [193]. A lot of evidence also supports the suggestion that a dysfunctional KKS may contribute to the pathogenesis of heart failure. It has been reported that decreases in the local production of kinin and NO formation have been reported in microvessels of failing human hearts [194]. BK antagonists worsen ischemia-induced effects [190]. Attenuation of the anti-arrhythmic effects of ischaemia preconditioning by the blockade of B2R and BK can counteract the cardioprotective effects of preconditioning. Accordingly, the reduction in cardiac infarct size by BK, after preconditioning in rabbits, was prevented by B2R antagonist (Hoe140) treatment [195].

1.3.3.2 Left Ventricular Hypertrophy

According to Linz, et al. [191], ventricular hypertrophy (LVH) in rats with hypertension caused by aortic banding can be prevented by a low dosage of BK, which has no effect on blood pressure. B2R antagonist and a NOS inhibitor can inhibit this anti-hypertrophic effect of BK. Based on these findings, BK plays an important role in protecting the heart against developing LVH by liberating NO.

1.3.3.3 Hypertension

Hypertension is a major risk factor for the development of cardiovascular diseases. Kinins circulating in the plasma are inactivated quickly and only reach very low concentrations in the blood. Local KKS are also found in the kidney, heart and vasculature, and their activity is of vital significance for the regulation of blood flow, blood pressure, and cardiovascular protection [196, 197]. BK exerts its physiological role in the modification of systemic blood pressure via a vasodilatory effect in most vasculature, in particular in resistance vessels, and the regulation of sodium excretion in the kidney [198, 199]. In human and experimental animals, a small decrease in KKS components leads to the developing of high blood pressure [189].

1.3.4 Angioedema

An increase in vascular permeability in the deeper layers of the skin including the dermis and the subcutaneous tissue leads to angioedema [200]. Angioedema attacks are challenging clinical issues because of their complex pathological mechanisms, the difficulty in determining the causes, and the diverse responses to symptomatic treatment among patients. Angioedema is classified as allergic or nonallergic. Allergic angioedema often occurs with an inflammatory focus and an allergy to food allergens, drugs, or insect venom. Histamine is an essential agent in this type of edema [201]. Nonallergic angioedema is grouped into 5 different types: 1) hereditary angioedema (HAE); 2) acquired angioedema (AAE) due to C1 inhibitor (C1-INH) deficiency; 3) angioedema

associated with the renin-angiotensin system blockade (The use of ACE inhibitors may cause BK-mediated angioedema by blocking the destruction of BK and by activating B2R); 4) pseudoallergic angioedema, which is a form of drug-induced angioedema; and 5) idiopathic angioedema [201, 202]. BK is the main mediator of nonallergic angioedema [200]. Excessive amounts of BK lead to increased permeability of capillaries, leading to the progression of local edema [202]. HAE is mainly known as an autosomal dominant disease, characterized by C1-INH quantitative (type I) or functional (type II) deficiency, with more than 500 mutations identified (The Human Gene Mutation Database, http: //www.hgmd.cf.ac.uk/ac/index.php). Its clinical description and hereditary characteristics were established in 19th century [203, 204], but C1-INH deficiency was only identified in the 1960s [205]. The characteristic symptoms are nonpruritic and nonpitting swellings of submucosal or subcutaneous tissues, involving the face, hands, feet, arms, legs, bowels, genitalia and upper airways, which can be life threatening [206]. Angioedema symptoms generally last 2 to 5 days before resolving spontaneously without treatment, and the most common triggering factors for HAE attacks include emotional stress, trauma, medical and surgical procedures, and oestrogens [207]. C1-INH is a secreted glycoprotein of the Serpin family that inhibits several proteases of the classical and lectin complement pathways [208], and other serine proteases such as PK, coagulation FXI and FXII, thrombin, plasmin and tissue plasminogen activator [209]. Its deficiency results in an uncontrolled BK release due to HK cleavage by PK activity, which has been recognized as the main responsible cause for HAE symptoms. In HAE type III, excessive BK formation is due to pathological activation of the contact system via FXII auto activation. A lot of evidence supports the hypothesis that edema formation is mediated by BK signalling in both HAE types, and although HAE patients present a huge variation regarding frequency, duration and localization of edemas, triggering factors and severity, the clinical symptoms among all types are undistinguished. The angioedema episodes are not followed by hives and are not benefited by antihistamines or corticosteroids, indicating that histamine is not a fundamental mediator, whereas HAE crises have been successfully treated with plasma kallikrein inhibitor (Ecallantide), B2R antagonist (Hoe140, Icatibant), as well as recombinant or plasma derived C1-INH [206]. It is not clear which elements lead to the large variation of HAE clinical manifestations, but the role of BK is evident, implying an involvement of contact system proteins, from FXII to B2R. It was shown that plasma PK is able to hydrolyse HK in vitro, releasing BK in a potential autoactivation mechanism that may be favoured in the lack of contact system inhibition [210]. Hormones are considered as a pronounced triggering factor for crises, with women presenting a worse prognosis, especially during hormonal reposition, contraceptive pill intake, pregnancy and menstruation. Oestrogen has been recognized as a regulator of the expression of gene coding for crucial proteins of the BK release pathway, including FXII, HK and PK genes, but the balance of this regulation is not completely understood [211, 212, 213]. The lack of suitable animal models with similar human clinical symptoms is a considerable problem in HAE research. Han et al. (2002) generated homozygous and heterozygous C1INH-deficient mice, which presented increased vascular permeability in the ears, rear paws and bowel, and an increased permeability response to external irritants. However, these animals do not present episodes of spontaneous angioedema that could be comparable to the human clinical symptoms [214]

2 Aims of the thesis

The aims of the thesis were to investigate the role of kinin B1 and B2 receptors in endothelial cells and to scrutinize the signalling mechanisms involved in B1R and B2R mediated vasorelaxation. To clarify their vascular function, we generated transgenic rats overexpressing B1R and B2R exclusively in the endothelium. The effect of kinin receptor overexpression on vascular reactivity was investigated in vitro in aorta rings using the organ bath technique. The effects on vascular homeostasis were evaluated in vivo by measurement of blood pressure and vascular permeability. Additionally, CPM KO rats were generated using the CRISPR/Cas9 technique to investigate the function of CPM as an important enzyme in the metabolism of BK, since it metabolizes BK, a B2R agonist, to the specific agonist for B1R, des-Arg^{9}-BK.

3 Materials

3.1 Chemicals and reagents

Table 5: Chemicals and reagents

Chemicals and reagents	Company (Location)
Agarose	Biozym (Oldendorf, Germany)
Bovine Serum Albumin (BSA)	Sigma-Aldrich (St. Louis, USA)
Chloroform	Merck (Darmstadt, Germany)
Deoxyribonucleotide (dNTP)	Bioline (London, UK)
Dimethyl sulfoxide (DMSO)	Sigma-Aldrich (St. Louis, USA)
DNase I recombinant	Roche (Basel, Schweiz)
Ethanol	Berkel AHK (Berlin, Germany)
Ethidium Bromide	Carl Roth (Karlsruhe, Germany)
Ethylenediaminetetraacetic acid (EDTA)	Serva (Heidelberg, Germany)
Ethylenediaminetetraacetic acid (EDTA)	Carl Roth (Karlsruhe, Germany)
Eukitt® Quick-hardening mounting medium	Sigma-Aldrich (St. Louis, USA)
First Strand buffer (5x) (Invitrogen)	Thermo Fisher Scientific (Waltham, USA)
GoTaq® qPCR Master Mix	Promega (Fitchburg, USA)
Hematoxylin Solution	Sigma-Aldrich (St. Louis, USA)
Heparin-Sodium (5 000UI/mL)	B. Braun Melsungen (Melsungen, Germany)
Isoflurane	Abbott (Chicago, USA)
Isopropyl	Carl Roth (Karlsruhe, Germany)
Magnesium chloride ($MgCl_2$; 50mM)	Sigma-Aldrich (St. Louis, USA)
Methanol	Chemsolute/ Th. Geyer (Renningen, Germany)
Normal donkey serum	dianova/ Jackson ImmunoResearch (West Grove, USA)
Odyssey® Blocking Buffer	LI-COR Bioscience (Lincoln, USA)
Paraffin	Carl Roth (Karlsruhe, Germany)
Paraformaldehyde (PFA) $%, buffered	Fischar (Saarbrücken, Germany)
Proteinase K	Carl Roth (Karlsruhe, Germany)
Quick-Load© 100 bp DNA ladder	New England Biolabs (Ipswich, USA)
Quick-Load© 1 kb DNA ladder	New England Biolabs (Ipswich, USA)
Random primers p(dN)6	Roche (Basel, Schweiz)
RedTaq ® DNA Polymerase	Sigma-Aldrich (St. Louis, USA)
RIPA Buffer (10X)	Cell Signaling Technology (Danvers, USA)
RNAse A	Promega (Fitchburg, USA)
RNAsin® Ribonuclease Inhibitor (Rnasin) RNAsin® Ribonuclease Inhibitor (Rnasin)	Promega (Fitchburg, USA) EURx (Gdansk, Poland)
Saline (NaCl 0.9%)	B. Braun Melsungen (Melsungen, Germany)
Sodium dodecyl sulfate (SDS)	Serva (Heidelberg, Germany)
Temed	Carl Roth (Karlsruhe, Germany)
Triton X-100	Sigma-Aldrich (St. Louis, USA)
Trizol® (Invitrogen)	Thermo Fisher Scientific (Waltham, USA)
Xylene	Carl Roth (Karlsruhe, Germany)
BSTYI	New England Biolabs (Ipswich, USA)

3.2 Agonists and antagonists

Table 6: Agonists and antagonists

Agonists and antagonists	**Company (Location)**
Glibenclamide	Tocris (Bristol, United Kingdom)
Indomethacin	Sigma-Aldrich (St. Louis, USA)
Tetraethylammonium chloride	Sigma-Aldrich (St. Louis, USA)
17-ODYA	Tocris (Bristol, United Kingdom)
Charybdotoxin	Alomone labs (Jerusalem, Israel)
Iberiotoxin	Alomone labs (Jerusalem, Israel)
Apamin	Tocris (Bristol, United Kingdom)
Capsazepine	Sigma-Aldrich (St. Louis, USA)
Capsaicin	Sigma-Aldrich (St. Louis, USA)
GSK1016790A	Sigma-Aldrich (St. Louis, USA)
AB159908	Sigma-Aldrich (St. Louis, USA)
SH045	Gift from Dr. Schaefer (Munich, Germany)
Dansyl-Ala-Arg-OH trifluoroacetate salt	Bachem (Bubendorf, Switzerland)
Recombinant human carboxypeptidase M protein, CF	Novus (Colorado, USA)
DL-2-Mercaptomethyl-3-guanidinoethylthio-propanoic Acid	Sigma-Aldrich (St. Louis, USA)
HPA002657	Sigma-Aldrich (St. Louis, USA)
RN 1734	Tocris (Bristol, United Kingdom)
SAR 7334	Tocris (Bristol, United Kingdom)
Pyr3	Tocris (Bristol, United Kingdom)
(Des-Arg^{9}) -Bradykinin-acetate salt	Bachem (Bubendorf, Switzerland)
Bradykinin-acetate salt	Bachem (Bubendorf, Switzerland)
(Des-Arg^{9}, Leu^{8}) -Bradykinin	Bachem (Bubendorf, Switzerland)
HOE140	Sigma-Aldrich (St. Louis, USA)
L-NAME	Sigma-Aldrich (St. Louis, USA)
R 715	R&D System (Minneapolis, Minnesota, United States)

3.3 Lab equipment

Table 7: Lab Equipment

Instruments and Materials	Company (Location)
Fluorescence microscope BZ-9000	Keyence (Neu-Isenburg, Germany)
Fluorescence stereo microscope M205 FA	Leica (Wetzlar, Germany)
Odyssey® infrared imaging system	LI-COR Bioscience (Lincoln, USA)
ACCU-Chek glucometer	Aviva/ Roche (Basel, Switzerland)
Agarose gel electrophoresis chamber	Biometra (Göttingen, Germany)
Centrifuge Biofuge 13	Heraeus (Hanau, Germany)
Centrifuge Labofuge 400e	Heraeus (Hanau, Germany)
Centrifuge Sorvall RC 5C	Heraeus (Hanau, Germany)
Cooling centrifuge 5804 R	Eppendorf (Hamburg, Germany)
Electroporator 2510	Eppendorf (Hamburg, Germany)
FastPrep™-24 instrument	MP Biomedicals (Eschwege, Germany)
Gel Imager C200	Azure Biosystems (Dublin, USA)
Imager Transilluminator Multi Image™ Light Cabinet	Alpha Innotech (San Leandro, USA)
Instruments for surgery and organ collection	FST Fine Science Tools (Heidelberg, Germany)
NanoDrop™ 1000 spectrophotometer	Peqlab (Erlangen, Germany)
pH Meter pH Level 1	WTW (Weilheim, Germany)
Pipettes	Discovery Abimed (Langenfeld, Germany)
Real-Time PCR System 7900HT AbiPrism	Applied Biosystems (Foster City, USA)
Real-Time PCR System QuantStudio 5	Applied Biosystems (Foster City, USA)
Roller mixer SRT1	Snijders (Tilburg, Netherlands)
Roller mixer SU1400	sunlab (Mannheim, Germany)
Rotable platform Polymax 1040	Heidolph Instruments (Schwabach, Germany)
Rotary microtome HM 355 S	Microm (Walldorf, Germany)
SDS-PAGE gel electrophoresis chamber	Bio-Rad Laboratories (Hercules, USA)
Schuler tissue bath system	Hugo Sachs Elektronik, Freiburg, Germany
Sonicator Bioruptor plus	diagenode (Seraing, Belgium)
Sonicator Ultrasound Sonoplus	Bandelin electronic (Berlin, Germany)
Thermocycler C1000	Bio-Rad Laboratories (Hercules, USA)
Thermocycler Master cycler nexus GX2	Eppendorf (Hamburg, Germany)
Thermocycler peqSTAR	Peqlab (Erlangen, Germany)
Thermomixer 5437	Eppendorf (Hamburg, Germany)
UV Stratalinker 1800	Stratagene (La Jolla, USA)
Vacuum pump BVC 21	Vacuubrand (Wertheim, Germany)
Vacuum pump BVC professional	Vacuubrand (Wertheim, Germany)
Water bath	GFL (Burgwedel, Germany)
384-well optical plate MicroAmp	Applied Biosystems (Foster City, USA)
Beads for tissue homogenization	MP Biomedical (Eschwege, Germany)
Falcon tubes (15 and 50 ml)	Greiner AG (Kremsmünster, Austria)
FastPrep™ lysing matrix tubes and caps	MP Biomedicals (Eschwege, Germany)
Filter tips (10, 20, 200 and 1000 ml) Surphob	Biozym (Oldendorf, Germany)
Latex gloves	Sänger (Schrozberg, Germany)

Instruments and Materials	**Company (Location)**
Nitrile gloves	Cardinal Health (The Hague, The Netherlands)
Pasteur pipettes	Carl Roth (Karlsruhe, Germany)
PCR strip tubes + caps Axygen	Corning (Corning, USA)
Plastipak™ Plastic Concentric Luer-Lock 50 mL Syringe	BD (Franklin Lakes, USA)
PVDF membranes	Amersham Life Science (Little Chalfont, UK)
Save-Lock Tubes	Eppendorf (Hamburg, Germany)
Whatman paper (3 mm)	Whatman (Maidstone, UK)

4 Methods

4.1 Genotyping of rat lines

4.1.1 DNA isolation for genotyping

To determine the genotype of rat lines, biopsies of ear, toenail, or tail were incubated with 25 µL (toe nail) or 100 µL (ear, tail) of Ear buffer (Table 8), shaking overnight at 55 °C. The buffer contained the broad-spectrum serine protease Proteinase K for digestion of proteins and hair, hence making the DNA accessible. To inactivate Proteinase K activity, the samples were heated to 95 °C for 10 min. and 250 µL (toe nail) or 750µL (ear, tail) of Tris-EDTA buffer were added. RNase A in the TE buffer degraded RNA, resulting in genomic DNA in solution. The solution contained the isolated genomic DNA of the respective animal. Samples were stored at 4 °C until usage.

Table 8: Solutions to isolate genomic DNA from animal biopsies

	Ingredient	End concentration
	NaCl	200 mM
	Tris-HCl pH 8.5	100 mM
	EDTA pH 8.0	0.1 mM
	SDS	1%
	Proteinase K	1 mg/mL
TE buffer (pH 8.0)	Tris-HCl pH 7.4	10 mM
	EDTA pH 8.0	1 mM
	RNase A	20 µg/ml

4.1.2 Primers for genotyping of rat lines

Primer sequences that were used to genotype animals are listed in Table 9 All oligonucleotides were synthetized by Biotez Berlin Buch GmbH and delivered in a lyophilized state. The primers were diluted in double-distilled water (ddH2O) to a concentration of 50 pmol/µL and stored at -20 °C.

Table 9: Primers for genotyping of rat lines

Rat line	Primer name	Sequence (5' to 3')
B1R-TGR	**Tie2-for**	5′-TTTCCTCCTCCCATTGGCTGCC
	Tie2-rev	5′- GAAGGAACCTTACTTCTGTGG
B2R-TGR	**B2R BK135-for**	5' -TCACAGCTCCTCCGATGAGA
	B2R BK137-rev	5' - TCAGTGTCTGGGCAGTTGAC
CPM KO	**CPM 5**	5'-GTGGGACCATCTTTACCTGG
	CPM 3	5'-GAGCGTGGCTCAGAACTAC

4.1.3 Polymerase Chain Reaction (PCR)

Genotyping was performed to distinguish wild type from transgenic animals. PCR was performed according to the manufacturer's instructions. PCR efficiency was optimized by adjusting the concentration of primers, deoxyribonucleotides (dNTPs), magnesium chloride ($MgCl_2$) and genomic DNA, as well as the duration and temperature for annealing and elongation. The standard steps of the PCR can be seen in Table 10.

Table 10: General steps of the PCR

PCR steps	Time	Temperature	Cycles
Initial denaturation	3 min	94°C	1x
Denaturation	20-30 sec	94°C	
Annealing	30 sec	55-65°C	34x
Elongation	30-60 sec	68/72°C	
Final elongation	5-10 min	68/72°C	1x

4.1.4 Agarose gel electrophoresis

PCR amplicons were visualized by gel electrophoresis. Agarose was dissolved in Tris-acetate-EDTA (TAE) buffer, diluted from Rotiphorese 50x TAE Buffer. To enable visualizing DNA in UV light, 5 µL of 0.2% ethidium bromide was added to 35 mL of dissolved agarose. The PCR amplicon was mixed with gel loading dye and loaded onto an agarose gel. PCR products were electrophoretically separated at constant voltage (80-110 V) for 20-40 min. Fluorescing bands were visualized with UV light using a gel imager Transilluminator Multi Image™ Light Cabinet or a gel imager C200. A Quick-Load 100 bp DNA ladder served as the molecular weight reference.

4.1.5 Genotyping of rat lines

The B1R-TGR, B2R-TGR and CPM-KO rat lines were genotyped according to the protocol shown in Table 11, Table 12 and Table 13, respectively. A PCR mix of 25 µL in total was prepared and run with its respective PCR program. The product was loaded onto a 2% agarose gel. Digestion resulted in one band of the sizes 300, 350 and 450 base pairs (bp), respectively.

Table 11: PCR protocol for genotyping the B1R-TGR

Stock conc.	Ingredients	Volume [µL]
10x	10x Self-made PCR Puffer	2.5
50mM	$MgCl_2$	1
5mM	dNTP	2
7.1 µM	Tie2 for	1
7.1 µM	Tie2 rev	1
	ddH_20	15.375
5000 U/mL	*Taq* DNA Polymerase (NEB)	0.125
	Genomic DNA	1

Time	Temperature	Cycles
2 min	94 °C	1x
20 sec	94 °C	35x
30 sec	58 °C	
30 sec	72 °C	
4 min	72 °C	1x
infinite	4°C	

Table 12: PCR protocol for genotyping the B2R-TGR

Stock conc.	Ingredients	Volume [µL]
10x	ThermoPol Buffer (NEB)	2.5
5mM	dNTP	1
5µM	B2R BK135	1
5µM	B2R BK137	1
	ddH20	18.075
5000 U/mL	*Taq* DNA Polymerase (NEB)	0.125
	Genomic DNA	1.3

Time	Temperature	Cycles
30 sec	95°C	1x
22 sec	95°C	34x
30 sec	60.5°C	
50 sec	68°C	
5 min	68°C	1x
infinite	4°C	

Table 13: PCR protocol for genotyping the CPM-KO 12576 and 12538 rat lines

Stock conc.	Ingredients	Volume [µL]
10x	ThermoPol Buffer (NEB)	2.5
5mM	dNTP	1
5µM	CPM3	1
5µM	CPM5	1
	ddH20	18.075
5000 U/mL	*Taq* DNA Polymerase (NEB)	0.125
	Genomic DNA	1.3

Time	Temperature	Cycles
30 sec	95°C	1x
22 sec	95°C	34x
30 sec	60.5°C	
50 sec	68°C	
5 min	68°C	1x
infinite	4°C	

4.2 Insertion Site Mapping by Circle PCR

Two lines of transgenic rats overexpressing kinin B2 receptor (TGR (VECDHB2), B2R-TGR) were generated: L-11248 and L-11206 (see Materials and Methods). In L-11248, we observed that in some litters all pups were positive for the transgene, although they were from heterozygous transgenic and non-transgenic parents. We were expecting 50% transgenic and 50% non-transgenic littermates. The explanation for this unexpected phenomenon could be that this line may have more than one transgene integrated into several of their chromosomes due to the random nature of an integration event. To clarify this, we mapped the B2 receptor transgene locations in this line. We used the inverse PCR method. Genomic DNA containing the inserted transgene from 20 transgenic rats was digested by a restriction enzyme (BstYI) (Table 14) which generates a restriction site within the transgene as well as within the neighboring genomic DNA.

Table 14: Protocol of Restriction Endonuclease Reaction

Restriction Endonuclease Reaction	
Restriction enzyme (BSTY 1)	1µL
DNA	1µg
Buffer (2.1 NEB) (1x)	5µL
H2O	x µL
Total reaction volume	50µL

This digestion of transgene-genomic DNA fragment was stopped in 80°C for 20 minutes and then ligated back to itself to form a circular DNA structure using T4 ligase kit, followed by 2 hours of incubation at 20°C (Table 15). In the next step, DNA was purified using the column-based DNA extraction method. PCR was performed (Table 16) using selected primers which were oriented in the reverse direction (Table 17). Next, nested PCR was performed to improve the sensitivity and specificity of the DNA (Table 18).

Table 15: Protocol of Ligase Reaction

Ligase Reaction	
DNA	40µL
Ligase buffer 10x	8µL
Ligase T4	4µL
H2O	48µL
Total reaction volume	100µL

Table 16: Protocol of PCR

Stock conc.	Ingredients	Volume [µL]
10x	ThermoPol Buffer (NEB)	2.5
5mM	dNTP	1
5µM	Map1 or 3	0.5
5µM	Map2 or 4	0.5
	ddH20	9
	MgCl2	0.5
5000 U/mL	*Taq* DNA Polymerase (NEB)	0.5
	DNA	10

Time	Temperature	Cycles
3 min	95°C	1x
20 sec	95°C	35x
30 sec	60°C	
1 min	72°C	
5 min	72°C	1x
infinite	4°C	

Table 17: Primers used for mapping by circle PCR

Primer name	Sequence (5' to 3')
BGHPAmap 1	5'-ACCTTCCAGGGTCAAGGAAG
BGHPAmap 2	5'-CTTCCTTTCTCGCCACGTTC
BGHPAmap 3	5'-GATGGCTGGCAACTAGAAGG
BGHPAmap 4	5'-CCGTCAAGCTCTAAATCGGG
B2outside	5'-ACAAGGCCTAAGGGGCTGC

Table 18: Protocol of Nested PCR

Stock conc.	Ingredients	Volume [µL]
10x	ThermoPol Buffer (NEB)	1.5
5mM	dNTP	1
5µM	Map3	0.5
5µM	Map4	0.5
	ddH20	15.4
	MgCl2	0.6
5000 U/mL	*Taq* DNA Polymerase (NEB)	0.5
	DNA	5

Time	Temperature	Cycles
3 min	95°C	1x
20 sec	95°C	35x
30 sec	60°C	
1 min	72°C	
5 min	72°C	1x
infinite	4°C	

PCR products were purified using Column based DNA extraction and inserted into T-vector (Table 19), followed by overnight incubation at 16°C. 10 µL of the sample containing DNA inserted into T-vector were transformed into One Shot™ TOP10F' Chemically Competent *E. coli.* The bacteria were kept on ice for 30 min, followed by an electroshock. After adding 1 mL LB medium (25 g LB Broth Luria/Miller, solved in 1 L ddH_2O) without antibiotics, the bacteria were cultured in a

shaking thermomixer at 37 °C for 45 min. This was followed by growth overnight on an agar dish (40 g of LB Agar Luria/Miller, solved in 1 L ddH_2O) at 37 °C, selection by ampicillin resistance (100 µg/mL, solved in 120 mM NaOH). The next day, seven clones were picked and each clone was cultured in 5 mL LB medium with ampicillin selection overnight in a shaking 37 °C incubator. Bacterial DNA was isolated from 4 mL of the overnight culture. In order to extract plasmid DNA from bacteria, the "mini prep" technique was utilized. For mini-preparation of DNA from the bacteria, 4 mL of the bacterial culture were pelleted for 5 min at 6000*g. The pelleted cells were solved in 250 µl of Solution A (Table 20). To lyse the cells, 250 µl of Solution B were added and mixed gently by inversion. After incubation for 3-5 min at room temperature, 250 µl of Solution C were added to neutralize the sample and stop the lysis. The mixture of precipitated DNA, protein and SDS was gently mixed, incubated on ice for 10-30 min and centrifuged for 10 min at 14 000*g. The supernatant was transferred to a new 1.5 ml tube, and 500 µL 99% isopropyl were added and mixed by inversion. After an incubation step for 10 min at room temperature, the DNA was pelleted by centrifugation for 15 min at 14 000*g. The pellet was washed with 500 µL 70% ethanol and centrifuged for 15 min at 13 000*g. The pellet was air-dried and resuspended in 50 µL H_2O DEPC. To visualize positive clones, 2 µL of DNA were linearized analogously to Table 21 and loaded onto a 1% agarose gel. Finally, the DNA was sequenced using a specific B2 outside primer (Table 17). We found that in these pups, the transgene was located in chromosome 19 and the integration was only on one site.

Table 19: Ligase reaction to ligate DNA into T-vector

Ligase Reaction	
DNA	2µL
Ligase buffer 10x	1µL
Ligase T4	1µL
H2O	5µL
Vector (easy T Vector)	1µL
Total reaction volume	10µL

Table 20: Ingredients of solutions to isolate DNA from small bacterial cultures

	Ingredients	**End concentration**
Solution A	Glucose	50 mM
	EDTA pH 8	10 mM
	Tris pH 8	25 mM
	RNase (4 mg/mL)	1%
Solution B	NaOH	0.2M
	SDS	0.1%
Solution C	Potassium acetate pH 5.5	3.1 M

Table 21: Digestion of T-vector

Linearization of vector pX330	**Volume [µL]**
Ligation product	2
ecor 1	1
Cutsmart	2
ddH_2O DEPC	6

Time	**Temperature**
1 h	37 °C

4.3 Quantification of B1R and B2R mRNA expression

4.3.1 RNA isolation

The tissue samples removed from rats were snap frozen and then ground to a fine powder using a mortar and pestle in liquid nitrogen. Then, some of the powder was transferred into FastPrep tubes containing 5 bead sand stored at -80 °C until RNA isolation. On the day of the RNA isolation, samples were homogenized with 1 mL of TriFast or TRIzol Reagent twice for 40 sec at speed level 4 using the FastPrep™-24 instruments with a 5 min resting period in between. Thereafter, the manufacturer's instructions for TRIzol or TriFast were followed. On the day of the RNA isolation, samples were thawed and the manufacturer's instructions for TRIzol or TriFast were followed. The RNA concentration and purity were assessed using a Nanodrop 1000 spectrophotometer and it was stored at -80 °C until use.

4.3.2 Complementary DNA synthesis

First, the remaining DNA in the RNA sample was degraded to avoid amplifying genomic DNA that would infer a higher gene expression of the respective gene. Therefore, 3µg of RNA were treated with DNase digestion mix (Table 22). After heat-inactivating the enzyme, the mix was quickly chilled on ice to avoid re-formation of RNA secondary structures. Secondly, 1 µg of RNA was reverse transcribed into complementary DNA (cDNA) according to Table 23. The cDNA samples were stored at -20 °C until use.

Table 22: Protocol for DNA digestion of RNA samples

Ingredient	Volume [µL]
10X buffer	1,5
Rnasin	1
DNase I	1
RNA	3µg
ddH_2O	ad 15 µL

DNA digestion steps	Time	Temperature
DNA digestion	20 min	37°C
Inactivation of DNase enzyme activity	10 min	75°C
		directly on ice

Table 23: Protocol for reverse transcription of RNA samples

Ingredient (Promega)	Volume [µL]
5x M-MLV Buffer (Promega)	4
Random primers	1
dNTP (5mM)	2.5
RNase inhibitor	0,5
M-MLV (200U, Promega)	0,8
RNA	1 µg
ddH_2O	ad 20 µL

RT steps	Time	Temperature
Priming	10 min	26°C
Transcription	60 min	37°C
Enzyme inactivation	10 min	75°C
Conservation	Infinite	4°C

4.3.3 Quantitative Real-Time PCR (qRT-PCR)

Gene expression on the RNA level of cells or tissues was determined using qRT-PCR. The quantification was performed using a 384-well plate format in the qRT-PCR 7900HT system or the Quant Studio 5 system with GoTaq® qPCR Master Mix, SyberGreen® Dye and CXR as reference dyes. The qRT-PCR program is shown in Table 24 and the forward and reverse primer pairs used are listed in Table 25. A melting curve was carried out at the end of the qRT-PCR program as a quality control for the amplicons. Reactions with signs of unspecific fragments or primer dimers were excluded. All samples were quantified in duplicates. SDS2.4.1 or QuantStudio™ Design and Analysis Software v1.3.1 (both Applied Biosystems, Foster City, USA) were used for analysis. The cycle threshold was set manually in the exponential phase of amplification. The expression of the gene of interest was normalized to the expression of the housekeeping gene TATA-binding protein (Tbp). Relative gene expression between groups was calculated using the $2^{-\Delta\Delta Ct}$ method that results in the fold change of gene expression compared to the housekeeping gene.

Table 24: Protocol for qRT-PCR with GoTaq enzyme

Stock conc.	qRT-PCR steps	Volume [µL]
	cDNA (1: 50)	9
2x	GoTaq® master mix	10
5 µM	Primer Forward	0.4
5 µM	Primer Reverse	0.4
100x	CXR reference dye	0.2

Steps	Time	Temperature	Cycles
Initial denaturation	10 min	95°C	1x
Denaturation	15 sec	95°C	40x
Annealing and elongation	60 sec	60°C	
Dissociation curve		60-99-60°C	

4.3.4 Primers applied for Real-Time PCR

Table 25: Primers applied for Real-Time PCR

Primers name	Sequence (5' to 3')
TRPV1-for	5'-ATGTGGCTTCCATGGTGTTCTC
TRPV1-rev	5'-GAACATAAACCGCCACAGGTCTC
TRPV3-for	5'-TTATCTGGGCCATGTGCATCTC
TRPV3-rev	5'-GGCATCTGACAGGATGGACTGA
TRPV4-for	5'-GCTGACAGGGACCTACAGCATC
TRPV4-rev	5'-CTCTGGTCCTCGTTACAGACCTTC
TRPC1-for	5'-TTCTGTGAACAGCAAAGCAA
TRPC1-rev	5'-CATGCGCTAAGGAGAAGATG
TRPC3-for	5'-ATGCAGTGCAAAGACTTCGT
TRPC3-rev	5'-ATTCAGAATGGCTTCCACCT
TRPC4-for	5'-TGCAGATATCTCTGGGAAGG
TRPC4-rev	5'-AGCACGAGGCAGTAGATGAA
TRPC5-for	5'-AACCCTTCAGTCGCTCTTCT
TRPC5-rev	5'-CGTAGCTCCCACAAACTCAG
TRPC5-for	5'-AGAATGCAGCCAGAAACAAA
TRPC5-rev	5'-AGCCCTTTGTAGGCATTGAT
Mouse B1R-for	5'-ATGCAGTGCAAAGACTTCGT
Mouse B1R-rev	5'-ATTCAGAATGGCTTCCACCT
Rat B1R-for	5'-AGAATGCAGCCAGAAACAAA
Rat B1R-rev	5'-AGCCCTTTGTAGGCATTGAT
Rat B2R-for	5'-AACCCTTCAGTCGCTCTTCT
Rat B2R-rev	5'-CGTAGCTCCCACAAACTCAG
TBP-for	5'-AGAATGCAGCCAGAAACAAA
TBP-rev	5'-AGCCCTTTGTAGGCATTGAT
EndogenousB2R-for	5'-AGAATGCAGCCAGAAACAAA
EndogenousB2R-rev	5'-AGCCCTTTGTAGGCATTGAT
Total B2R-for	5'-ATGCAGTGCAAAGACTTCGT
Total B2R-rev	5'-ATTCAGAATGGCTTCCACCT
TBP-for	5'-GGGCATTATTTGTGCACTGAGA
TBP-rev	5'-TAGCAGCACGGTATGAGCAACT

4.4 Quantification of protein expression

4.4.1 Protein isolation

Tissue powder samples were collected in FastPrep tubes containing 5 beads and stored at -80 °C until protein isolation. On the day of the protein isolation, samples were homogenized with an adequate volume of RIPA buffer containing protease and phosphatase inhibitors for 40 sec several

times at speed level 4 with a 5 min resting period in between, in which the samples were stored on ice using the FastPrep-24 instrument. Sample homogenates were sonicated for 30 sec to disrupt double membranes and incubated at 4°C or on ice for 30 min with intermittent mixing. Cell debris was removed by centrifugation at 13 000*g for 10 min at 4°C. The supernatant with the dissolved proteins was transferred to a new 1.5 mL tube and stored at -20°C until usage.

4.4.2 Determination/estimation of protein concentration

The concentration of proteins was determined using a bicinchoninic acid kit. Protein bonds reduce Cu^{2++} to Cu^{+}, which reacts with bicinchoninic acid. This complex has a purple colour; therefore, the colour intensity correlates to the amount of protein in the reaction. Samples were measured in pure duplicates and in a 1: 10 dilution. A standard series of bovine serum albumin (BSA) solved in RIPA buffer was used as reference. A 7-fold 1: 2 dilution series was made starting from 1 mg/mL BSA downwards. In a 96-well plate, 5 µL of sample or standard and 100 µL of working solution containing bicinchoninic acid and 4% (w/v) copper sulphate at a ratio of 50: 1 were mixed. After 30 min at 37 °C, the colorimetric biochemical reaction was quantified at 562 nm using a microplate reader. The protein concentration was calculated using Excel 2013 (Microsoft, Redmond, USA).

4.4.3 SDS-polyacrylamide gel electrophoresis (SDS-PAGE)

SDS-PAGE was performed to separate proteins according to their size. Denaturing gels with 1 mm thickness were cast using the Bio-Rad electrophoresis system. Separating gels containing 8-15% acrylamide was cast and overlaid with isopropanol to straighten the separating gel-stacking gel interface. After polymerization, the isopropanol was removed with Whatman paper and the stacking gel containing 5% acrylamide and an appropriate comb were added. The polymerized gels were stored in a humid bag at 4 °C overnight (Table 26).

Table 26: Ingredients for separating and stacking gels

	8% separating gel	**10% separating gel**	**15% separating gel**	**5% stacking gel**
ddH_2O	9.36 mL	7.9 mL	6.54 mL	5.5mL
1.5 M Tris pH 8.8	5.0 mL	5.0 mL	5.0 mL	
1 M Tris pH 6.8				1.0mL
SDS 10%	200 µL	200 µL	200 µL	80 µL
Acrylamide	5.44 mL	6.8 mL	8.16 mL	1.3 mL
APS	100 µL	100 µL	100 µL	50 µL
Temed	20 µL	20 µL	20 µL	20 µL

Table 27: Ingredients for Lysis, SDS-PAGE and Western blot buffers

Electrophoresis buffer	
Glycine	196 mM
Tris-HCl (pH8.4)	20 mM
SDS	0.1%

Transfer buffer	
Glycine	200 mM
Tris	20 mM
Methanol	20%

TBST buffer	
NaCl	150 mM
Tris	50 mM
Tween-20	0.05%

RIPA buffer
sodium chloride 150 mM Triton X-100 1.0% sodium deoxycholate 0.5% SDS0.1% Tris, pH 8.0 50 mM

Protein samples were adjusted to an equal amount of 10-50 µg protein with ddH_2O and one part of 4x Roti-load reducing loading buffer in a total volume of 20-30 µL. Samples were denatured at 95 °C for 5 min. Gels were immersed in electrophoresis buffer (Table 27) and 16 µL of the protein samples and 5 µL of a molecular weight marker - either Precision plus protein™ standards all blue or Odyssey® two-colour protein molecular weight marker - were loaded onto the gel. Electrophoresis was performed first at 80 mV until the proteins migrated from the stacking into the separating gel, followed by 100-110 mV until the dye front migrated out of the gel.

4.4.4 Western blotting

Electrophoretically separated proteins were transferred from the SDS-PAGE gel onto a polyvinylidene difluoride (PVDF) membrane using a wet transfer system from Bio-Rad. The membrane was activated for 5 min with methanol. The stacking gel was removed and the separating gel was placed in a "sandwich" next to the activated membrane in between one sponge and two Whatman papers on each side. Air bubbles between the gel and the membrane were removed carefully. The blotting was performed in ice-cold transfer buffer at 4 °C. The blotted membrane was blocked with Odyssey blocking buffer for a minimum of 30 min at room temperature. The primary antibody (Table 28) was diluted in a mix of 2.5 mL Tris-buffered saline containing 0.5% Tween-20 (TBST) and 2.5 mL of Odyssey blocking buffer, and incubated at 4 °C overnight under constant rolling. Unbound primary antibody was removed with 3-4 washes of 10 min each with 20 mL TBST. The membrane was incubated with Odyssey IR Dye secondary antibody, diluted 1: 10,000 in TBST, for 2 h at room temperature under constant rolling. After 3-4 washes of 10 min each with 20 mL TBST, the membrane was scanned using an Odyssey infrared imaging system. The signals were analysed using Image Studio Lite software version 5.2.5 (2015, LI-COR Bioscience, Lincoln, USA). The same membrane was incubated with anti-glyceraldehyde-3-phosphate dehydrogenase (Gapdh) antibody (Table 28) to normalize the signal on the membrane. Alternatively, the whole protein staining solution Revert was applied directly after blotting and before blocking according to the manufacturer's instructions.

4.4.5 Antibodies applied for western blotting

Table 28: Primary and secondary antibodies

Protein	Antibody	Host	Method	Dilution	Company
Gapdh (secondary)	Gapdh 14C10, mAb #2118	rabbit	WB	1: 1000	Cell Signaling Technology (Danvers, USA)
CPM (primary)	Anti-CPM #HPA002657	rabbit	WB	1: 1000	Sigma-Aldrich (St. Louis, USA)

4.4.6 Immunohistochemistry

Organs were fixed in 4% PFA for several days to ensure thorough fixation. Then, samples were washed twice in PBS (Table 29) and dehydrated in an alcohol series (2x 70% ethanol 30 min, 2x 80% ethanol 30 min, 2 x 96% ethanol 60 min, 2x isopropyl 60 min, 2x xylene 90 min). Organs were infiltrated with paraffin twice for 90 min and embedded in fresh paraffin. Then, the organs were cut with a rotary microtome, placed on a microscope slide and air-dried overnight at room temperature.

Paraffin sections were deparaffinized and rehydrated as follows: 3x xylene; 3x 100%, 1x 90%, 1x 80%, 1x 70%, 1x 60%, 1x 50%, 1x 40%, 1x 30% ethanol; and 2x ddH_2O, each for 5 min. Antigens were unmasked by boiling the sections in sodium citrate buffer (10 mM sodium citrate, 0.05% Tween-20, pH 6.0) for 20 min. Sections were washed twice in PBS for 5 min and blocked with 10% normal donkey serum/PBS for 10 min. The primary antibody diluted in PBS was incubated in a humid chamber overnight at 4 °C. The next day, sections were washed 3 times for 5 min with PBS. If two different antigens were stained, the second primary antibody was applied again for one night and washed 3 times for 5 min with PBS. The respective secondary antibodies diluted in PBS were applied separately in the dark at room temperature for 2 h each and washed 3 times for 5 min with PBS. Sections were mounted with nuclei staining 4, 6-diamidino-2-phenylindole (DAPI) in Vectashield mounting medium and covered with a cover slip.

Table 29: Ingredients of 10x phosphate-buffered saline (PBS)

	Ingredients	End concentration of 10x
10 x PBS pH 7.4	NaCl	137 mM
	KCl	2.7 mM
	Na_2HPO_4	10 mM
	KH_2PO_4	1.7 mM

4.5 Analysis of α and ß cells in pancreas with hematoxylin and eosin

Hematoxylin and eosin staining was used to quantify α and ß cells in pancreas. Sections were deparaffinized and rehydrated as described above (Chapter 3.4.6) and washed with tap water for 10 min. Nuclei were stained with hematoxylin for 5 min and washed with tap water for 3 times for 10 min each. Differentiation was achieved with a hydrochloric acid solution (0.11% HCl, 67.2% ethanol) for 3 sec. Sections were washed thoroughly with tap water, and an eosin solution was incubated for 5-10 sec. Sections were dehydrated in increasing alcohol series (briefly in 80%, 90%, 100% ethanol, then isopropyl, and finally xylene for 30 min), mounted with Eukitt mounting medium and covered with a cover slip. Pictures were obtained with the BZ-9000 light microscope.

4.6 In Situ mRNA detection using RNAscope method

In situ hybridization (ISH) was performed using the RNAscope technology to localize B2R mRNA in formalin fixed paraffin embedded tissues. 5 µm tissue sections mounted on super frost glass slides were deparaffinised with xylene, and rehydrated with a series of ethanol washes. Endogenous peroxidase was blocked by incubating the sections with H2O2. The sections were then heated in antigen retrieval buffer (RNAscope Target Retrieval, Ref. #322001, ACD) in a steamer and digested by proteinase solution at 40°C for 30 min (RNAscope H2O2 & Protease Plus Reagents, Ref. #322330, ACD). The sections were incubated with ISH target probe pairs at 40°C in a hybridization oven for 2 h. The forty ZZ-ISH probes targeting rat B2R RNA were designed and synthesized by Advanced Cell Diagnostics (ACD, Newark, USA) (Rn-Bdkrb2, Ref. #463571, Lot #191984). The sections were washed with buffer (RNAscope Washing Buffer, Ref. #320058, ACD). The signal was amplified using the pre-amplifier and amplifier conjugated to alkaline phosphatase and incubated with a Fast-Red substrate solution for 10 min at room temperature according to the instructions of the provider (RNAscope 2.5 HD Detection Reagent-RED, ACD). The sections were then counterstained with hematoxylin for 10 sec, air-dried, incubated in xylene for 30 minutes and coverslipped using xylene based mounting medium (EcoMount, Biocare Medical, Ref. #EM897L). On the next day, images were taken using an inverse Keyence bright light/Fluorescence microscope (Keyence BZ9000, Germany), and evaluated.

4.7 Carboxypeptidase M activity assay

CPM activity was determined using the substrate Dansyl-Ala-Arg-OH (100 µM) in Tris-HCl50 mM, pH 7.4, NaCl 50 mM buffer and MERGETPA (MGTA, 100 µM) as specific inhibitor during the incubation. After 30 minutes of incubation at 37°C, the reaction was stopped using citric acid (1 M), pH 3.1 (Table 30).

Table 30: Protocol of CPM enzyme assay

Buffer (0.2 Mm HEPES)	**rhCPM (0.04 µg/mL)**	**MGTA (100 µM)**	**water (µL)**	**Incubation time (on ice)**	**Dansyl (1mM)**	**Incubation time (37c)**	**Citric acid (stop solution,1 M)**
125 µL	50 µL	Ø	25 µL	10 min	50 µL	3h	150 µL
125 µL	50 µL	25 µL	Ø	10 min	50 µL	3h	150 µL
125 µL	Ø	25 µL	25 µL	10 min	50 µL	3h	150 µL
125 µL	Ø	Ø	75 µL	10 min	50 µL	3h	150 µL
125 µL	50 µL	Ø	75 µL + 25 µL	10 min	Ø	3h	150 µL

Chloroform (500 µl) was added to each reaction tube, which was mixed vigorously for 15 sec to extract the Dansyl-Ala-OH product. Centrifugation at 800 g for 10 min separated the solution in the tubes into two phases. The fluorescence in the chloroform layer (bottom layer) was measured relative to a chloroform blank at 340 nm excitation wavelength and 495 nm emission wavelengths. The peptidase activity of CPM was also tested at pH values ranging from 5.0 to 9.0 (Table 30).

4.8 Flow Cytometry

4.8.1 Preparation of cells for Flow Cytometry

Peripheral blood (~ 1ml) was incubated 1-2x with 2 ml 1x BD™ Pharm Lyse™ reagent for 5 min at RT in order to lyse the red blood cells. The reaction was stopped by addition of an equal amount of FACS buffer (5% FBS in PBS) and centrifuged for 2 min at 1200 rpm. The supernatant was discarded, and cells were resuspended in blocking buffer (rat: rat serum 1: 100 in FACS buffer; mouse: CD16/CD32 1: 1000 in FACS buffer) and kept at 4°C for 15 min. Both femur and tibia were dissected and carefully cleaned of adherent tissue. The tip of each bone was removed with scissors and the bones were flushed with 2 ml PBS by using a 23 G needle and a 1 ml syringe. Red blood cells were lysed as described above and cell suspensions were filtered using 40 µm nylon filters, followed by blocking at RT for 15 min. Splenic tissue was homogenized using scissors and cells were resuspended in 2 ml PBS and filtered using 100 µm nylon filters. Red blood cell lysis and blocking was performed as described above.

4.8.2 Antibody staining and measurement

Upon blocking, cells were centrifuged for 2 min at 1200 rpm, resuspended with fluorescence-labeled antibody dilution (usually 1: 500 - 1: 4000 in FACS buffer), and incubated at 4°C for 30 min. The samples were centrifuged for 2 min at 1200 rpm, washed twice with FACS buffer, and fixed by incubation with 2% PFA (diluted in FACS buffer) for 5 min at RT. After another centrifugation step, cells were resuspended in FACS buffer and stored at 4°C until use. For flow cytometry, 250 µl of PBS were added and between 50,000 - 600,000 cells were analysed per sample using the BD™ LSR II or LSR Fortessa™ benchtop cell analyzers as well as the BD FACSDiva™ software. Data were analysed with the FlowJo software (Tree Star Inc., OR, USA).

4.9 Isometric tension recording experiments

Rats were sacrificed in deep anesthesia using isoflurane and the thoracic aorta was carefully removed. The aorta was cleaned of excess fat and connective tissue, cut into 2–3mm long rings and placed in cold physiological salt solution (PSS) containing (mM) 119 NaCl, 4.7 KCl, 1.2 KH_2PO_4, 25 $NaHCO_3$, 1.2 Mg_2SO_4, 11.1 glucose and 1.6 $CaCl_2$, with a pH of 7.4. The rings were mounted in an organ bath chamber (Hugo Sachs Elektronik, Freiburg, Germany) filled with 20 ml PSS gassed with 95% O_2 and 5% CO_2, and maintained at 37 °C. The rings were gradually stretched to 1 g and allowed to equilibrate for 60 min until a stable resting tension was acquired. To evaluate maximal contractility, each aortic ring was then exposed to a high K^+ (60 mmol/L) solution. After ca. 10-15 min, when the high K^+-induced contraction reached a plateau, the rings were washed with PSS and allowed to re-equilibrate for 30 min. Afterwards, the rings were contracted with 10^{-6} M phenylephrine (PE), and after stabilization (10–15 min), endothelium integrity and functionality was assessed by the cumulative addition of acetylcholine (10^{-9} - 10^{-6} M). The vascular response was expressed as a percentage of the 'plateau' constriction evoked by PE (10^{-6}M). The software MYODAQ 2.01M610+ (Danish Myo Technology, Denmark) was used for data acquisition and display.

5 Animal experiments

5.1 Animal husbandry

All rat lines were kept in pathogen-free conditions in the MDC animal facility according to the German Animal Protection Law. Rats were housed in ventilated cages at a temperature of 21-23 ˚C, with a light/ dark cycle of 12 h each. Chow (0.25% sodium) and water were provided *ad libitum.* The genotype was determined in DNA isolated from either toe nail (p5-9) or ear (after p14), or, at the end of an animal experiment, in DNA from the tip of the tail for verification of the genotype. Animal experiments were reviewed and approved by the LaGeSo (G0124/17, Berlin, Germany).

5.1.1 Endothelial cell-specific kinin B1 receptor transgenic rats

B1R-TGR overexpressing B1 receptor in endothelial cells were already generated and used in previous studies by our group [215]. Briefly, endothelium-specific expression was achieved using the mouse Tie2 promoter/enhancer (gift from Dr. T. Sato, University of Texas Southwestern Medical Center, Dallas, TX, USA[13]). A 2.1-kb Tie2 promoter fragment was subcloned into Bluescript SK+ (Promega, Madison, WI, USA) flanking a 1.2-kb mouse B1R coding region, a 0.8-kb SV40 polyadenylation signal sequence, and an 8.6-kb partial XbaI fragment containing the Tie2 enhancer sequence. The resulting 12.7-kb transgene fragment (Figure 15) was microinjected into the pronuclei of fertilized zygotes from Sprague Dawley (SD) rats.

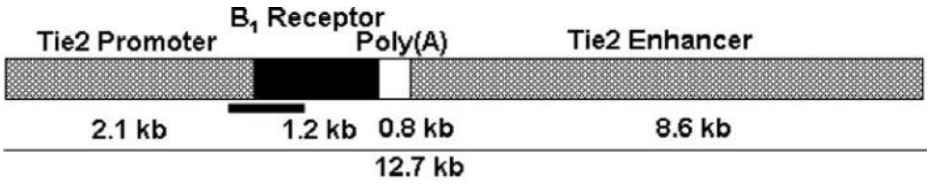

Figure 15: DNA construct used for the generation of transgenic rats with endothelial kinin B1 receptor overexpression.

5.1.2 Generation of endothelial cell-specific kinin B2 receptor transgenic rats

The sequences of the endothelium-specific promoter of the mouse VE-Cadherin (VECDH) gene (available in the EMBL databank under accession number Y10887) and rat B2R cDNA were inserted in a pcDNA3.1 (-) vector (Invitrogen, Carlsbad, CA) to create the construct to be injected in pronuclei of rat zygotes. For this purpose, specific primers (BioTez, Berlin-Buch GmbH) were designed to amplify 2,800 bp of the mouse VECDH gene promoter region with the addition of restriction site sequences for the Mlu I and Xba I enzymes, VECDH5 (5'-TCGTACGCGTGAGCTCCTCAATGTG3') and VEDCH3 (5'GATGTCTAGAGCACAGTTGATTGCCTCAG-3'). The purified construct (Figure 16) was microinjected in the zygote's pronucleus and the surviving fertilized oocytes were transferred on the same day to the foster mothers by Elena Popova [216]. The first four litters yielded a total of 34 pups. They were genotyped, but none of the animals was identified as a founder. Later, another 11 pups were genotyped and one was identified as a male founder (Figure 17 A). Later, a new female founder was identified between 18 new pups (Figure 17 B).

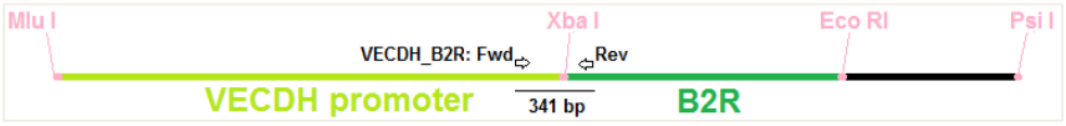

Figure 16: Construct for B2R-TGR rats and representation of the primers designed to recognize the transgene in the DNA of the rats.

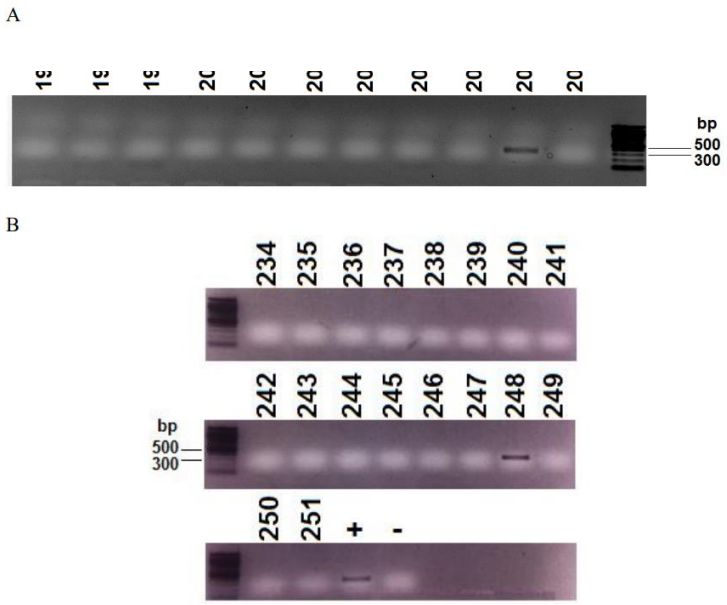

Figure 17: Transgene identification in the founders. The genotyping was performed using DNA extracted from tail biopsies. A: The first founder (206) is a male rat from a litter of 11 pups. B: The second founder (248) is a female rat from 18 pups. The positive control is indicated by "+" symbol, and the negative control by "- ". The identification number of each rat is according to our maternity records.

5.1.3 Generation of CPM knockout rat model

CPM-knockout (KO) rats were generated using CRISPR-Cas9 technology (Figure 18). For this purpose, the DNA for the gRNA sequence (AAAAGCACCGACTCGGTGCC) was synthesized as a double-stranded oligonucleotide by the company BIOTEZ, phosphorylated by T4 polynucleotide kinase, and inserted into the plasmid pX330 via the BbsI site. PCR-amplification by T7sgRNA CPM (TAATACGACTCACTATAGGTTCCATCTCTAGGACATGGA) and gRNA31 (AAAAGCACCGACTCGGTGCC) primers, followed by transcription of the PCR product with T7 polymerase, produced the gRNA which was co-injected with Cas9 mRNA into pronuclei of Sprague-Dawley rat zygotes by Elena Popova. The injected embryos were transferred into foster mothers and the offspring was analysed for mutations by PCR using the primers CPM5 and CPM3, followed by sequencing of the PCR products with CPM3. The sequence analysis of two animals with mutations revealed a 6 base pair deletion including the ATG start codon and a T insertion in the coding sequence. Both should be functional knockouts. The lines L-38 and L-76, respectively, were both bred to homozygosity (Figure 19).

gtgagacgggtcgtgcggaagggtgctgctgcggggacacgggcgggctgcggggctccg
gtgggaccatctttacctggctcctcagaggagggagcgtggagctcaggtgttccggag
ggcggagaggactccgggctggcggtacccgcgcttccccgggcggtcctcaactgctca
ctccttctcttccatctctag
GACATGGACGGCGCGCGCTCTGTGGCTGGGGCTTCTGCTGCCCGTGGTGGCCGCCTTGGAT
TTCCGATACCACCACCAGGAAGGGATGGAGGCTTTCCTAAAGAGCGTGGCTCAGAACTAC
AGTTCGATCACGCACTTGCACAGCATCGGGAAATCGGTGAGAG
gtaggtggcctcccgcgcacgtccccaaccctcaacccacgtttaaaagttaagttgaat
ggcactgtctggtcctctgttggtgaggctccccggacgcgctcctcgcaggtaaagcat

Figure 18: Mutations in the rat CPM gene introduced by CRISPR/Cas9. The Exon 2 of the CPM gene is shown in capital letters and introns are shown in lower case letters, and red letters mark the two genotyping primers, CPM5 and CPM3. The gRNA sequence is underlined and the PAM is in italic. Blue and green letters mark the deletion in one rat line (38) and the insertion in the other line (76), respectively.

Figure 19: Lung cDNA of homozygous CPM-KO rats from both lines was amplified by CPM5 and CPM3 primers. The PCR products were sent to sequence analyses with CPM3. The DNA from line 38 showed the expected 6 bp deletion and from line 76 the single T insertion.

5.2 Measurements of blood pressure in conscious rats

Male rats (12–16 weeks) were equipped with catheters in the femoral artery and vein, under chloral hydrate (400mg/kg) anesthesia. After a 48h recovery period, the arterial catheter was connected to a pressure transducer (PowerLab, ADI Instruments Co., Colorado Springs, CO, USA) and mean arterial pressure and heart rate were recorded under basal conditions as well as after intravenous (i.v.) administration of increasing doses (0.01–1µg/kg) of BK and des-Arg^9-BK in B2R and B1R-TGR, respectively and also in SD rats.

5.3 Angioedema induction and vascular permeability assays

5.3.1 Short term treatment to induce angioedema using Mustard oil

Male B2R-TGR, edemic B2R-TGR and Sprague Dawley (SD) rats (12 weeks) were used in each experiment. All angioedema induction tests were performed in conscious animals. Angioedema induction was performed with local irritants able to induce plasma leakage and local inflammation such as mustard oil, as previously described [207]. Briefly, Evans blue dye (EB, 30mg/ml in 100 µl PBS) was injected into the tail vein of 12-week-old rats. After 1 and 15 minutes of EB injection, mustard oil diluted to 5% in mineral oil was applied to the dorsal surface of the right ear and tissue samples from ear, feet, tongue, larynx, duodenum, and lung were dissected and the dye extracted and measured as described above. Pieces of organs were collected, weighed and incubated in formamide for 48 h at 55°C to extract the dye. EB extravasation was measured by spectrophotometry at 620 nm and quantified according to a standard curve.

5.3.2 Hoe140 treatment in B2R-TGR and spontaneously edemic TGR rats

In this experiment, we considered four groups of rats (male, 12-16 weeks old): group 1, B2R-TGR (control group, n=3); group 2, B2R-TGR treated with Hoe140 (n=4); group 3, EdemicB2R-TGR (control group, n=5); and group 4, EdemicB2R-TGR treated with Hoe140 injection (n=5). Rats from groups 2 and 4 were treated with Hoe140 (10µg/kg) intravenously (i.v. lateral tail vein), and groups 1 and 3 were treated with vehicle (physiological saline, i.v.). 24h after the treatment, vascular permeability was analysed in all four groups 30 min after EB tail vein injections. One hour after the EB treatment, rats were sacrificed and the organs were collected for the analysis of extravasations. Pieces of organs were weighed and incubated in 1 ml formamide for 48 h at 55°C

to extract the dye. EB was quantified by measuring the optical density of the formamide extract at 620 nm absorbance and was compared with the standard curve of EB (0.005 μg to 3000 μg/100 μL) diluted in formamide. Extravasations are expressed as mg of EB/g tissue.

5.3.3 Chronic enalapril treatment to induce angioedema

In this experiment male rats (12-16 weeks) were divided into four groups: group 1, B2R-TGR (n=6); group 2, B2R-TGR received enalapril in drinking water for 30 days (1mg/KG/BW) (n=8); group 3, SD rats (n=6); and group 4, SD rats also received enalapril in drinking water for 30 days (1mg/kg/BW) (n=6). The daily drinking water amount and every week body weight were measured and the dose of enalapril was adjusted accordingly. At the end of the treatment period, vascular permeability was analysed 30 min after Evans blue (EB) tail vein injections (30 mg/kg body-weight). Rats were sacrificed and organs collected for the extravasation analyses as described above.

5.4 Statistics

All data were subjected to statistical analysis using GraphPad Prism 5 or 6 software (San Diego, CA, USA). Results in this study are presented as mean ± SEM (standard error of mean). The Student's t-test was applied for comparisons between independent pairs of means. Differences between two groups with a p-value of <0.05 were considered to be statistically significant. The following categorization applies to all displayed graphs in this study: * $p < 0.05$; ** $p < 0.01$; *** $p < 0.001$; **** $p < 0.0001$; and applies in the same way for all other symbols.

6 Results

6.1 Transgenic rats overexpressing bradykinin B2 receptors in endothelial cells (VECDHB2)

Two lines of transgenic rats overexpressing kinin B2 receptor (TGR (VECDHB2); B2R-TGR) were generated; L-11248 and L-11206 (see 4. Animals). In L-11248, we observed that in some litters all pups were positive for the transgene, although they were from heterozygous transgenic and non-transgenic parents. We were expecting 50% transgenic and 50% non-transgenic littermates. This unexpected phenomenon could be explained by the possibility that this line may have more than one transgene integrated into more than one of their chromosomes due to the random nature of an integration event. To clarify this, we mapped the B2R transgene locations. We used the inverse PCR method. Genomic DNA containing the inserted transgene from 20 transgenic rats was digested by a restriction enzyme (BstY1) which generates a restriction cut within the transgene as well as within the neighboring genomic DNA. This transgene-genomic DNA fragment was then ligated back to itself to form a circular DNA structure using ligase (T4 Ligase). PCR was performed using selected primers (Table 17) which were oriented in the reverse direction. PCR products were cloned using T-vector. In order to extract plasmid DNA from bacteria, the "mini prep" technique was utilized, and finally the DNA was sequenced using specific primers (Table 17). We found that in these pups the transgene was located in chromosome 19 and the integration was only on one site (Figure 20).

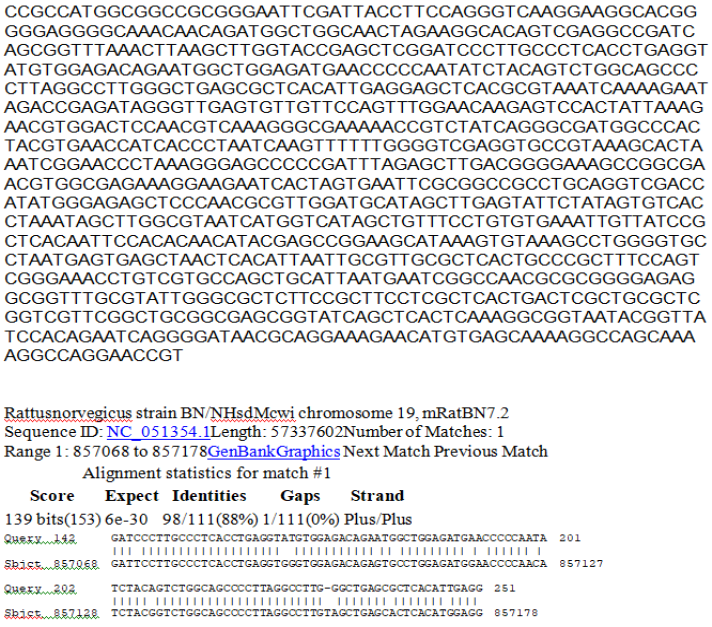

Figure 20: Transgene flanking sequence in B2R-TGR line 11248 and comparison with the rat genomic DNA (chromosome 19).

6.1.1 Verification of B2 receptor expression in different organs at the level of mRNA

We had two lines for the B2R-TGR, as mentioned above. The expression levels of mouse and rat B2R were determined by quantitative real-time PCR (qPCR) in different tissues isolated from non-transgenic control SD and the two lines of B2R-TGR (L-11248 and L-11206). Transgene (mouse B2R) overexpression was determined by qPCR using primers targeting the endogenous (rat, 5' - AGGAGAAGTTGGTGGGCTAC -3', 5' -TCATCAGGGTGTCGACGAAA -3') and the total B2R expression (transgene + endogenous) (5' - GGTGCTGAGGAACAACGAGA -3', 5' - CCCAACACAGCACAAAGAGC -3'). The total B2R expression was significantly higher in all organs of L-11248 B2R-TGR tested when compared to non-transgenic SD rats, while the expression of endogenous B2R was slightly reduced or not affected (Figure 21). The expression levels were calculated related to TBP (TATA-binding protein) as housekeeping gene. However, L-11206 did not express the transgene at all in all organs tested, even though they were transgenic according to our genotyping data. Therefore, we only used the L-11248 rats for all further experiments.

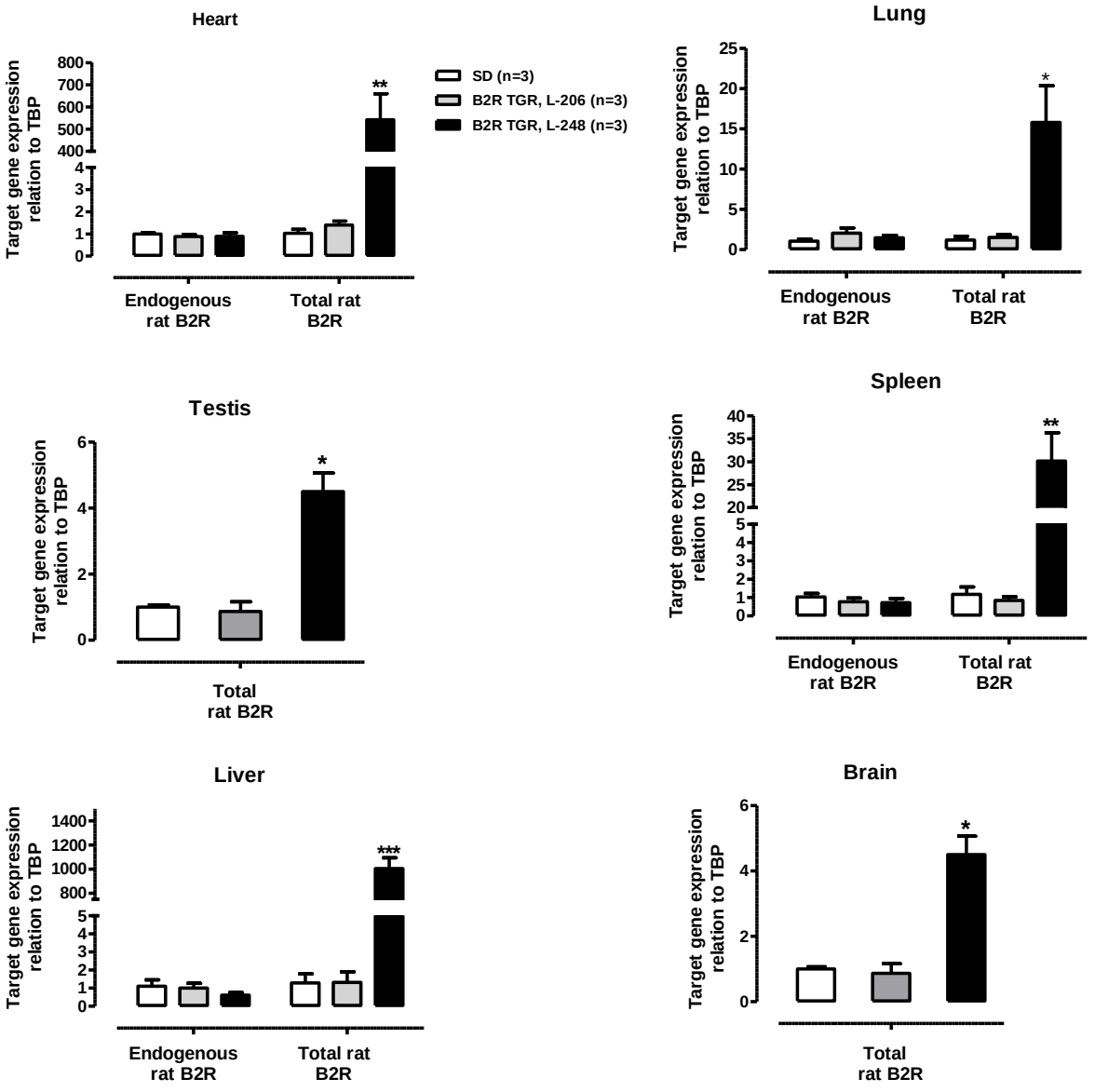

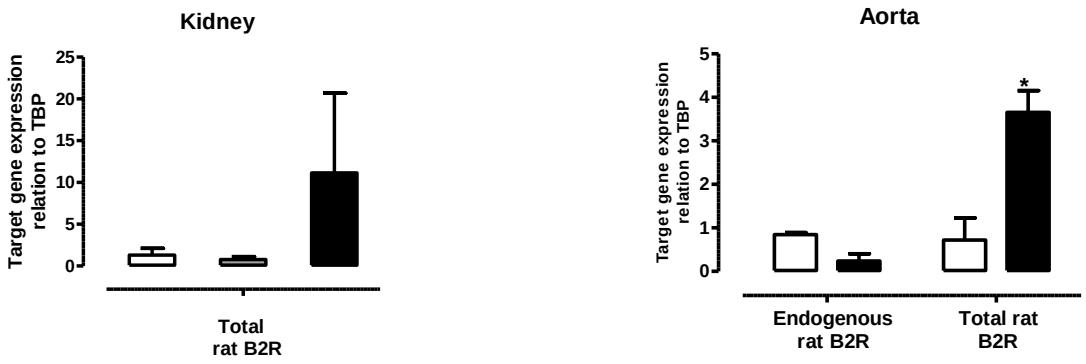

*Figure 21: Quantitative analysis of mRNA levels of rat endogenous and mouse transgene B2 receptor in two lines of B2R-TGR (L-11248 and L-11206). Data are expressed as mean ± SEM. *p<0.05; **p<0.01; ***p<0.001 when compared with other groups, unpaired t-test.*

6.1.2 Localization of B2R on endothelial cells in rat blood vessels using "RNAscope" in-situ hybridisation technique

The exclusive overexpression of B2R in endothelial cells of B2R-TGR of L-11248 was demonstrated using the RNAscope method. RNAscope enables the detection of almost any RNA with single-molecule sensitivity and high specificity in tissues. RNAscope was performed on sections of aorta and other tissues from age-matched adult B2R-TGR, and with SD rats as negative control. Figure 22 demonstrates significant overexpression of transgenic B2R only in the endothelium of aorta and neighbouring small vessels of B2R-TGR compared to SD controls (red dots).

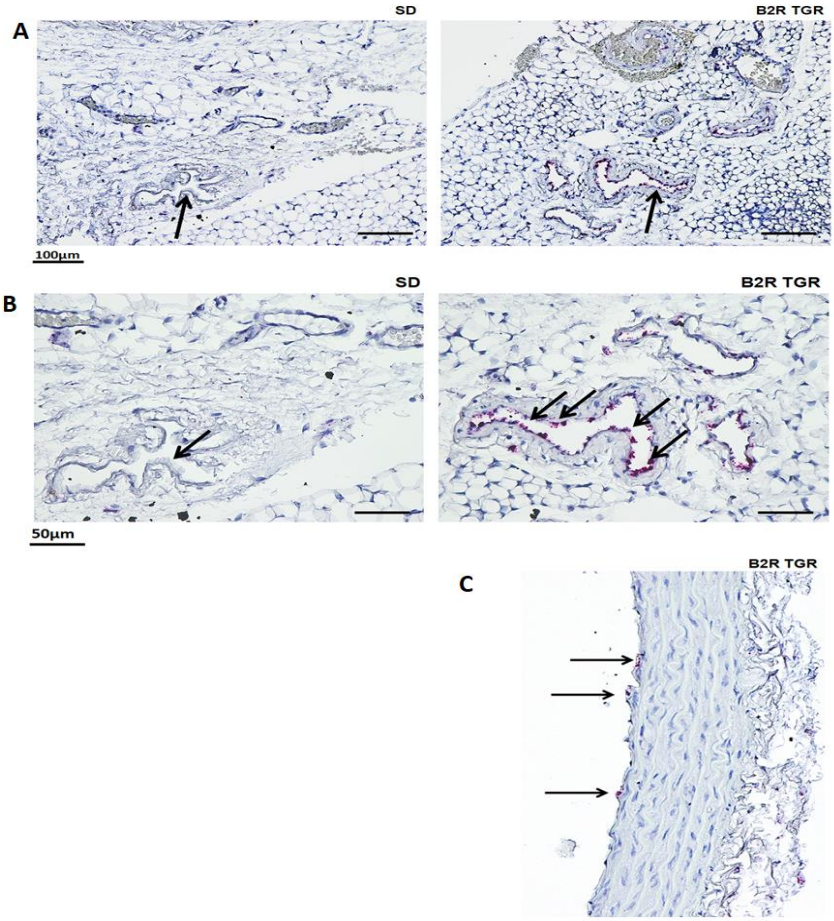

Figure 22: In-situ hybridization using the RNAscope technique. RNAscope was performed on formalin fixed paraffin-embedded sections of aorta from adult B2R-TGR and SD (control) rats. Arrows show B2R mRNA overexpression (red dots) on endothelial cell lining. A: small arteries located adjacent to aorta; B: higher magnification; and C: aorta in B2R-TGR.

6.2 Verification of B1 receptor expression in different organs at the level of mRNA

To determine the expression levels of the transgene in heart, lung and aorta, we performed quantitative real-time PCR (qPCR) in non-transgenic control SD rats and B1R transgenic rats (B1R-TGR, L-7065). Figure 23 shows the expression levels of mouse transgenic B1R as well as rat endogenous B1R and B2R. The expression levels were calculated related to TBP as housekeeping gene. The transgenic and endogenous B1R were significantly overexpressed in heart, lung and aorta of B1R-TGR compared to SD rats. Surprisingly, endogenous B2R was significantly overexpressed in B1R-TGR aorta compared to SD aorta.

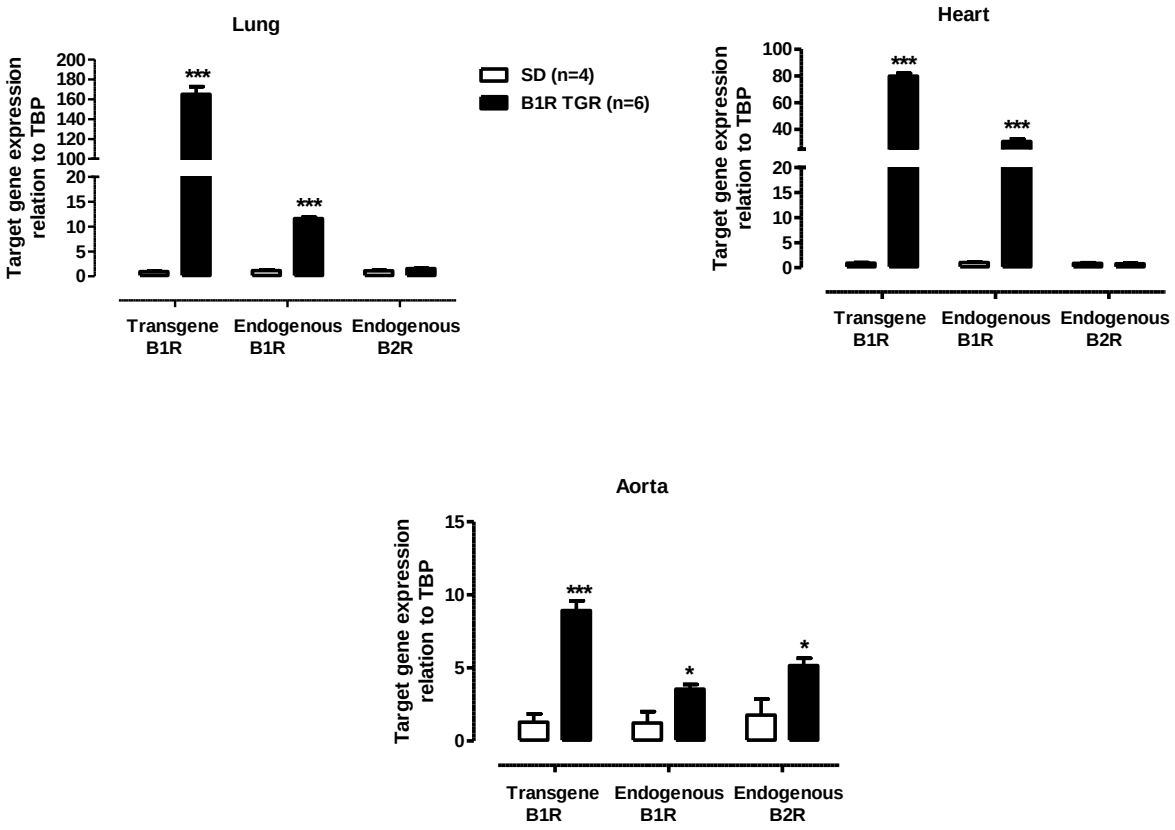

*Figure 23: Quantitative analysis of mRNA levels of mouse transgenic B1R, rat endogenous B1R and rat endogenous B2R in B1R-TGR. Data are expressed as mean ± SEM. *p<0.05; ***p<0.001 when compared with control groups, unpaired t-test.*

6.3 Blood pressure response to B1 and B2 receptor agonists in vivo

B1R- and B2R-TGR showed normal levels of mean arterial pressure vs. SD rats at baseline. BK and des-Arg^9-BK (0.01–1µg/kg) [215] produced a dose-dependent hypotension when administered (i.v.) to B2R- and B1R-TGR, respectively, whereas control SD rats did not respond to these treatments (Figure 24).

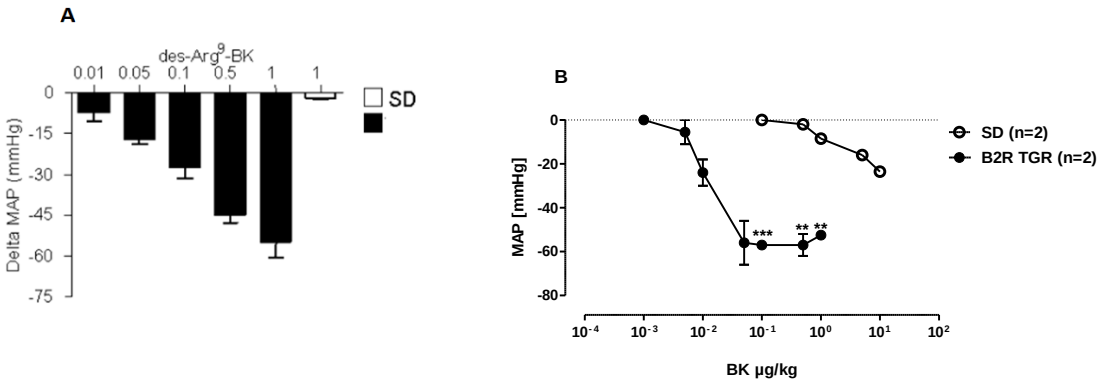

*Figure 24: Effect of kinin receptor agonists on mean arterial blood pressure. A: Hypotension dose-dependently induced by B1 receptor agonist (des-Arg^9-BK) administration (i.v.) to B1R-TGR and control rats (SD), respectively (modified from Merino et al., 2008 [208]). B: Hypotension dose-dependently induced by BK administration (i.v.) to B2R-TGR and control rats (SD). **p<0.01; ***p<0.001 when compared with control groups, unpaired t-test.*

6.4 Kinins induced endothelium-dependent vasorelaxation in B1R- and B2R-TGR

B1R and B2R agonists on the relaxant responses induced by des-Arg^9-BK or BK, respectively, were tested in aortic rings isolated from B1R- and B2R-TGR. The aortic rings were characterized in terms of the vascular reactivity through isometric relaxation and contraction recordings following application of the respective agonists, and in addition, pretreatment of tissue with the respective antagonists. To perform the experiments, we used the in vitro "organ bath" technique. The des-Arg^9-BK (specific B1R agonist) had no effect on the aortic rings isolated from control SD rats. In contrast, B1R-TGR aortic rings responded with a dose-dependent relaxation to des-Arg^9-BK. This effect was abolished by pre-incubation of aortic rings with R-715, a specific B1R antagonist (Figure 25 A and B). With BK, the B2R agonist induced a significant vasorelaxation in B2R-TGR aortic rings but not in control SD, and this effect was abolished by pre-incubation of aortic rings with Hoe140, the specific B2R antagonist (Figure 26 A and B).

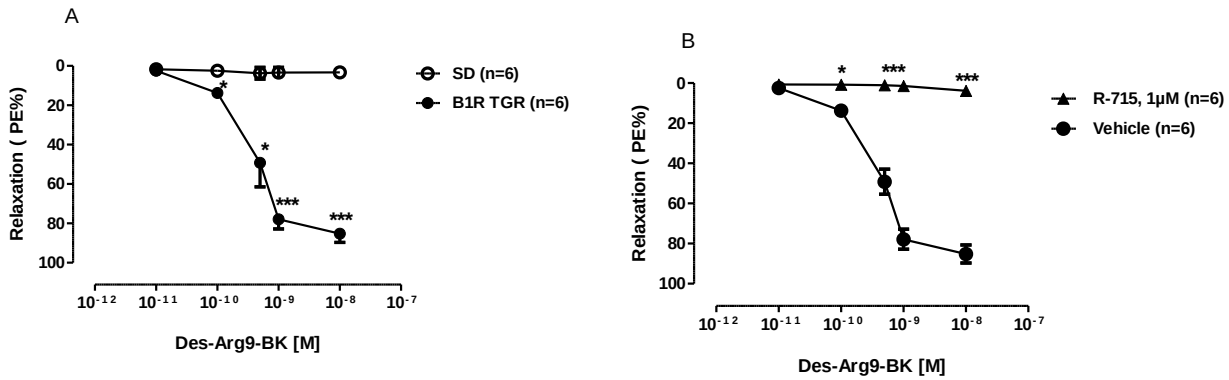

*Figure 25: Effect of: A) B1 receptor agonists (des-Arg^9-BK), and B) pre-incubation with B1 receptor antagonist (R-715, 1µM) on isolated aortic rings from B1R-TGR and SD rats. Data are expressed as mean ± SEM. *p<0.05; ***p<0.001 when compared with control groups, unpaired t-test.*

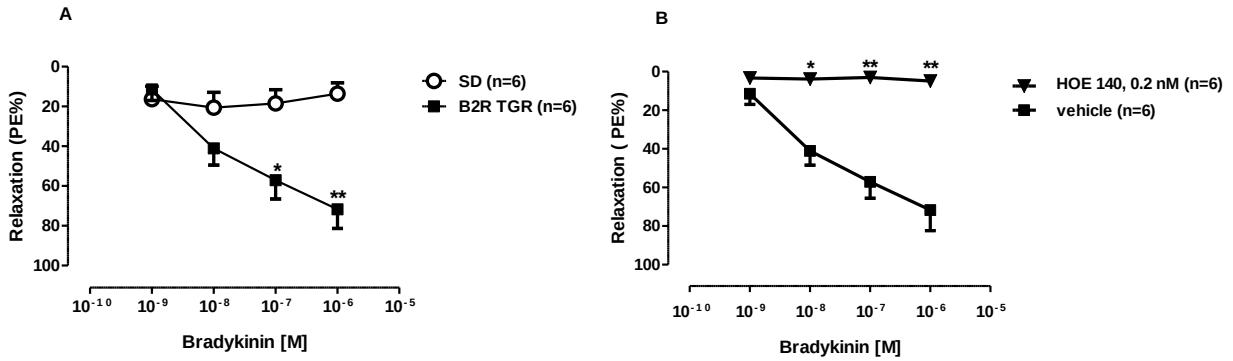

*Figure 26: Effect of: A) B2 receptor agonist (bradykinin), and B) antagonist (Hoe140, 0.2 nM) on isolated aortic rings from B2R-TGR and SD rats. Data are expressed as mean ± SEM. *p<0.05; **p<0.01, ***p<0.001 when compared with control groups, unpaired t-test.*

To investigate functional up-regulation of the other kinin receptor subtype in each transgenic model (vice versa), BK and des-Arg^9-BK were applied on B1R-TGR and B2R-TGR, respectively. Des-Arg^9-BK had no effect on the aortic rings isolated from B2R-TGR rats, whereas BK surprisingly showed a significant relaxant effect on the aortic rings from B1R-TGR rats - however, only at a higher concentration (Figure 27). To evaluate whether the enhanced relaxant responses induced by BK were due to the activation of B1R or B2R, the aortic rings isolated from B1R-TGR rats were pre-incubated with R-715 (B1R antagonist) or Hoe140 (B2R antagonist). As can be seen in Figure 28, R-715 completely abolished BK-induced relaxation; however, Hoe140 did not show any effect on BK relaxation response, indicating vasorelaxation through B1Rs. We then tested whether this was due to the degradation of BK to des-Arg^9-BK by the enzyme CPM in the tissue. Therefore, the aortic rings were pre-incubated with the CPM inhibitor MERGETPA. It did not affect the vasorelaxation induced by BK (Figure 28 C).

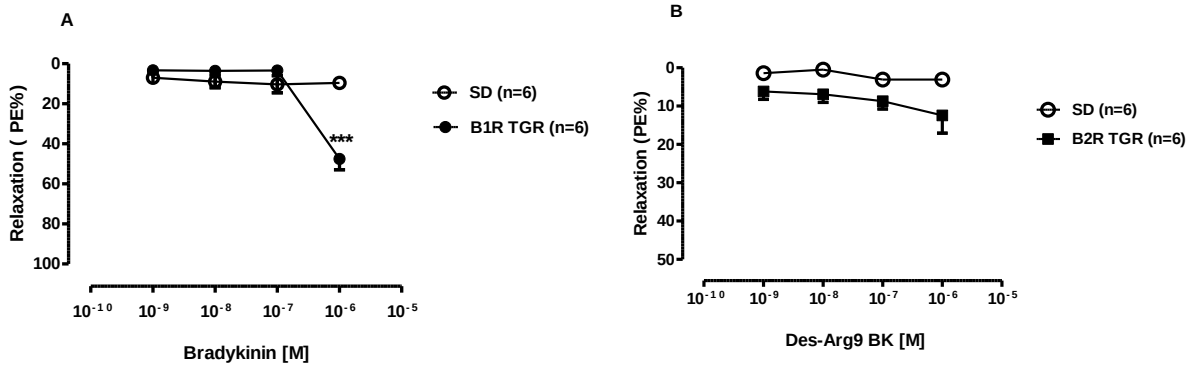

*Figure 27: Effect of: A) B2 receptor agonist (bradykinin) on isolated aortic rings from B1R-TGR, and B) B1R agonist (des-Arg^9-BK) on isolated aortic rings from B2R-TGR (B). Data are expressed as mean ± SEM. ***p<0.001 when compared with control groups, unpaired t-test.*

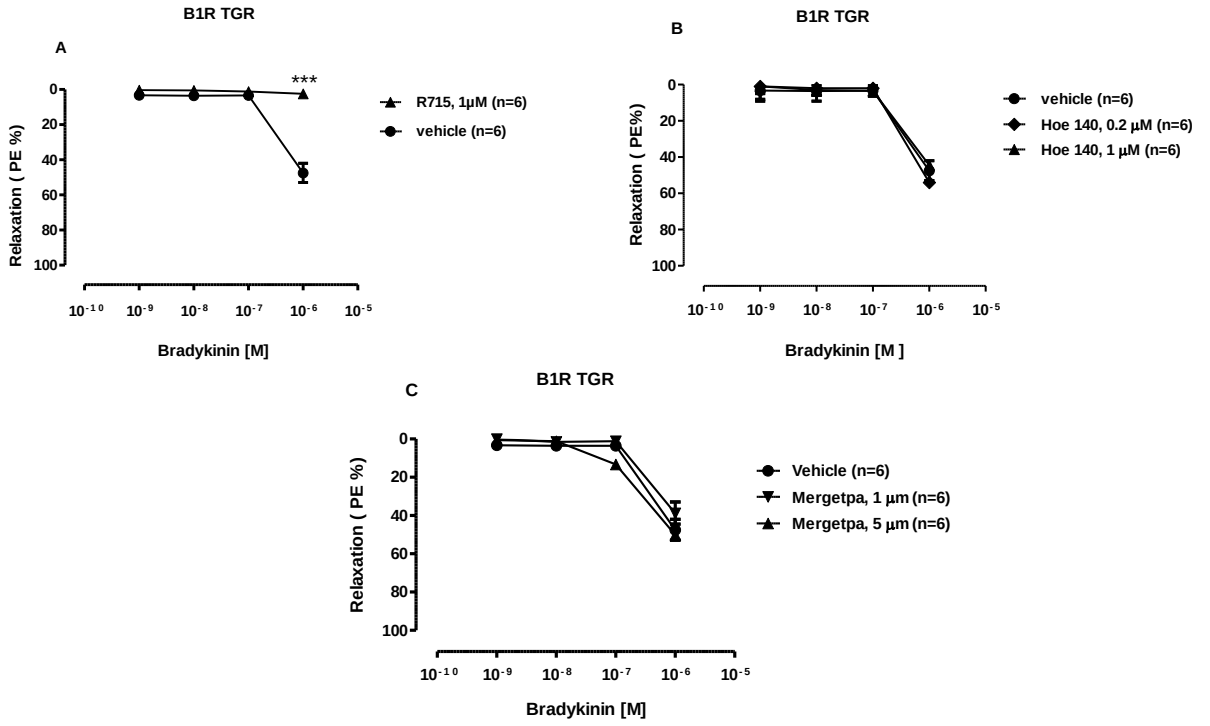

*Figure 28: Effect of: A) R715 (B1R antagonist), B) Hoe140 (B2R antagonist) and C) MERGETPA (CPM inhibitor) on isolated aortic rings from B1R-TGR. Data are expressed as mean ± SEM. ***p<0.001 when compared with control group, unpaired t-test.*

6.5 Bradykinin-induced endothelium-dependent vasorelaxation

The relaxant response to BK in rats and humans depends on the endothelium [217, 218]. To establish whether endothelium-dependent mechanisms are involved in the response of B2R-TGR vessels to BK, the endothelium was removed by gentle rubbing of the intimal surface of aorta before the ring was mounted in the bath. The absence of endothelial cells was confirmed physiologically by testing the relaxant response to acetylcholine, which is abolished by endothelial denudation. Endothelial denudation completely abolished the BK-induced relaxation (Figure 29).

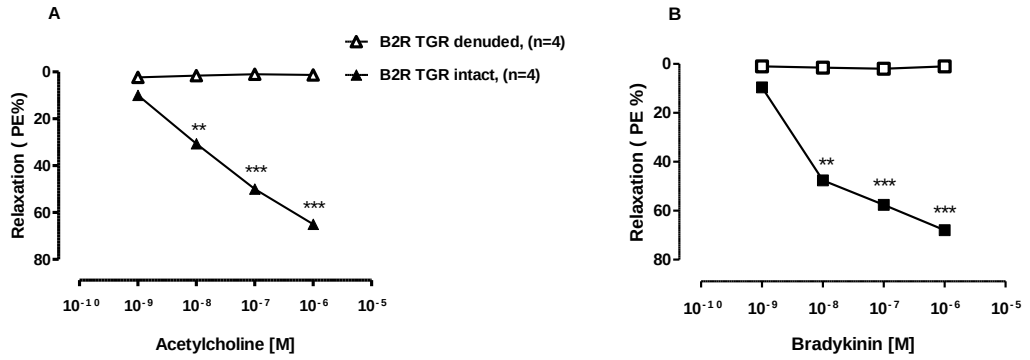

*Figure 29: Relaxations of: A) B2R-TGR aortic rings to acetylcholine, and B) Bradykinin in the absence and presence of endothelium. Data are expressed as mean ± SEM. **p<0.01; ***p<0.001 when compared with segments without endothelium, unpaired t-test.*

6.6 Signaling pathways involved in kinin receptor-induced vasodilation

There are three major signaling pathways characterized for kinin-induced vasodilatory effects: nitric oxide (NO), prostacyclin and endothelial-derived hyperpolarizing factor (EDHF). It is known that these pathways do not contribute to the same degree in different types of blood vessels. To find out what percentage each pathway contributes to the relaxation mediated by kinins, we used receptor blockers/inhibitors for these three different pathways. First, we studied the NO signaling pathway. It turned out that L-NAME completely abolished the relaxation induced by B1R and B2R agonists in both transgenic rats. Therefore, it was clearly evident that, most probably, the dominant signaling pathway which mediates kinin-induced vasorelaxation in rat aorta is the NO-signaling pathway (Figure 30 A and B). As depicted in Figure 30 B, preincubation of aortic rings with L-NAME resulted in vasoconstriction at higher concentrations of BK. It is known that BK induces not only relaxation but also contraction in an endothelium-dependent manner [219].

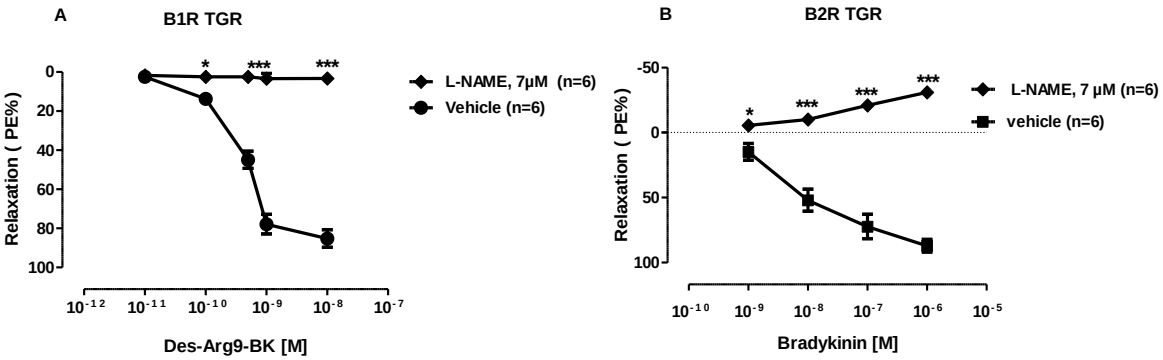

*Figure 30: Effect of: A) NO synthesis inhibitor L-NAME on isolated aorta from B1R-TGR, and B) B2R-TGR. Data are expressed as mean ± SEM. *p<0.05; ***p<0.001 when compared with control group, unpaired t-test.*

Next, the contribution of the prostacyclin signaling pathway was investigated. Indomethacin, a non-selective COX inhibitor, was used on kinin-induced vasorelaxation and it was found that B2R-TGR aortic ring relaxation was in fact significantly potentiated (at 10^{-8}/10^{-7} M BK) compared to vehicle treated aortic rings. Indomethacin also did not inhibit the relaxation induced by des-Arg^{9}-BK in B1R-TGR. The results clearly indicate that the vasorelaxation response induced by kinins in aorta was not mediated via the prostacyclin pathway (Figure 31 A and B).

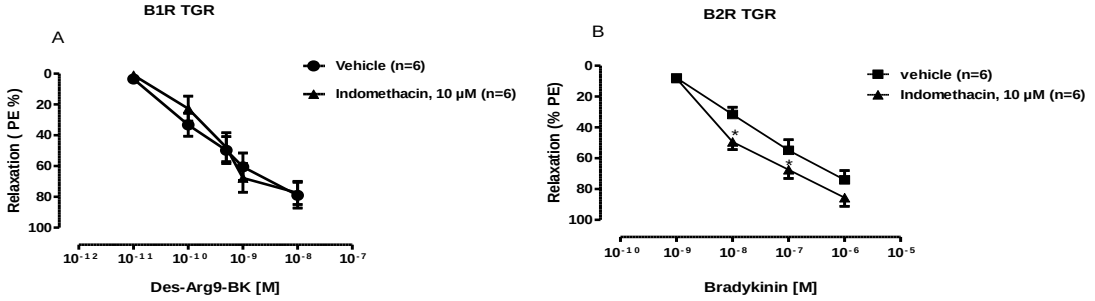

*Figure 31: Effect of COX inhibitor indomethacin on isolated aortic rings from B1R- (A) and B2R- (B) TGR. Data are expressed as mean ± SEM. *p<0.05 when compared with control group, unpaired t-test.*

Next, we investigated the possible involvement of K^+ channels in vasorelaxation induced by kinins. In this experimental protocol, we applied non-selective and selective K^+ channel blockers. The non-selective K^+ channel blocker tetraethylammonium (TEA) was used in both B1R- and B2R-TGR, which partially blocked the vasorelaxation induced by BK and des-Arg^9-BK (Figure 32 A and B). Glibenclamide, a specific K_{ATP} channel blocker, showed no involvement in the relaxation induced by BK (Figure 32 C and D). On the other hand, Iberiotoxin, a $BKca^{2+}$ (big conductance calcium sensitive potassium channel) blocker, strongly attenuated the vasorelaxation effect induced by kinins in both B1R- and B2R-TGR rats. This indicates the involvement of large conductance Ca^{2+} sensitive potassium channels in kinin-induced vasorelaxation (Figure 32 E and F).

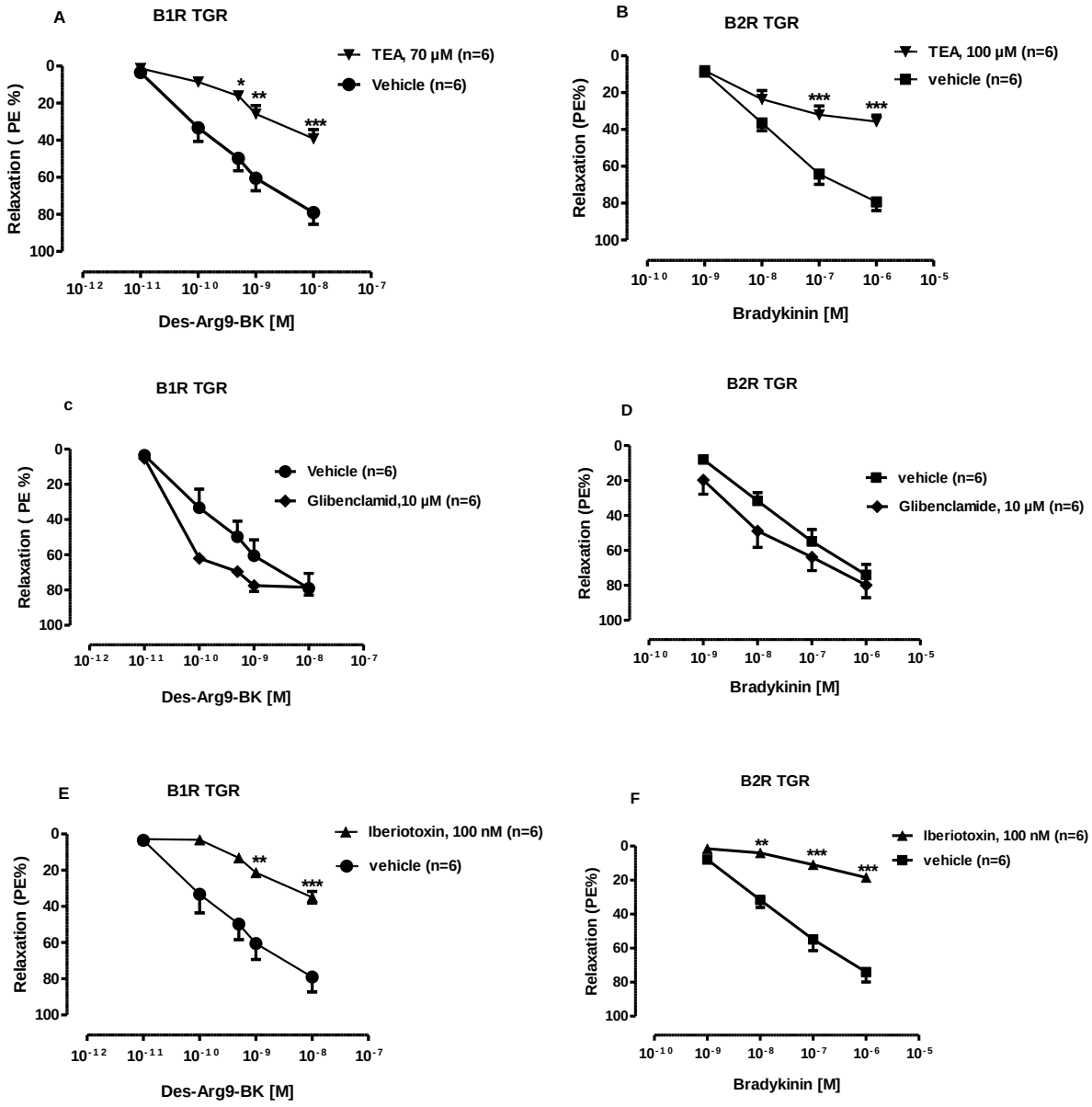

*Figure 32: Effect of: A) and B) non-selective K+ channel blocker, TEA; C) and D) specific K_{ATP} channel blocker, Glibenclamide; E) and F) BKca2+ channel blocker Iberiotoxin, on isolated aortic rings from B1R- (A, C, E) and B2R-TGR (B, D, F). Data are expressed as mean ± SEM, *p<0.05, **p<0.01; ***p<0.001 when compared with control groups, unpaired t-test.*

It has been shown that triggering of all relaxation pathways requires Ca^{2+} ions and that intracellular Ca^{2+} should be increased in endothelial cells. There are different Ca^{2+} channels on the cell membrane. Transient receptor potential channels (TRP) are the most important Ca^{2+} channels, which are a family of cation channels grouped into six subfamilies, namely: TRPV 1-6; TRPC 1-7; TRPM 1-8; TRPML 1-3; TRPP 2, 3, 5; and TRPA1. To investigate the role of TRPV (transient receptor potential vanilloid channel), particularly 1 and 4, in the vasorelaxation induced by kinins, specific inhibitors were used. There was no significant difference between B1R- and B2R-TGRaortic rings inhibited by TRPV1 (Capsazepine) and TRPV4 (RN-1724) inhibitors compared to vehicle treated aortic rings (Figure 33, A-B and C-D, respectively). We also assessed the role of different TRPC inhibitors on kinin-induced vasorelaxation, including the TRPC3 inhibitor Pyr3 (Figure 34 A and B), the TRPC4 inhibitor ML204 (Figure 34 C and D), the TRPC5 inhibitor AC1903 (Figure 34 E and F), and the TRPC6 specific inhibitor SAR7334 (Figure 34 G and H). Our results showed the involvement of TRPC4 channels only, and all other inhibitors did not affect the kinin-induced vasorelaxation. It seems that TRPC4 plays a central role in B1R- and B2R-induced vasorelaxation in rat aorta.

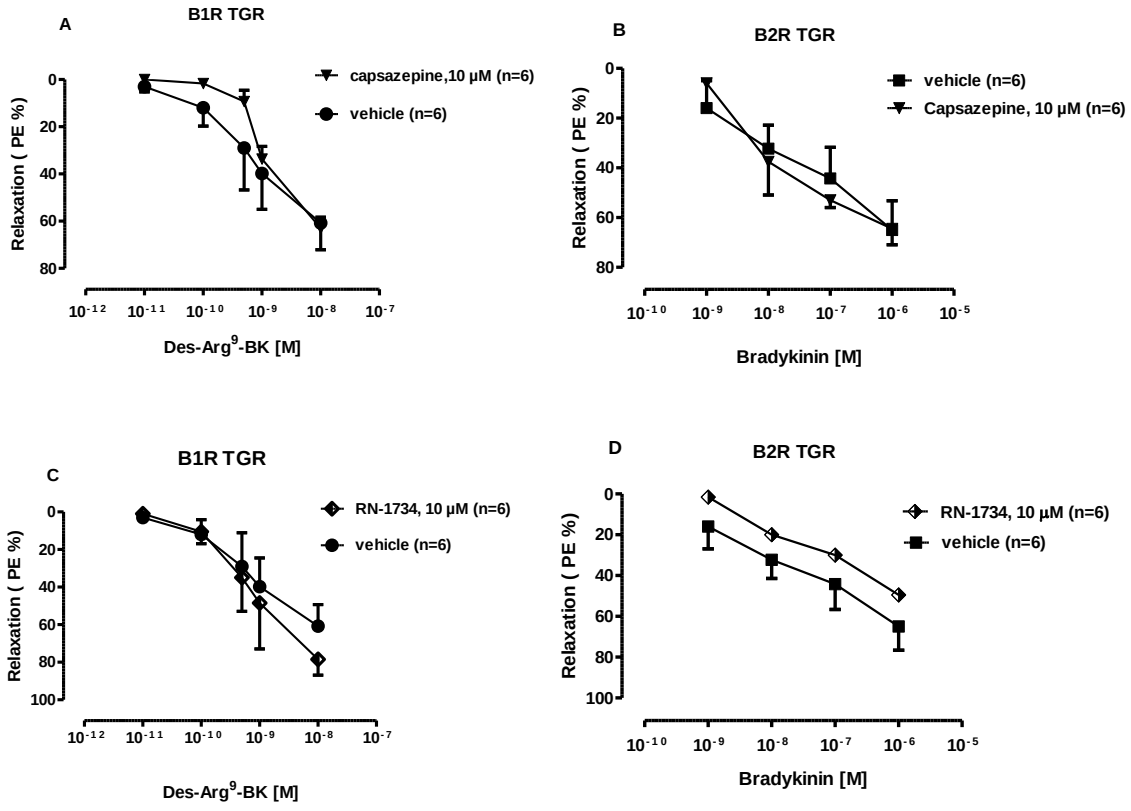

Figure 33: Effect of: A) and B) TRPV4 (capsazepine); C) and D) TRPV1 (RN-1734) inhibitors on isolated aorta from B1R- and B2R-TGR. Data are expressed as mean ± SEM.

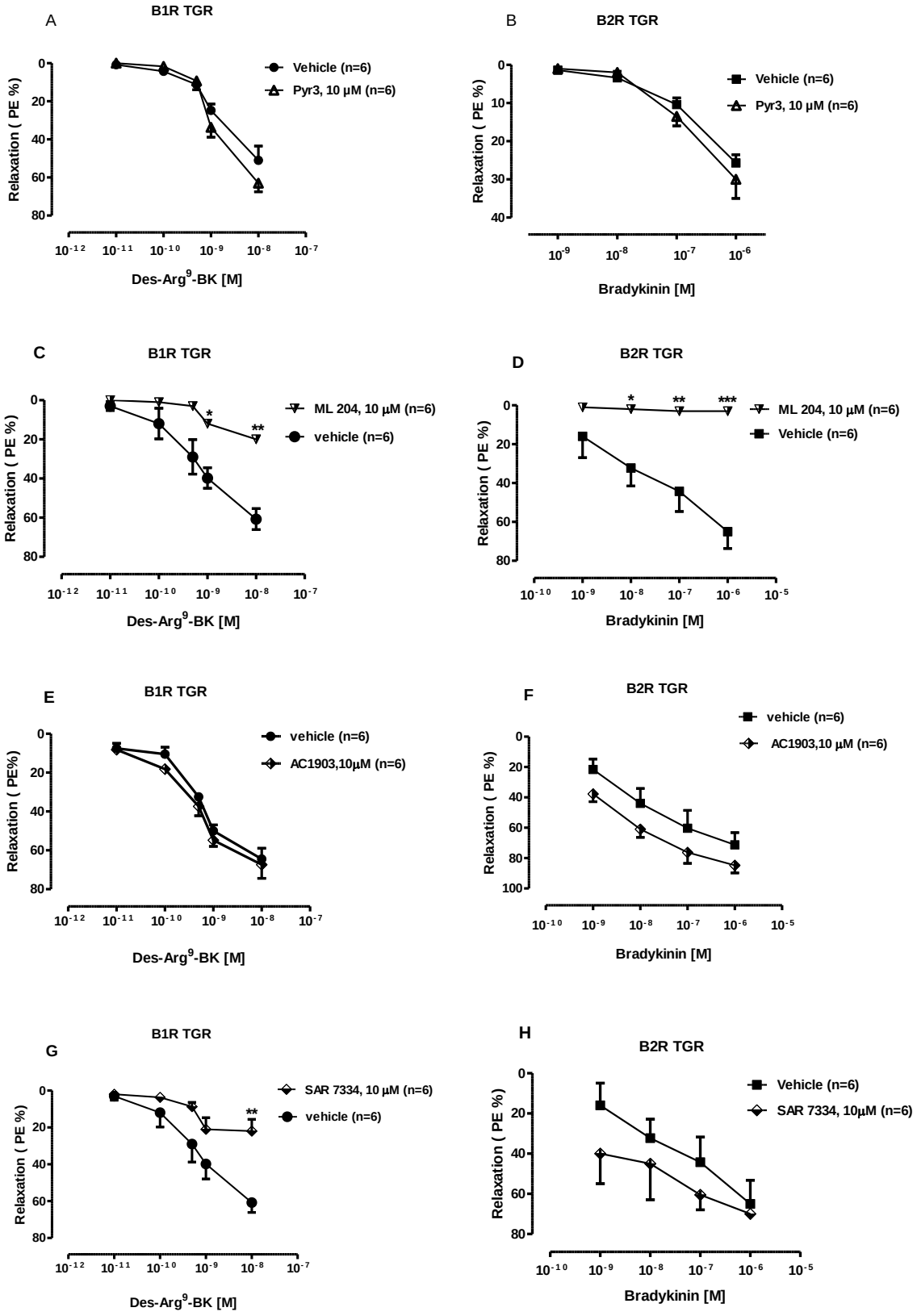

*Figure 34: Effect of: A) and B) TRPC3 (Pyr3); C) and D) TRPC4 (ML204); E) and F) TRPC5 (AC1903); G and H) TRPC6 (SAR7334) inhibitors on isolated aorta from B1R- and B2R-TGR. Data are expressed as mean ± SEM, *p<0.05; **p<0.01; ***p<0.001 when compared with control groups, unpaired t-test.*

ML204 is a potent antagonist that selectively modulates native TRPC4/C5 ion channels. Initially 10 μM of ML204 was applied, which has been suggested to block both TRPC4 and 5 (Figure 34 C, D). According to some studies, concentrations smaller than 10 μM of ML204 show more affinity and specificity toward TRPC4 channels. Therefore, it was decided to assess 300 nM of the inhibitor in kinin induced vasorelaxation, and it induced the same relaxation pattern as 10 μM (Figure 35). Since there was an effect by SAR7334 at high concentrations of BK in B1R-TGR (Figure 34 G), we also assessed a second inhibitor of TRPC6 with a high specificity named SHO45 (Gift from Dr. Schaefer, Munich, Germany), confirming that this subtype is not involved in kinin receptor signaling (Figure 36).

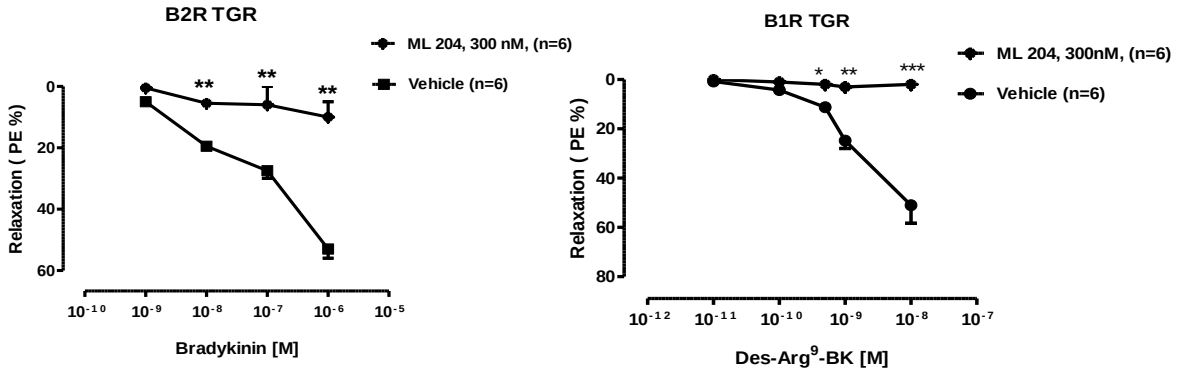

*Figure 35: Effect of TRPC4/5 inhibitor, ML204, low dose, on isolated aortic rings from B1R- and B2R-TGR. Data are expressed as mean ± SEM, *p<0.05; **p<0.01; ***p<0.001 when compared with control group, unpaired t-test.*

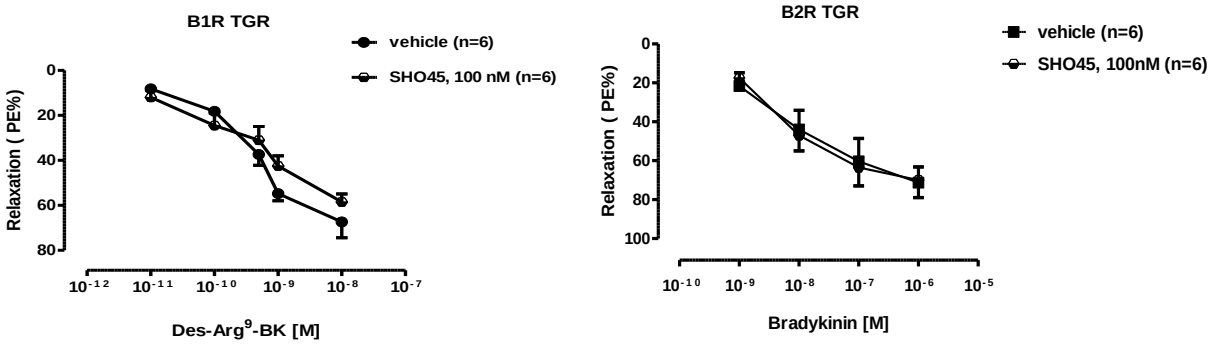

Figure 36: Effect of TRPC6 inhibitor, SHO45, on isolated aortic rings from B1R- and B2R-TGR. Data are expressed as mean ± SEM.

6.7 Detection and quantification of TRP channel transcripts in aorta at the level of mRNA

Figure 37 shows the expression levels of TRPC3, TRPC4, TRPC5, TRPC6, TRPV1 and TRPV3 channels in aorta isolated from B1R- and B2R-TGR. The expression levels were calculated related to TBP (TATA-binding protein) as housekeeping gene. The non-transgenic SD rats were taken as control. Using qPCR, we detected signals for all above mentioned TRP channel transcripts. There were no significant differences in TRPC3, 4, 5, TRPV1 and 3 expression levels in B1R- and B2R-TGR compared to control groups. A slight decrease of TRPC6 was detected in B2R-TGR aorta compared to the SD group. The expression levels of TRP channels were also calculated in aorta isolated from WT rats. To understand how high the expression of the TRP channels was relative to one another in the aorta, we compared their ΔCT values (Figure 38).

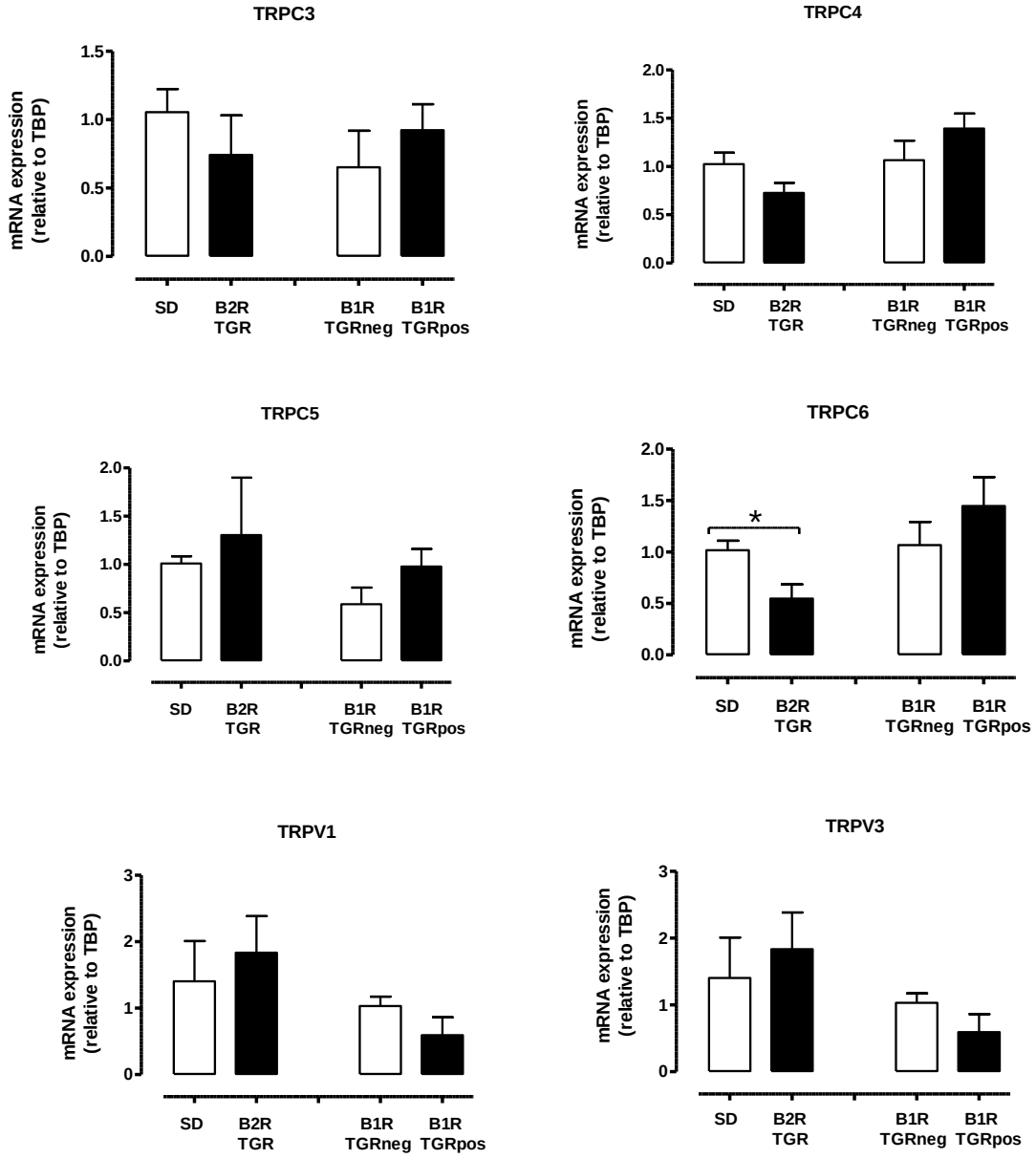

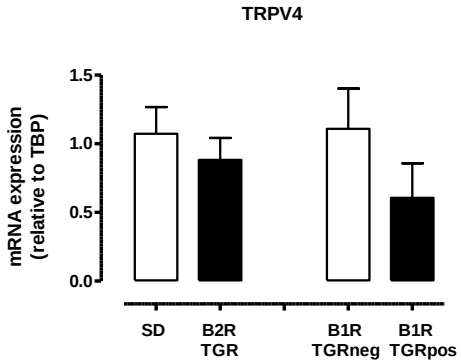

*Figure 37: Quantification of TRP channel transcripts in aorta at the level of mRNA using real-time qPCR. Expression levels of TRPC3, TRPC4, TRPC5, TRPC6, TRPV1 and TRPV3 channel mRNA from B1R- and B2R-TGR. The non-transgenic SD rats were taken as control for B2R-TGR, and B1Rneg (negative) litter mates were taken as control for B1R-TGR. The mRNA levels of TRP ion channels are given in relation to the housekeeping gene, TBP. Means ± S.E.M, * p<0.05 when compared with control group, unpaired t-test, n = 4–6.*

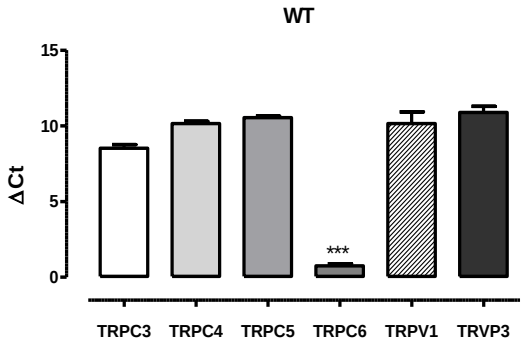

*Figure 38: Quantification of TRP channel transcripts in aorta at the level of mRNA using real-time qPCR. Expression levels of TRPC3, TRPC4, TRPC5, TRPC6, TRPV1 and TRPV3 channel mRNA from WT. The mRNA levels of TRP ion channels are given in relation to the housekeeping gene, TBP. Means ± S.E.M, ***p<0.001 when compared with other groups, unpaired t-test. n = 4–6.*

6.8 Angioedema induction in rats overexpressing the kinin B2 receptor

6.8.1 Vascular permeability assay in B2R transgenic rats after Mustard oil short-term (acute) treatment to induce angioedema

Vascular permeability was analyzed 30 min after Evans blue (EB) tail vein injections in 12-week-old conscious B2R-TGR rats (30 mg/kg bodyweight). EB extravasation was measured spectrophotometrically. Acute angioedema attacks were induced by two topical applications of

mustard oil. On the dorsal/outer side of the ear, where mustard oil was applied, EB extravasation was more than 4-fold higher in B2R-TGR rats when compared to WT (Figure 39 A), and additionally the skin surrounding the region, such as on the skull, and surrounding the eye and snout, showed higher vascular permeability (Figure 39 B, C and D).

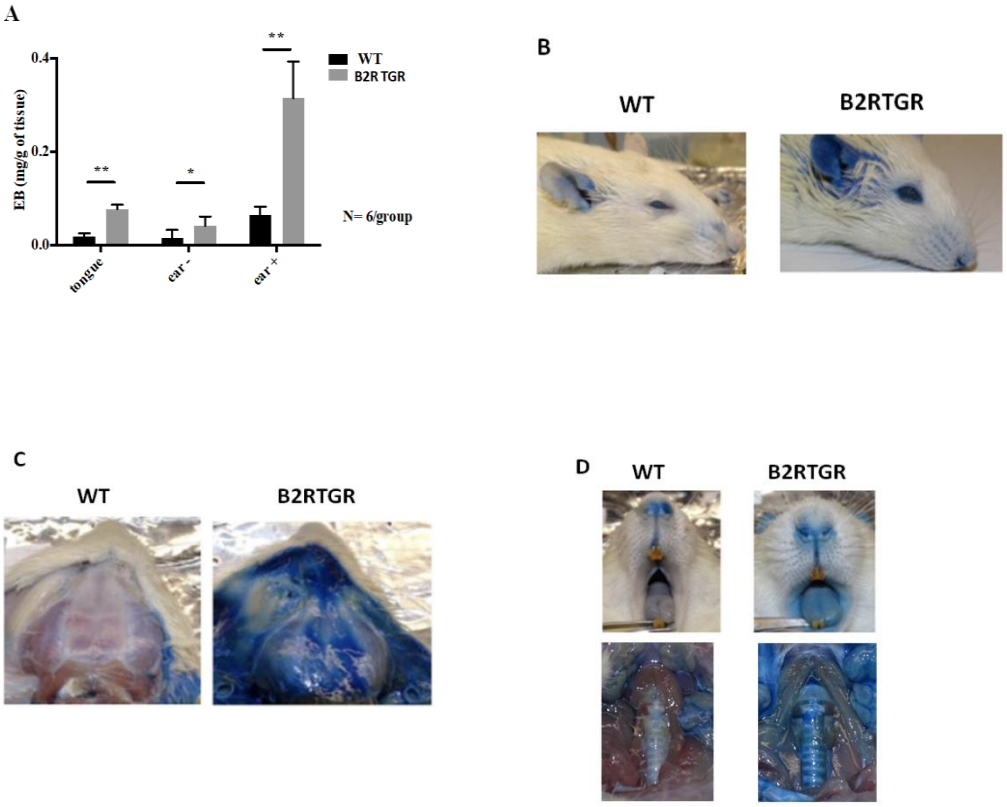

*Figure 39: Evans blue extravasation after mustard oil challenge. (A) The median Evans blue (EB) extravasation was significantly higher in the B2R-TGR ear where mustard oil was applied (ear+), but also in the other ear (ear-) and in the tongue compared to control rats. (B) Ear, (C) head skin, (D) tongue and trachea after mustard oil application. *p<0.05, **p<0.01 when compared with control group, unpaired t-test, n=6.*

We also evaluated internal tissues to assess any possible systemic effect of mustard oil-induced EB extravasation. After mustard oil challenge, EB extravasation in male B2R-TGR rats was significantly higher in kidney compare to all other organs tested (Figure 40 A). We assume that this increased vascular permeability remote from the application site was most probably independent of mustard oil treatment. Accordingly, 12-week-old female transgenic rats presented increased vascular permeability under basal conditions in bowel, uterus, liver and kidney when compared to age-matched WT females (Figure 40 B). This exacerbated vascular permeability in females compared to males supports the potential of the transgenic rat model as a tool for the study of the influence of sexual hormones on the regulation of the BK-release pathway and HAE.

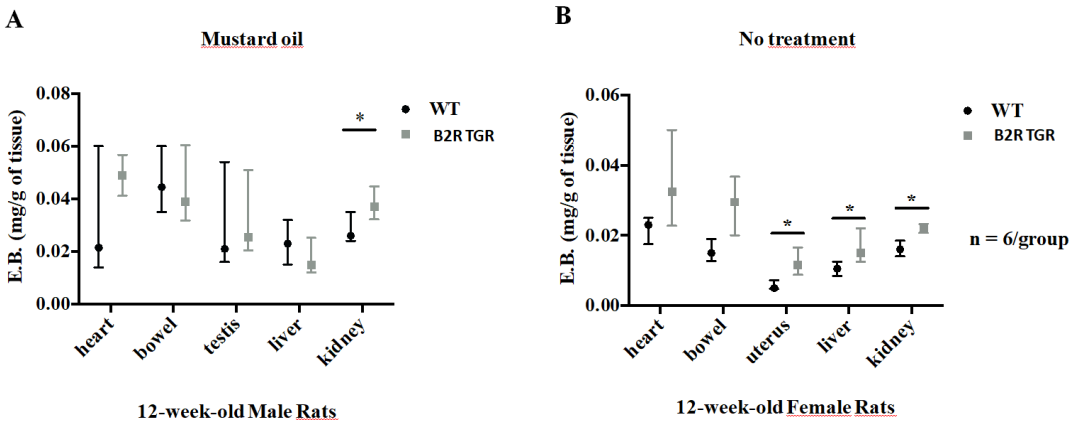

*Figure 40: Evans blue extravasation in different tissues. (A) Comparison of Evans blue (EB) extravasation in male rats after mustard oil challenges revealed significantly increased permeability only in kidney of B2R-TGR compared to WT. (B) Female rats presented higher median EB extravasation in all analyzed organs under basal conditions. Data are expressed as median with interquartile range. *p<0.05 when compared with control groups, unpaired t-test.*

6.8.2 Spontaneous angioedema in B2R-TGR

During the mustard oil short term experiments, although no skin swelling occurred, we observed that 12% percent of B2R-TGR rats (10/84) presented intestinal swellings independent of sex (5/49 male vs. 5/35 female). This phenotype was not observed in the analysed age-matched WT rats (42 male, 18 female). Neither EB nor mustard oil was determinant for the development of this phenotype (4/10 rats underwent no procedure), indicating a spontaneous and sporadic occurrence of abdominal angioedema. We then carefully analysed more B2R-TGR animals and found that almost 9% of them developed intestinal swelling, which was prominent around the age of 4-6 weeks. We also observed pancreatic lesions characterized by blood clots spread throughout the tissue, whereas B2R-TGR littermates with no intestinal swelling have normal pancreatic tissue. Comparing B2R-TGR pancreas with and without hemorrhagic clots (Figure 41 B), an increase in the size and amount of Langerhans islets was observed (Figure 41 D). Immunohistochemical analysis indicated a large increase in the number of α-cells and a decrease in β-cells when compared to non-affected B2R-TGR rats (Figure 41 E). The pancreatic lesions observed can be a consequence of pancreatic edema or represent a secondary event to intestinal swelling, which can induce partial or complete ductal obstruction resulting in pancreatitis.

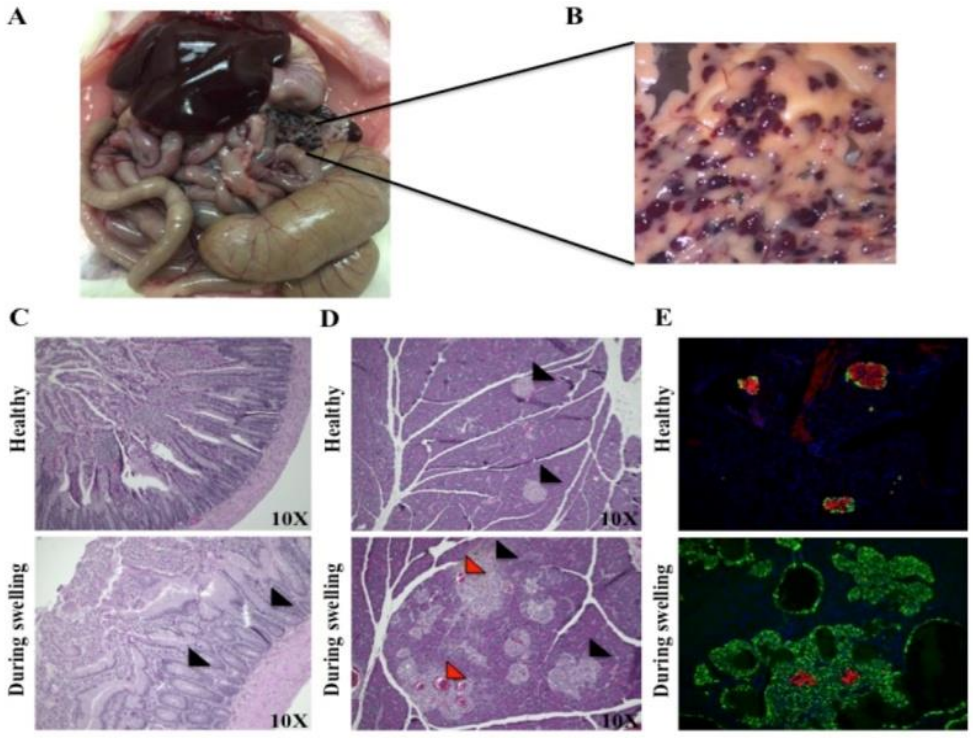

Figure 41: Spontaneous angioedema affecting intestine and pancreas. B2R-TGR presented sporadic spontaneous episodes of angioedema affecting intestine (A) and pancreas (B). Haematoxylin-eosin stained ileum (C) and pancreas (D) sections of healthy B2R-TGR rats (upper panels) and B2R-TGR rats during intestinal swellings (lower panels). Thickened villi can be observed during abdominal swellings in the intestine (C, black arrow heads). Langerhans islets (D, black arrow heads) are larger during swelling episodes, and contain thrombi (red arrow heads). (E) Anti-insulin (red) and anti-glucagon (green) staining revealed a decrease in β-cells and an increase in α-cells, respectively.

6.8.3 Vascular permeability assay after Hoe140 treatment in B2R-TGR

In order to evaluate whether B2R-TGR with angioedema showed an increased B2R-dependent vascular permeability in general, we measured this parameter by tail-vein injection of EB in the presence of the B2R antagonist Hoe140. In this experiment, we used four groups of rats (male, 12-16 weeks old): group 1, B2R-TGR (control group, n=3); group 2, B2R-TGR treated with HOE140 (n=4); group 3, EdemicB2R-TGR (control group, n=5); and group 4, EdemicB2R-TGR treated with HOE140 injection (n=5). Rats from groups 2 and 4 were treated with Hoe140 (10µg/kg) intravenous (i.v. lateral tail vein) and groups 1 and 3 were treated with vehicle (physiological saline, i.v.). 24h after the treatment, vascular permeability was analysed in all four groups 30 min after Evans blue (EB) tail vein injections. One hour after the EB treatment, rats were sacrificed and organs were collected for the analysis of extravasations. Statistical differences were determined by t- and F-test. Unlike the t-test which shows the significance of means, an F-test is used to compare the two standard deviations of two samples and check the variability. In the edemic B2R-TGR group which received Hoe140, the EB extravasations were significantly decreased in the heart when evaluated by t-test, and significantly decreased in the stomach,

rectum, skeletal muscle, skin and submandibular gland when evaluated by F-test compared to the edemic B2R-TGR vehicle-treated control group. In most of the organs from the B2R-TGR+Hoe140 group, especially the stomach, colon, uterus (t-test) and duodenum, ileum, skin and urinary bladder (F-test), to our surprise, EB extravasation was increased when compared to the vehicle-treated B2R-TGR group (Figure 42).

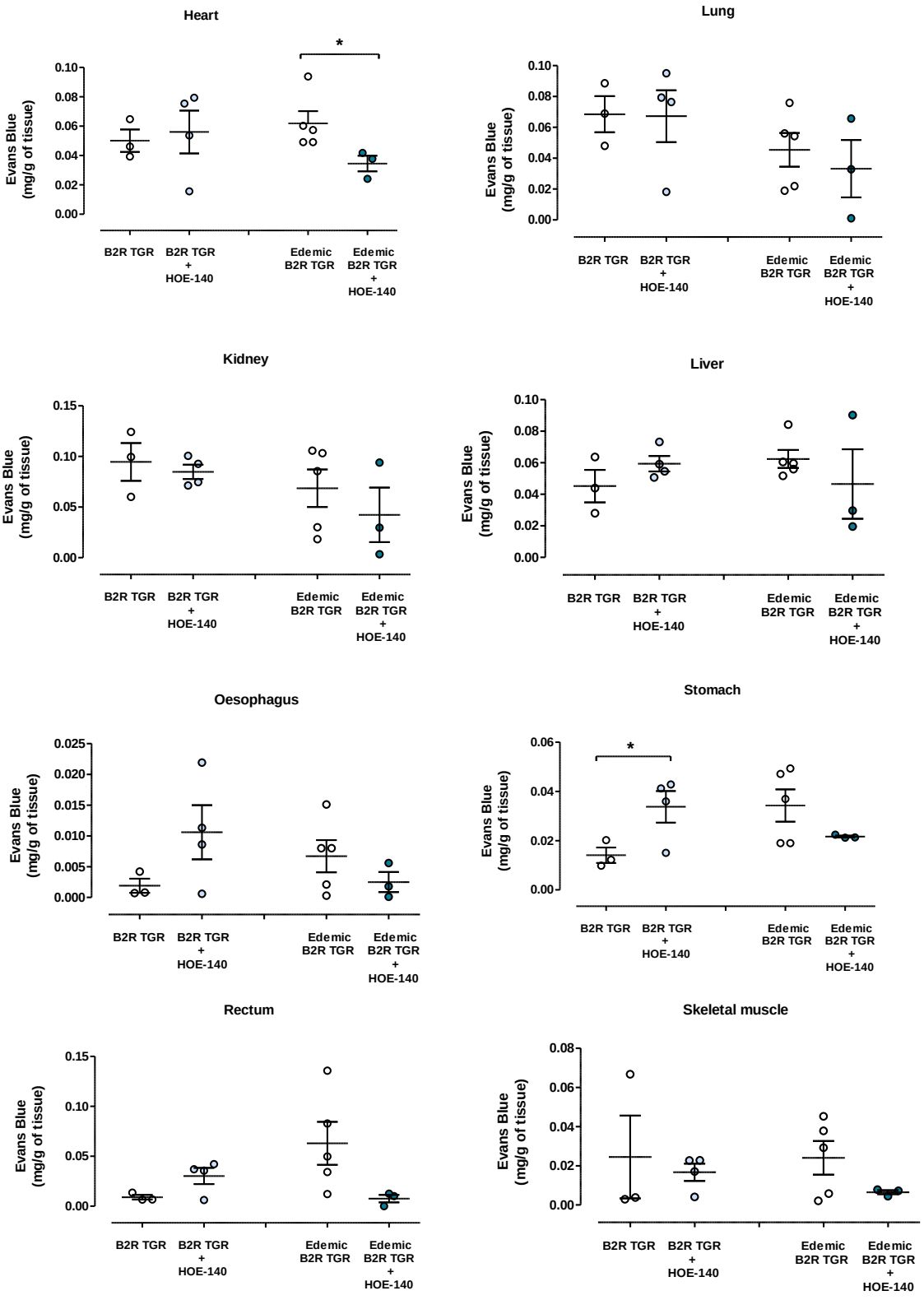

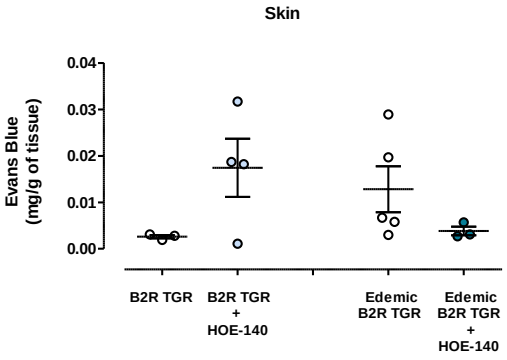
Skin
Evans Blue (mg/g of tissue)
0.04
0.03
0.02
0.01
0.00
B2R TGR
B2R TGR + HOE-140
Edemic B2R TGR
Edemic B2R TGR + HOE-140

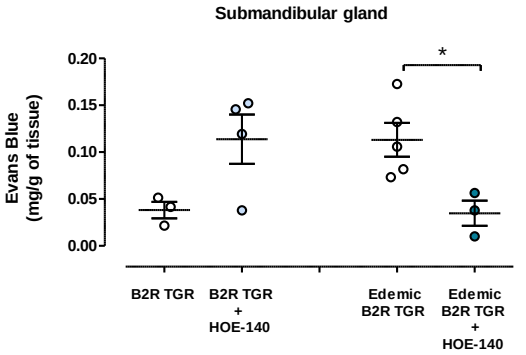
Submandibular gland
Evans Blue (mg/g of tissue)
0.20
0.15
0.10
0.05
0.00
*
B2R TGR
B2R TGR + HOE-140
Edemic B2R TGR
Edemic B2R TGR + HOE-140

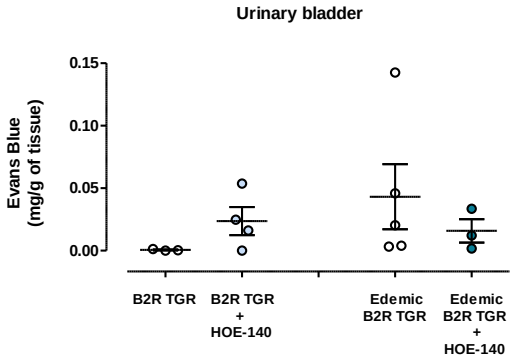
Urinary bladder
Evans Blue (mg/g of tissue)
0.15
0.10
0.05
0.00
B2R TGR
B2R TGR + HOE-140
Edemic B2R TGR
Edemic B2R TGR + HOE-140

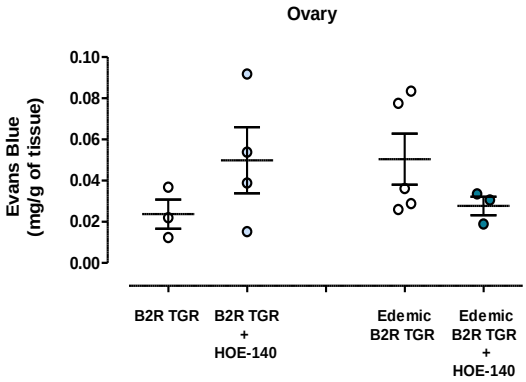
Ovary
Evans Blue (mg/g of tissue)
0.10
0.08
0.06
0.04
0.02
0.00
B2R TGR
B2R TGR + HOE-140
Edemic B2R TGR
Edemic B2R TGR + HOE-140

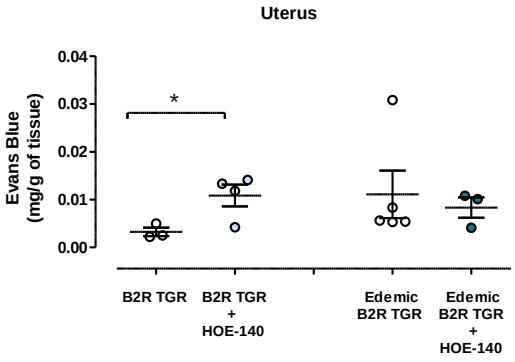
Uterus
Evans Blue (mg/g of tissue)
0.04
0.03
0.02
0.01
0.00
*
B2R TGR
B2R TGR + HOE-140
Edemic B2R TGR
Edemic B2R TGR + HOE-140

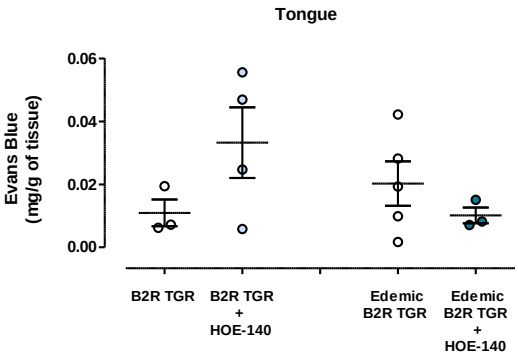
Tongue
Evans Blue (mg/g of tissue)
0.06
0.04
0.02
0.00
B2R TGR
B2R TGR + HOE-140
Edemic B2R TGR
Edemic B2R TGR + HOE-140

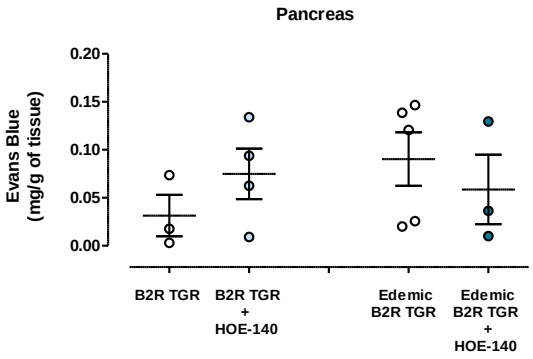
Pancreas
Evans Blue (mg/g of tissue)
0.20
0.15
0.10
0.05
0.00
B2R TGR
B2R TGR + HOE-140
Edemic B2R TGR
Edemic B2R TGR + HOE-140

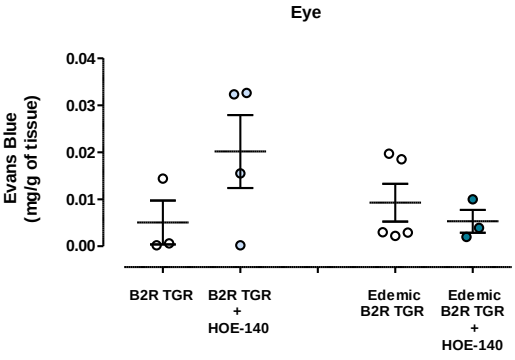
Eye
Evans Blue (mg/g of tissue)
0.04
0.03
0.02
0.01
0.00
B2R TGR
B2R TGR + HOE-140
Edemic B2R TGR
Edemic B2R TGR + HOE-140

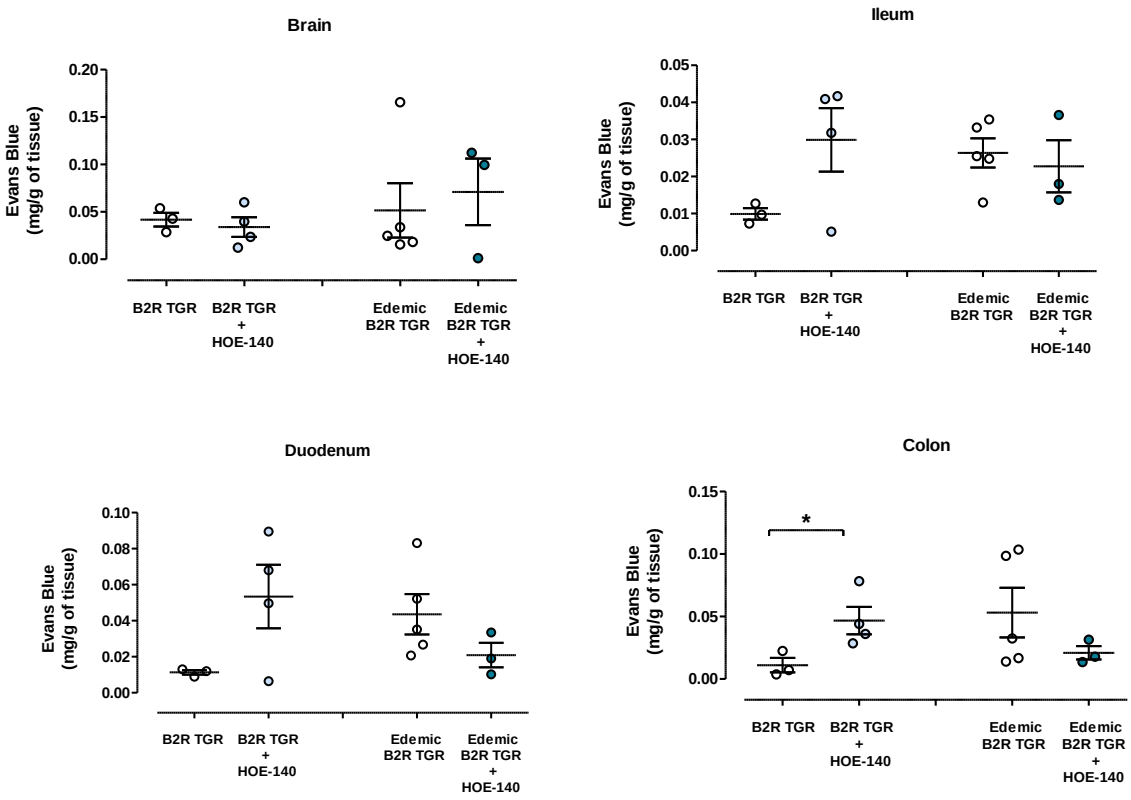

*Figure 42: Evans blue extravasation in different tissues of vehicle- and Hoe140-treated healthy (non-edemic) B2R-TGR and edemic B2R-TGR (n=3-5). Data are expressed as median with interquartile range. *p<0.05 when compared with control group, unpaired t-test.*

6.8.4 Vascular permeability measurement after chronic treatment with enalapril

Next, we wanted to assess whether B2R-TGR are more sensitive than controls to inducers of angioedema, such as ACE inhibitors. In this experiment male rats (12-16 weeks) were divided into four groups: group 1, B2R-TGR (n=6) control; group 2, B2R-TGR received the ACE inhibitor enalapril in drinking water for 30 days (1mg/KG/BW) (n=8); group 3, SD rats (n=6) as control group; and group 4, SD rats also received enalapril in drinking water for 30 days (1mg/kg/BW) (n=6). The control group received normal drinking water. At the end of the treatment period, vascular permeability was analysed 30 min after Evans blue (EB) tail vein injections (30 mg/kg body-weight). Rats were sacrificed and organs were collected for the extravasation analyses as described above. In the B2R-TGR group which received enalapril, the EB extravasations were significantly increased in the testis (t-test) and significantly increased in the stomach, heart, lung, kidney, trachea, tongue, oesophagus, duodenum, colon, brain, eyes and pancreas (F-test) compared to the vehicle-treated control B2R-TGR. In the trachea (F-test) and liver (t-test) of the SD treated with enalapril group, EB extravasations were significantly increased compared to the vehicle-treated control SD group (Figure 43).

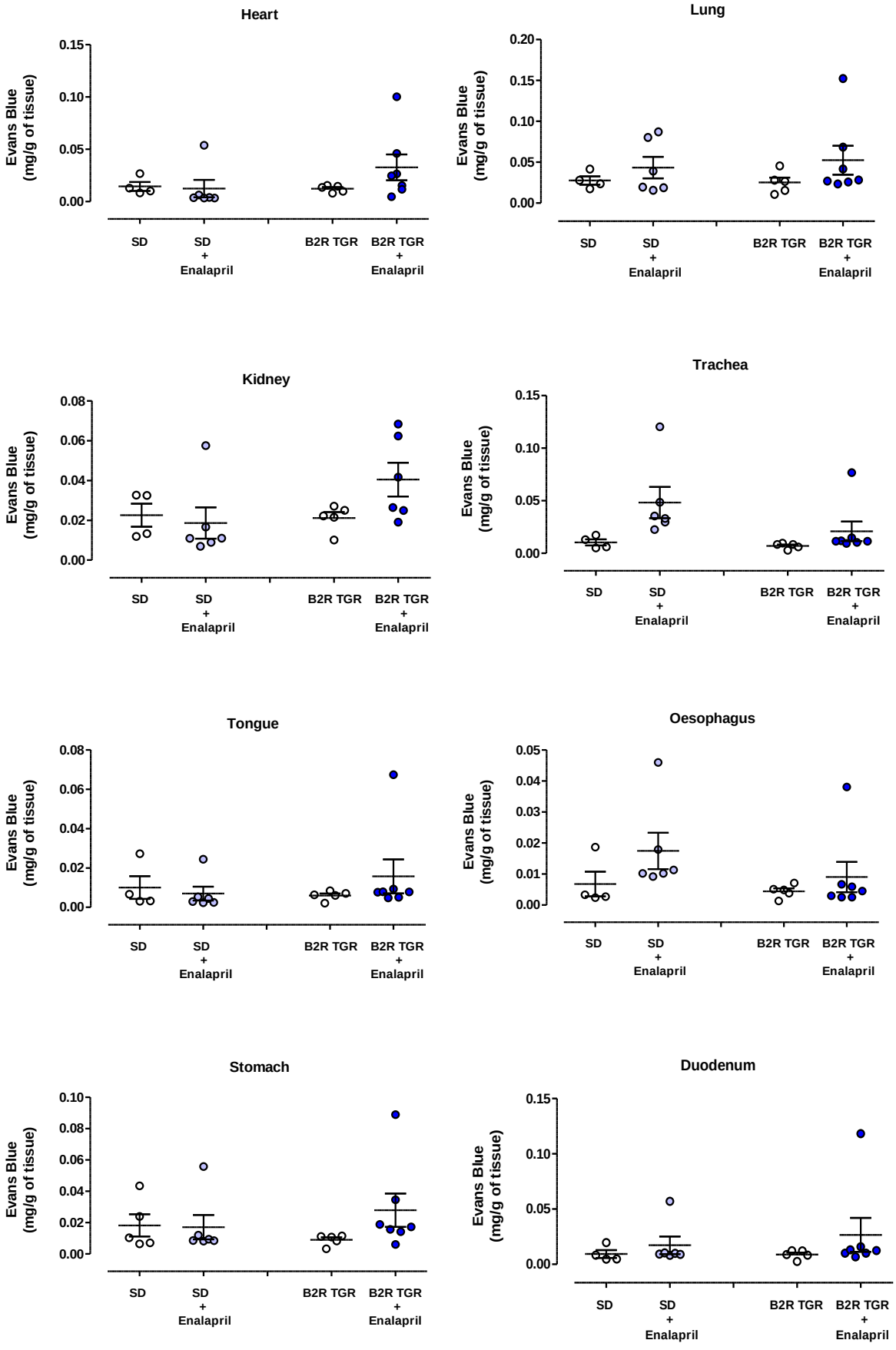
Heart
Evans Blue (mg/g of tissue)
0.15
0.10
0.05
0.00
SD
SD + Enalapril
B2R TGR
B2R TGR + Enalapril
Lung
Evans Blue (mg/g of tissue)
0.20
0.15
0.10
0.05
0.00
SD
SD + Enalapril
B2R TGR
B2R TGR + Enalapril
Kidney
Evans Blue (mg/g of tissue)
0.08
0.06
0.04
0.02
0.00
SD
SD + Enalapril
B2R TGR
B2R TGR + Enalapril
Trachea
Evans Blue (mg/g of tissue)
0.15
0.10
0.05
0.00
SD
SD + Enalapril
B2R TGR
B2R TGR + Enalapril
Tongue
Evans Blue (mg/g of tissue)
0.08
0.06
0.04
0.02
0.00
SD
SD + Enalapril
B2R TGR
B2R TGR + Enalapril
Oesophagus
Evans Blue (mg/g of tissue)
0.05
0.04
0.03
0.02
0.01
0.00
SD
SD + Enalapril
B2R TGR
B2R TGR + Enalapril
Stomach
Evans Blue (mg/g of tissue)
0.10
0.08
0.06
0.04
0.02
0.00
SD
SD + Enalapril
B2R TGR
B2R TGR + Enalapril
Duodenum
Evans Blue (mg/g of tissue)
0.15
0.10
0.05
0.00
SD
SD + Enalapril
B2R TGR
B2R TGR + Enalapril

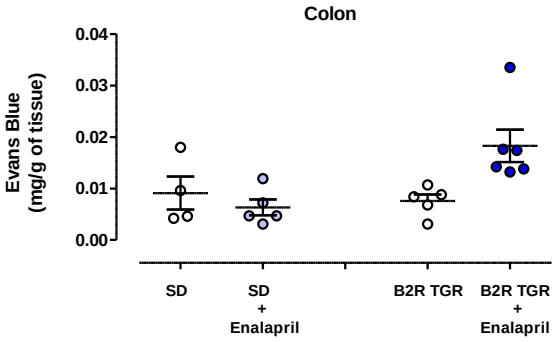
Colon
Evans Blue (mg/g of tissue)
0.04
0.03
0.02
0.01
0.00
SD
SD + Enalapril
B2R TGR
B2R TGR + Enalapril

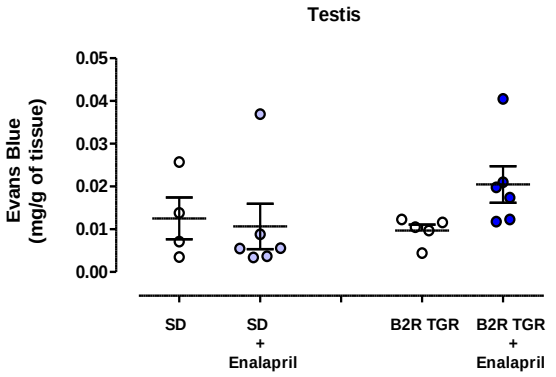
Testis
Evans Blue (mg/g of tissue)
0.05
0.04
0.03
0.02
0.01
0.00
SD
SD + Enalapril
B2R TGR
B2R TGR + Enalapril

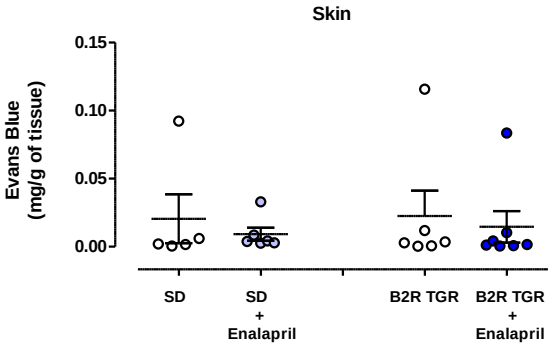
Skin
Evans Blue (mg/g of tissue)
0.15
0.10
0.05
0.00
SD
SD + Enalapril
B2R TGR
B2R TGR + Enalapril

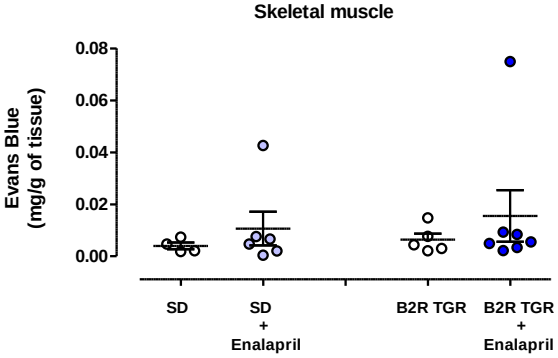
Skeletal muscle
Evans Blue (mg/g of tissue)
0.08
0.06
0.04
0.02
0.00
SD
SD + Enalapril
B2R TGR
B2R TGR + Enalapril

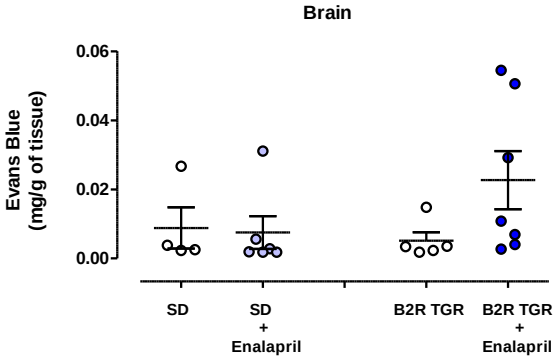
Brain
Evans Blue (mg/g of tissue)
0.06
0.04
0.02
0.00
SD
SD + Enalapril
B2R TGR
B2R TGR + Enalapril

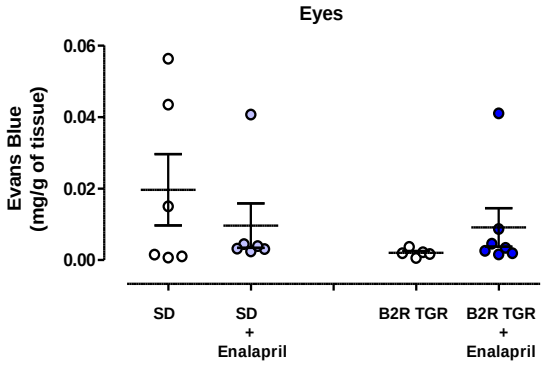
Eyes
Evans Blue (mg/g of tissue)
0.06
0.04
0.02
0.00
SD
SD + Enalapril
B2R TGR
B2R TGR + Enalapril

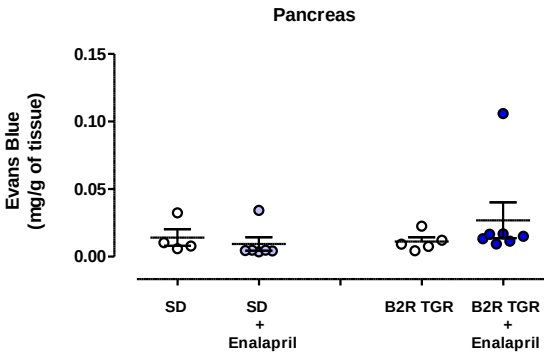
Pancreas
Evans Blue (mg/g of tissue)
0.15
0.10
0.05
0.00
SD
SD + Enalapril
B2R TGR
B2R TGR + Enalapril

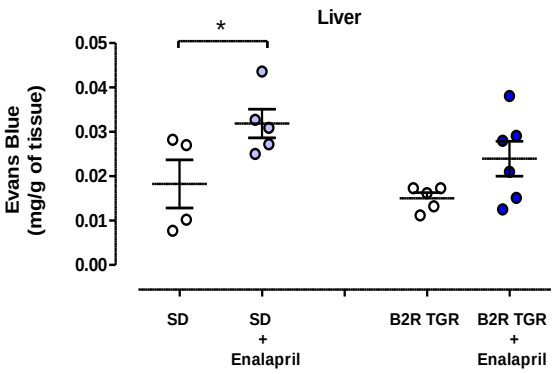
Liver
*
Evans Blue (mg/g of tissue)
0.05
0.04
0.03
0.02
0.01
0.00
SD
SD + Enalapril
B2R TGR
B2R TGR + Enalapril

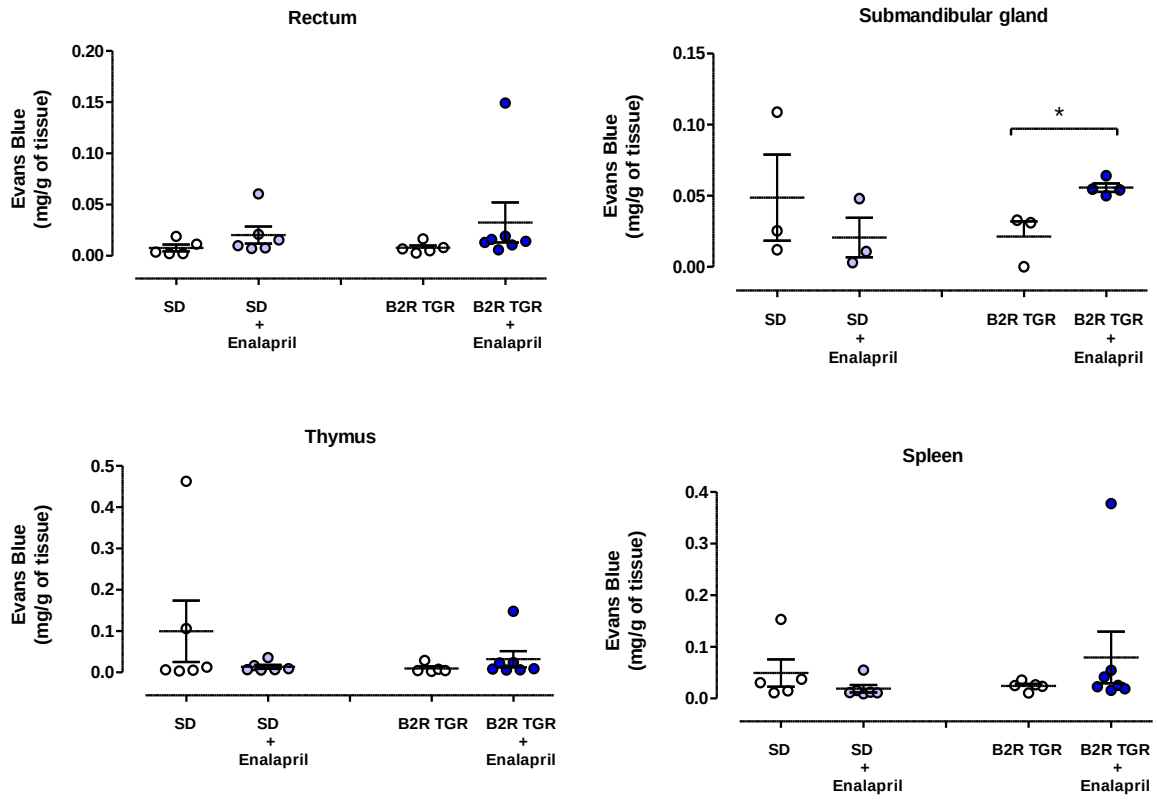

*Figure 43: Evans blue extravasation in different tissues of wild type SD and B2R-TGR rats after chronic treatment with enalapril (1 mg/KG/BW in drinking water for 4 weeks); control groups received vehicle (tap water). n=6-8. Data are expressed as median with interquartile range. *p<0.05 when compared with control group, unpaired t-test.*

6.9 Knockout rats for carboxypeptidase M

6.9.1 Generation of CPM-KO rats

BK as the main product of the KKS is released from kininogens and exerts its biological activities through B2R. BK is further converted to its metabolite des-Arg^9-BK, which is an active endogenous ligand to B1R. This conversion occurs through the enzymatic action of CPM, which is also known as kininase 1. To investigate the role of CPM in KKS and beyond, we decided to generate a rat model lacking CPM globally. The CRISPR/Cas9 technique was applied to introduce mutations in the rat CPM gene in exon 2. Two lines of CPM KO were generated, one line carrying a 6 base pair deletion including the ATG start codon (L-38), and another line (L-76) with a thymidine insertion in the coding sequence. Both were expected to be functional knockouts.

6.9.2 CPM expression in different organs at the level of mRNA

To determine the expression level of the CPM mRNA in different tissues of CPM-KO and WT rats, quantitative real-time PCR was performed. Figure 44 shows the expression levels of both lines in lung and heart calculated related to TBP (TATA-binding protein) as the housekeeping gene. SD rats were taken as positive control. The expression levels of CPM mRNA in both lines were almost 50% lower in lung and heart compared to the control group, but not fully absent. Therefore, it was important to check protein expression and enzyme activity to prove that the CPM is functionally inactive.

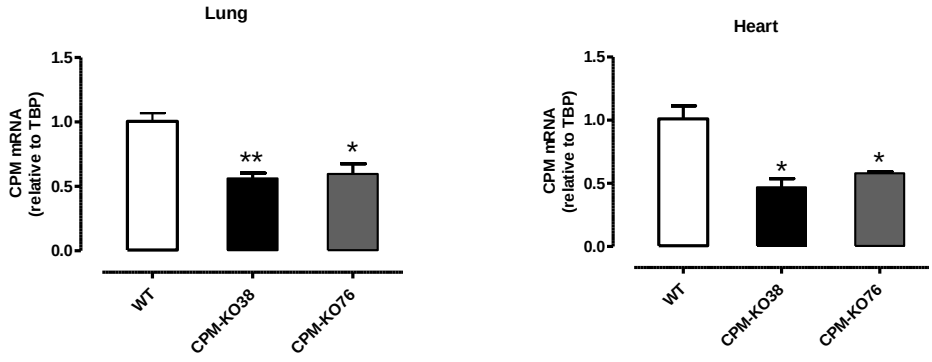

*Figure 44: Quantitative analysis of mRNA levels in two lines of CPM-KO rats (L-38 and L-76) Data are expressed as mean ± SEM. n=2-3. *p<0.05; **p<0.01 when compared with control group, unpaired t-test.*

6.9.3 CPM protein expression in CPM-KO and WT lungs

To investigate the CPM protein expression, Western blotting of CPM-KO and WT lung, this being the main expressing organ of this enzyme, was performed. Recombinant human CPM (rhCPM) was applied as positive control. According to previous studies [23], a specific band was detected for CPM at approximately 55-65 KDa in WT but not in our CPM-KO tissue. A rhCPM band was detected at about 50 KDa (Figure 45). Since rhCPM is purified from overexpressing cells, the difference in molecular mass may be explained by differential glycosylation states of the recombinant and the native CPM. Therefore, we decided to deglycosylate our tissue CPM to see whether the detected band sizes drop. The protein was stripped of N-linked oligosaccharides attached to asparagine residues using the specific amidase PNGase F. CPM was in fact strongly glycosylated, and deglycosylation led to a decreased size of about 47 KDa and to a more distinct shape of the band. This size was even smaller than that of rhCPM, which is not surprising since rhCPM is probably also partially glycosylated (Figure 45 B).

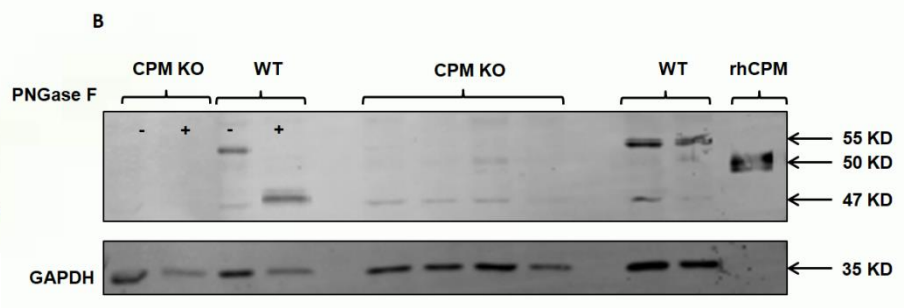

Figure 45: A: CPM protein expression of CPM-KO and WT lung. B. Deglycosylation of CPM protein CPM-KO and WT lung by PNGase F. GAPDH was used as the internal protein loading control. rhCPM, recombinant human CPM.

6.9.4 Estimation of CPM activity in CPM-KO and WT lungs

The peptidase activity of CPM was tested with Dansyl-Ala-Arg substrate at pH 7, which is the optimum pH for CPM activity [220]. Protein samples were from lung of WT and both CPM-KO lines (L-38 and L-76). Samples were incubated for 3 hrs and the enzyme activity was measured using a fluorometer. Substrate metabolism increased linearly over time in WT, but less in both CPM-KO lines, but did not reach a plateau. In Figure 46 A, it is shown that the hydrolysis of Dansyl-Ala-Arg by CPM was completely inhibited by the CPM inhibitor MERGETPA (MGTA) in both WT and CPM-KO. CPM-KO showed a dramatically dropped CPM activity compared to WT, but there was still some activity left (Figure 46 B). This could be due to other types of carboxypeptidases (CPs) found in the tissues besides CPM. These peptidases have different pH optima for their enzyme activity. To distinguish CPM activity from other CPs, we investigated the CP activity in the lung of WT and CPM-KO at pH values ranging from 5 to 8.5. In Figure 46 C, both lines of CPM-KO show a significant decrease in enzyme activity compared to WT on the whole range of pH. In WT, the maximal CP activity was obtained at pH 7, but the enzyme still retained about 90% of its activity at pH 7.5 and 70% at pH 8. The activity dropped sharply at acidic pH. In CPM-KOs, there was still a slight enzyme activity, mainly at acidic pH. We speculate that this slight activity could not be due to CPM because it does not follow the pH/activity pattern of CPM in WT, so that what we saw is the activity of other carboxypeptidases like CPD or CPH. These enzymes show their maximum activity in the range of pH 4.5 to 6 and are inactive at pH 7.5 [221].

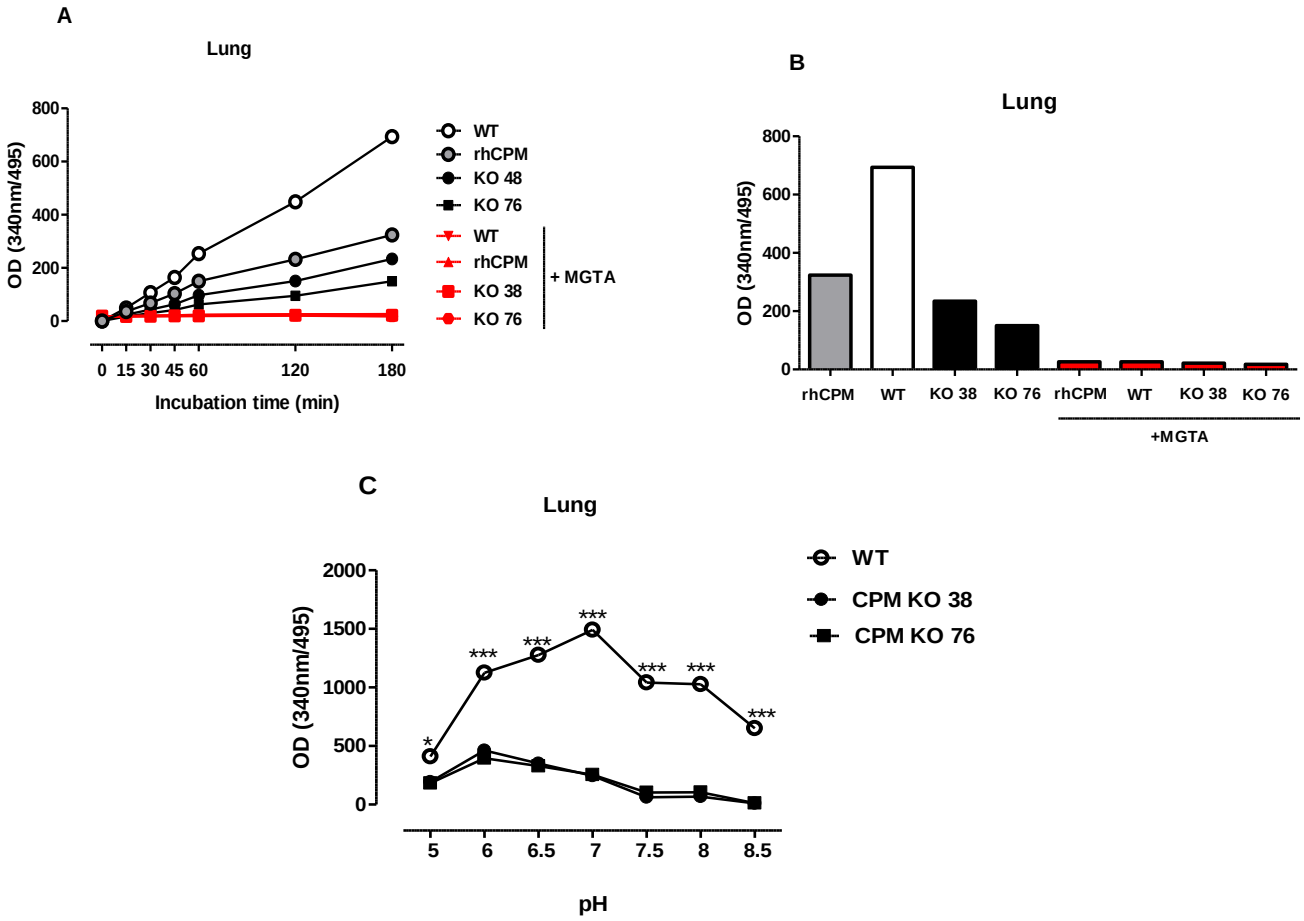

*Figure 46: A: CPM enzyme activity assay of CPM-KO, WT and rhCPM lung, 3 hours of incubation. B: CPM enzyme activity assay of CPM-KO and WT lung after 6 hours of incubation. C: Effect of pH on CPM activity of CPM-KO and WT lung after 3 hours of incubation. WT (n=3), CPMKO L-38 (n=3) and CPMKO L-76 (n=2). Data are expressed as mean ± SEM, *p<0.05; ***p<0.001 when compared with other groups, unpaired t-test.*

6.9.5 Effects of CPM deletion on the hematopoietic system

SDF-1, or CXCL12, is a chemokine produced by bone marrow (BM) stromal cells. This factor provides a potent retention signal for hematopoietic stem/progenitor cells (HSPC) and strongly attracts HSPC cells in the bone marrow. When SDF-1 is exposed to CPM, lysine is rapidly cleaved from the C-terminus producing des-lysSDF-1, and thereby reducing the ability of SDF-1 to stimulate chemotaxis and to mediate the retention of HSPCs in the bone marrow, facilitating their entry to the blood circulation [222]. Based on these findings, we decided to investigate our CPM-KO rats for changes in hematopoiesis. BM, spleen and blood samples were taken from WT and CPM-KO rats and blood cells were evaluated by fluorescence activated cell sorting (FACS). The number of blood cells per mg spleen was not significantly different between SD and CPM-KO samples (Figure 47 A). The percentage of non-classical monocytes decreased in CPM-KO spleen and the percentage of CD8+T cells increased compared to WT (Figure 47 B). There was no alteration in the other cell types between CPM-KO and WT. In BM, CD8+T cells increased per µL BM in CPM-KO compared to the WT, and there was no alteration in other cell types (Figure 47 C). In Figure 47 D, we compared cell percentages of all leukocytes in BM. The percentage of T cells, CD8+ T cells and classical monocytes from BM increased in CPM-KO compared to WT. Blood samples were also

evaluated by FACS analysis in both male and female animals (Figure 48 A and B). In males and females, there was a significant reduction of B cells in CPM-KO in blood compared to WT. But it was only in male rats that we saw an additional dramatic reduction in different cell types including all leukocytes, neutrophils, non-classical monocytes, T cells, T helper cells, and cytotoxic T cells in CPM-KO whole blood samples when compared to WT (Figure 48 B).

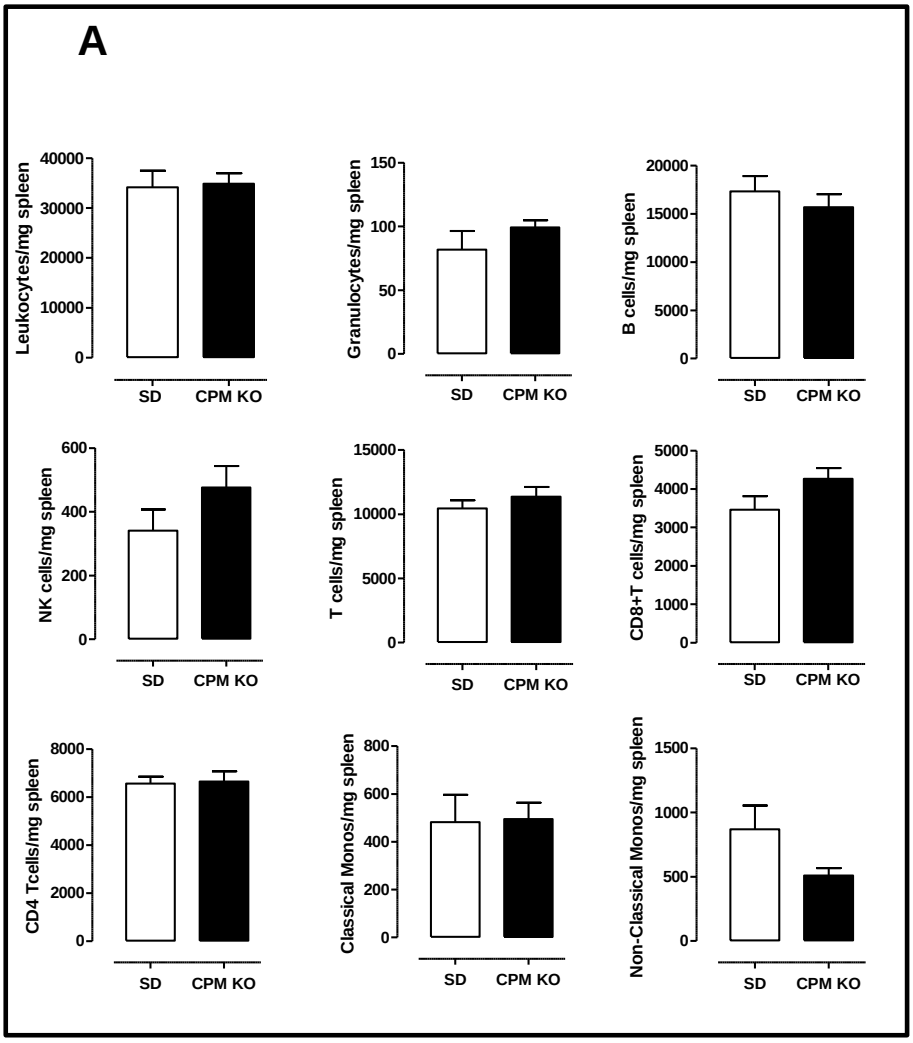

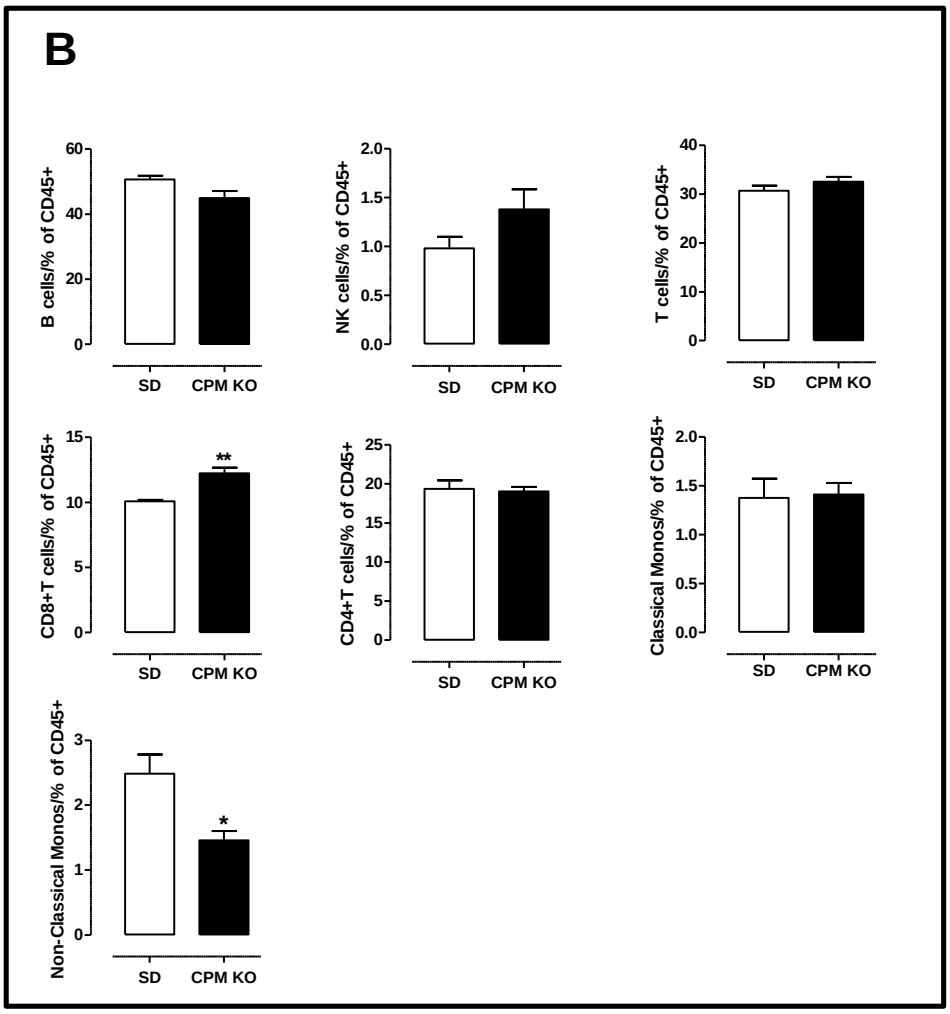
B
B cells/% of CD45+
60
40
20
0
SD
CPM KO
NK cells/% of CD45+
2.0
1.5
1.0
0.5
0.0
SD
CPM KO
T cells/% of CD45+
40
30
20
10
0
SD
CPM KO
CD8+T cells/% of CD45+
15
10
5
0
**
SD
CPM KO
CD4+T cells/% of CD45+
25
20
15
10
5
0
SD
CPM KO
Classical Monos/% of CD45+
2.0
1.5
1.0
0.5
0.0
SD
CPM KO
Non-Classical Monos/% of CD45+
3
2
1
0
*
SD
CPM KO

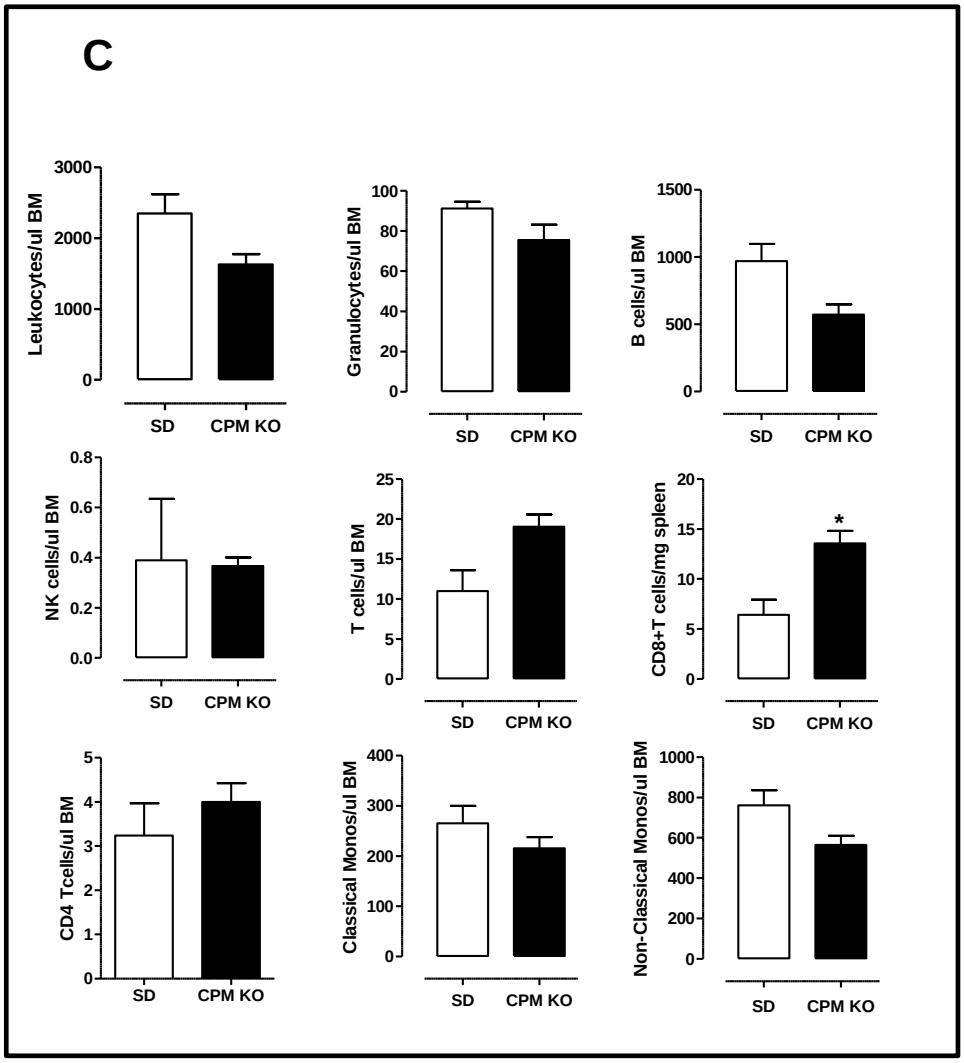
C
Leukocytes/ul BM
3000
2000
1000
0
SD
CPM KO
Granulocytes/ul BM
100
80
60
40
20
0
SD
CPM KO
B cells/ul BM
1500
1000
500
0
SD
CPM KO
NK cells/ul BM
0.8
0.6
0.4
0.2
0.0
SD
CPM KO
T cells/ul BM
25
20
15
10
5
0
SD
CPM KO
CD8+T cells/mg spleen
20
15
10
5
0
*
SD
CPM KO
CD4 Tcells/ul BM
5
4
3
2
1
0
SD
CPM KO
Classical Monos/ul BM
400
300
200
100
0
SD
CPM KO
Non-Classical Monos/ul BM
1000
800
600
400
200
0
SD
CPM KO

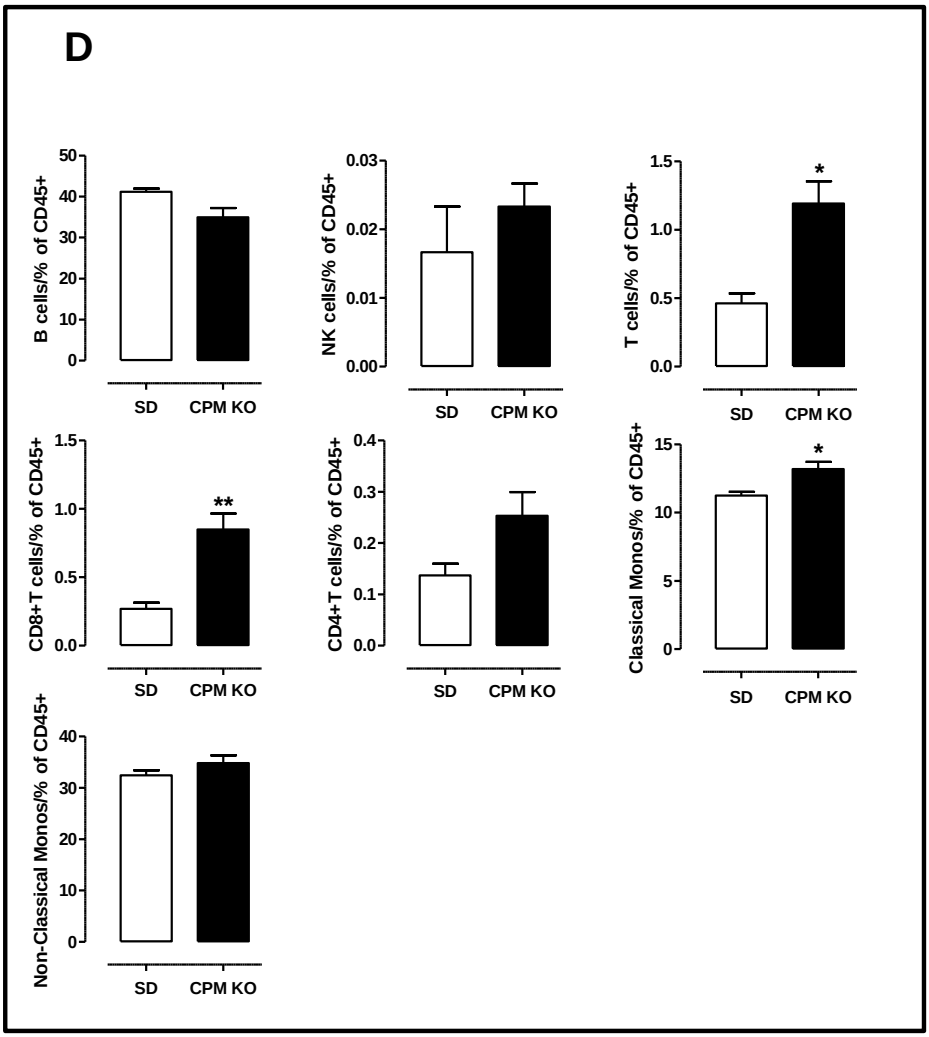

*Figure 47: FACS analysis of leukocytes in bone marrow and spleen of WT and CPM-KO rats. A: Number of leukocytes/ per mg spleen, and B: Percentage of leukocytes per CD45+cells in spleen. C: Number of leukocytes/ per µl bone marrow, and D: Percentage of leukocytes/µl bone marrow, and D: Percentage of leukocytes per CD45⁺cells in bone marrow. WT (n=3) and CPM-KO (n=3). Data are expressed as mean ± SEM, *p<0.05; **p<0.01 when compared with control groups, unpaired t-test.*

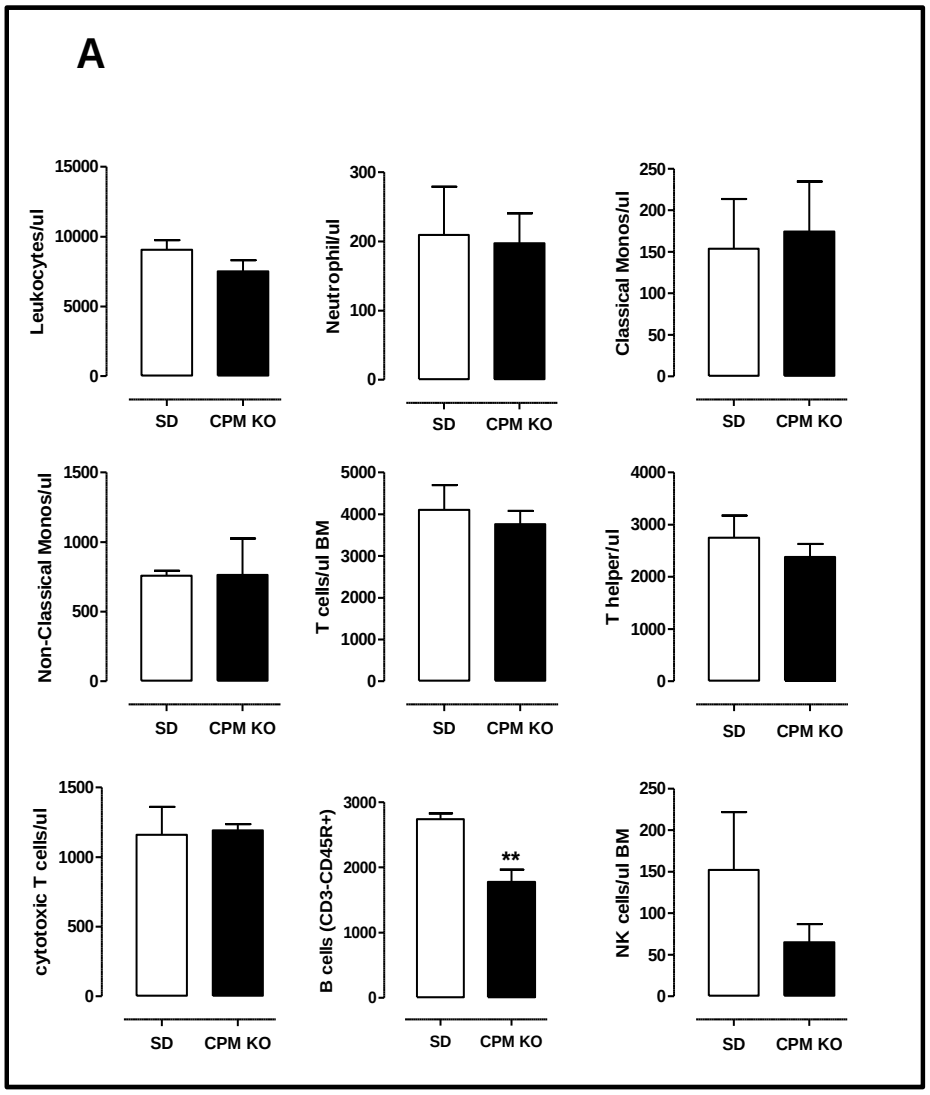
A
Leukocytes/ul
15000
10000
5000
0
SD
CPM KO
Neutrophil/ul
300
200
100
0
SD
CPM KO
Classical Monos/ul
250
200
150
100
50
0
SD
CPM KO
Non-Classical Monos/ul
1500
1000
500
0
SD
CPM KO
T cells/ul BM
5000
4000
3000
2000
1000
0
SD
CPM KO
T helper/ul
4000
3000
2000
1000
0
SD
CPM KO
cytotoxic T cells/ul
1500
1000
500
0
SD
CPM KO
B cells (CD3-CD45R+)
3000
2000
1000
0
**
SD
CPM KO
NK cells/ul BM
250
200
150
100
50
0
SD
CPM KO

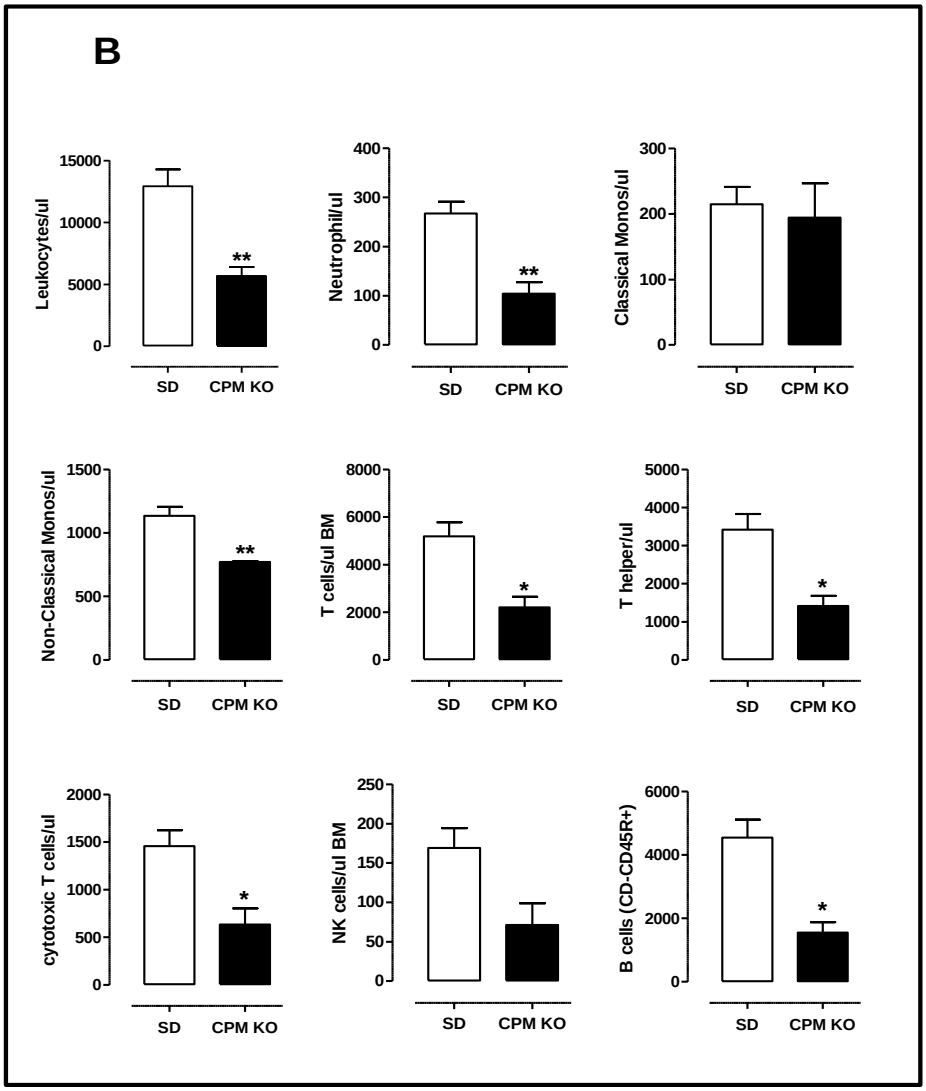

*Figure 48: FACS analysis of leukocytes per µl blood in WT and CPM-KO female (A) and male (B) rats. WT (n=3) and CPM-KO (n=3). Data are expressed as mean ± SEM, *p<0.05; **p<0.01 when compared with control group, unpaired t-test.*

7 Discussion

7.1 Transgenic rats constitutively overexpressing kinin B2 and B1 receptors exclusively in the endothelium

As the only animal model for HAE, a C1-INH deficient mouse [214], does not present characteristics that can be compared with human clinical symptoms, our group intended to generate an alternative animal model, which can reproduce the human clinical symptoms of HAE. For this purpose, we generated a rat which overexpresses the B2R, which is the main receptor for BK, in the endothelium. With the knowledge that BK is considered as the major effector of swelling in angioedema without wheals [223], we expected that an animal overexpressing its receptor would be prone to reproduce the angioedema attacks when stimulated. The choice of overexpressing the B2R only in the endothelium was made based on the fact that only the proteins of the plasma KKS seem to be involved in HAE, leading mainly to the activation of endothelial B2R. Because of their large size compared to the mouse, rats are more accessible to microsurgical techniques, tissue sampling, and for the in vitro study of organ function. The development of transgenic technology in the rat was particularly important for cardiovascular research, for which this species is the most common animal model [224]. Therefore, we decided to generate a B2R-TGR on a Sprague Dawley rat background.

We had two founders of B2R-TGR, generating the Lines (L)-11248 and L-11206. During the course of genotyping of the B2R-TGR, we observed in L-11248 that in some litters all pups were positive for the transgene, although they were from heterozygous transgenic and non-transgenic parents. Initially the explanation for this unexpected phenomenon was the random nature of an integration event. This means that one or multiple transgenes can integrate at one or multiple chromosome locations in the host genome as a result of pronuclear injection. So, these pups may have had more than one transgene integrated into their chromosomes. To clarify this, the B2R transgene location in these litters was mapped using the inverse PCR method. We found that the transgene was integrated on chromosome 19 and all transgenic animals were supposed to carry this integration site in only one site. So, the only explanation of the unexpected phenomenon observed in some litters of our pups (all were positive for the transgene) would be that it occurred by chance.

In the beginning, we had two lines for the B2 receptor transgene, as mentioned above (L-11248 and L-11206). Transgene over-expression at the level of mRNA was determined in different organs of both lines with primers targeting the endogenous and the total B2R expression (transgene + endogenous). The total B2R expression was significantly higher in all organs of L-11248 rats when compared to WT, while the expression of endogenous B2R was slightly reduced or not affected. However, L-11206 did not express transgenic B2R at all in all organs tested, although genotyping confirmed the existence of the B2Rtransgene in this line. One possible

explanation could be that this transgene might be inserted in an inactive domain of a chromosome and is therefore not transcribed. Consequently, L-11206 was excluded from further studies and we continued using only the L-11248 rats for all experiments.

It was necessary to confirm that the B2R transgene was expressed only in endothelial cells. The exclusive overexpression of B2R mRNA in B2R-TGR of L-11248 was demonstrated by in situ hybridization using the RNAscope method. This new technology enables the detection of almost any RNA with single-molecule sensitivity and high specificity in tissues. RNAscope was performed on sections of aorta and other tissues from adult B2R-TGR. As expected, there was an overexpression of B2R exclusively in the endothelium of B2R-TGR compared to controls. In addition, the overexpression of B2R mRNA was also evaluated taking RNA from intact and denuded aorta. There was a decrease in the total B2R in denuded aorta from B2R-TGR. This further confirmed that our transgenic animals were suitable for the planned experiments.

In order to study inparallel the effects of the other kinin receptor, B1R, and also in an overexpression model, besides B2R-TGR, we also included B1R-TGR in our experimental protocols. These transgenic rats overexpressing B1R exclusively in the endothelium had already been generated and published by our group [215]. It is a fact that the expression of B1R in different cell types is induced under pathological conditions [10]. For instance, B1R expression in endothelial cells is induced in vitro by incubating endothelial cells with interleukin-1β and interferon-γ [225], high glucose [209]or angiotensin-converting enzyme inhibitors like enalaprilat [226]. Furthermore, in vivo studies demonstrated the induction of B1R in endothelial cells under hypertension [227], heart failure [228], endotoxic shock [229] and atherosclerosis [230]. In a study done by Lagneux et al., agonist induced vasorelaxation mediated by B1R occurred only after receptor induction by LPS and not under physiological conditions [231]. I confirmed the data of Merino et al. [215], showing that the mouse transgene was significantly over-expressed in heart and lung tissue and also in aorta. Surprisingly, not only the exogenous B1R transgene but also the endogenous rat B1R was significantly over-expressed in heart, lung and aorta. As mentioned above, B1Rs are normally not expressed under physiological conditions, but induced after pathological conditions such as tissue injury or during certain inflammatory processes. Studies have shown that some cytokines and growth factors - including IL-1β, IL-2, interferon-γ, and epidermal growth factor - increase the expression of B1 receptor and consequently its response to tissue isolation and incubation [232]. The endogenous B1 receptor induction in B1R-TGR may not be related to the trauma of isolating tissues ex vivo, since endogenous B1R is not increased in WT rats. It is noteworthy that all animal groups were treated under the same conditions throughout the experiment. Up-regulation of endogenous B1R brought us to an assumption that constitutive expression of B1R might have a positive feedback on its own expression. Our finding could be explained by an investigation done by Schanstra et al. in 1998 [233]. They studied the molecular mechanism of B1R up-regulation in cultured human lung fibroblasts. They observed that the B1R is up-regulated by its own agonist mediated by the induction of the transcription factor NF-kappa B, which bound to the NF-kappa B binding site located in the promoter region of the human B1R gene to induce B1R expression. Since B1R has considerable ligand-independent constitutive activity, its transgenic overexpression may also induce NF-kappa B and thereby endogenous B1R expression.

In this study, the over-expression of B2R in the thoracic aorta from B1R-TGR was unexpected because a down-regulation should occur as a regulatory mechanism for over-expression of B1R. It has been reported that deletion of B2R is compensated by the up-regulation of the B1R subtype and vice versa [234, 235, 236]. There is evidence indicating that the induction of B1R expression by angiotensin II, laminar shear stress, high glucose, heart failure, tissue damage, myocardial

infarction, diabetic cardiomyopathy and ischemia-reperfusion injury lead to the co-expression of B1R and B2R in endothelial and heart cells, and in some cases it is vice versa [237, 238, 239, 240, 94, 228, 241]. A co-expression of B1R and B2R has also been reported in lung, esophageal squamous carcinoma and prostate cancer [242, 243, 244]. The mechanism by which B2R mRNA expression is increased in rats overexpressing kinin B1R is not clear and needs further investigation.

7.2 Overexpression of B1 and B2 receptors induces hypotensive responses to agonists in vivo

B1R-TGR rats showed normal levels of mean arterial pressure and heart rate compared to wild type rats. These findings were in accordance with the study done by Ni et al., in which transgenic mice over-expressing B1R were normotensive [245]. In a previous study done by our group, normotensive B1R knockout mice were reported, which showed a significantly reduced hypotensive response to LPS injection [181]. Taken together, these studies showed that B1R is not involved in basic blood pressure regulation. However, very low doses of des-Arg^9-BK already produced a dose-dependent hypotension when administered intravenously (i.v.) to B1R-TGR as compared to wild type rats [215].

The B2R-TGR rats used in the present study also presented normal levels of mean arterial pressure and BK produced a significant dose-dependent hypotension when administered i.v., whereas control SD rats did not respond to this treatment. The existence of different in vivo compensatory mechanisms could be one reason for unaltered blood pressure in B1R- and B2R-TGR rats. It is known that the KKS and RAS are connected all over the cardiovascular system. Activation of one system results in the counter activation of the other system to maintain physiological homeostasis. ANG II from RAS counterbalances some of the functions of BK by inducing vasoconstriction and the elevating of blood pressure [217].

7.3 Vascular reactivity and signalling pathways in B1R- and B2R-TGR aorta

Relaxant responses induced by the kinin B1 and B2 receptor agonists des-Arg^9-BK and BK were tested in B1R- and B2R-TGR aorta. Our transgenic rats were characterized in terms of vascular reactivity through isometric relaxation and contraction recordings following application of the respective agonists and, in addition, pretreatment of tissue with the respective antagonists. To perform the experiments, the in vitro well characterized organ bath technique was applied. The organ bath is a traditional experimental set-up that is commonly used to investigate the physiology and pharmacology of different kinds of vessels or tissue preparations. B1R-TGRaortic rings responded dramatically with a dose-dependent relaxation to des-Arg^9-BK. This effect was abolished by pre-incubation of aortic rings with R-715 (B1R antagonist). BK also induced a significant vasorelaxation in B2R-TGR aortic rings compared to wild type aorta, and this effect

was abolished by pre-incubation of aorta with Hoe140 (B2R antagonist). These results confirmed the over-expression of B1R and B2R in our transgenic rats. In a previous study of Lagneux et al., wild type rat aortic rings showed a relaxation to B1R agonists only after B1R induction by heat stress or LPS [231], confirming the absence of B1R in normal rat aorta. Aortic rings of WT rats in the present study did not respond to BK confirming previous studies. For instance, there is a report by Siltari et al. demonstrating that BK induces relaxation in mesenteric arteries from normotensive young rat, but not in aorta [246]. In general, it is assumed that, unlike mesenteric arteries, the aorta is a conduit vessel with a different endothelial function than resistance vessels. However, we observed that in phenylephrine preconstructed B2R-TGR aorta, BK induced a dose-dependent relaxation at very low doses (10^{-8} M) and even a biphasic response, i.e., relaxation followed by constriction, at higher doses (10^{-5} M). Normally aorta does not respond to kinin receptor agonists but transgenic overexpression allowed us to investigate kinin agonist induced vasodilatory effects in aorta.

7.3.1 BK-induced vasorelaxation in B1R-TGR aorta

Since we had observed the upregulation of B2R in B1R-TGR, we investigated the agonists for the other kinin receptor subtypes (BK and des-Arg^9-BK) in each transgenic model, i.e., B1R-TGR and B2R-TGR, respectively. Des-Arg^9-BK had no effect on the aorta isolated from B2R-TGR rats, whereas BK surprisingly showed a significant relaxant effect on the aortic rings from B1R-TGR rats at a higher concentration (10^{-6} M) in vitro, consistent with the increased expression level of B2R mRNA in B1R-TGR aorta. However, the relaxation of aortic rings induced by BK was not abolished by the B2R antagonist Hoe140, whereas R-715 as the B1R antagonist completely inhibited the relaxation response of BK. We then tested whether this was due to the degradation of BK to des-Arg^9-BK by CPM in the tissue and pre-incubated the aorta rings with the CPM inhibitor, MERGETPA. It also did not affect the vasorelaxation induced by BK. The complete blockade of the response of BK by the B1R antagonist showed that only direct B1R activation was responsible for the enhanced responses in B1R-TGR aorta induced by BK at higher concentrations.

7.3.2 BK-induced relaxation is endothelium dependent in B2R-TGR

A series of studies have shown that BK-induced relaxation in rats and humans depends on the endothelium [247, 217, 218]. The involvement of endothelium-dependent mechanisms in the relaxation response of B2R-TGR aorta was established, using endothelial denuded aorta rings of B2R-TGR. Endothelial denudation completely abolished the BK-induced relaxation in B2R-TGR aorta. The results of the current study clearly indicated that endothelium integrity is an essential prerequisite for BK-induced relaxation. The role of the endothelium in BK-induced relaxation has been described in various studies. Initially the essential role of endothelial cells in acetylcholine (ACh) induced relaxation was described by Furchgott[248]. Afterwards, Altura and Chand in 1981 also demonstrated the need for functional integrity of the endothelium in BK-mediated

vasodilation [249]. A study done by Cherry et al. in 1982 demonstrated BK-induced relaxation in different isolated arteries of dogs like the coronary, celiac, mesenteric, renal, pulmonary and femoral arteries, and the relaxation response of these arteries failed after endothelial cell removal [250]. Vasodilator agents such as ACh and BK induce vasorelaxation responses through endothelial cells and their release of vasodilatation factors [251]. Therefore, endothelium integrity is an essential prerequisite for ACh and BK-induced relaxation.

7.4 Signalling pathways involved in kinin receptor-induced vasodilation

7.4.1 The BK-induced relaxation response of B1R- and B2R-TGR aorta relies on the endothelium-derived NO

Based on several studies, there are three major signaling pathways characterized for the kinin-induced vasodilatory effects: nitric oxide (NO), prostacyclin and endothelial derived hyperpolarising factor (EDHF). Each of these endothelium-derived relaxing factors induces relaxation of vascular smooth muscle cells through its own pathway. It is known that these pathways do not contribute to the same degree in different types of vessels [252, 253, 248]. It has been shown that conduit vessels present more NO-mediated relaxation, and that the contribution of EDHF-mediated relaxation is considerably high in small resistance vessels [254]. The data of the current study indicate that relaxation in aorta induced by BK and des-Arg^9-BK is completely abolished after incubation of aortic rings with L-NAME, which showed that BK and des-Arg^9-BK induced relaxation mainly relies on the endothelium-derived NO. Another study demonstrated that BK stimulates B2R in endothelial cells in culture as well as in mouse carotid arteries and releases NO to regulate the vascular muscle tone [255]. Many studies have been published on the important role of NO in BK-induced coronary vasodilatation. Some of these investigations indicated that blocking NO synthesis dramatically abolished BK-induced relaxation of canine coronary arteries; however, several other investigations have suggested that inhibition of NO synthesis only partially reduced the BK-induced dilation of porcine coronary arteries [256, 257, 258, 77]. In a study done by Ignjatovic in 2004, it was shown that the activation of B1R by des-Arg^{10}-kallidin leads to prolonged NO release by activating eNOS in bovine and iNOS in stimulated human endothelial cells [226]. In our study, we have shown that BK and des-Arg^9-BK induced relaxation in aortic rings of B2R- and B1R-TGR mainly relies on the endothelium-derived NO.

7.4.2 The BK-induced relaxation response of B1R- and B2R-TGR aorta does not rely on the prostacyclin signaling pathways

In general, prostacyclin and EDHFs contribute to the relaxant effect of BK that is not inhibited by NO-synthesis (NOS) inhibition [259, 123, 260]. The contribution of the prostacyclin signaling pathway was investigated in the present study, despite having seen a complete blockade induced by L-NAME, to rule out any possibility of a prostacyclin effect. Indomethacin, as a COX (Cyclooxygenase) inhibitor, did not reduce the agonist-induced relaxant response in both B1R- and B2R-TGR aorta. The results clearly indicate that the vasorelaxation response mediated by kinins was not mediated via the prostacyclin pathway. Surprisingly, we observed that after pre-applying indomethacin on B2R-TGR aortic rings, the relaxation response induced by BK significantly increased compared to the control aortic rings. This phenomenon could be explained by previous studies demonstrating that BK induced not only relaxation but also contractions generating prostaglandins directly acting on smooth muscle cells [261, 262, 263, 252]. For the first time, Ihara et al. in 2000 indicated that BK could also induce contraction in an endothelium-dependent manner in the porcine interlobar renal artery mediated by the generation of TXA2 (thromboxane A2) and PGH2 (prostaglandin H2) [264]. Therefore, the increased relaxant effect of BK observed in B2R-TGR aorta after indomethacin treatment can be attributed to the inhibition of the prostaglandin-mediated contraction response, which allows BK to induce the actual extending of vasodilatation with no contractile effect.

7.4.3 Big conductance calcium sensitive potassium channels ($BKCa^{2+}$) are involved in the vasorelaxation induced by BK

The eventual hyperpolarization of the smooth muscle cells (VSMC) found in the vessels leads to relaxation. To reach hyperpolarization, Ca^{2+} influx should be decreased by reducing the open probability of voltage-dependent calcium channels [142, 265]. Vascular endothelial and smooth muscle cells possess different potassium channels, which play an essential role in the regulation of hyperpolarizing electrical events. The opening of K^+ channels results in the efflux of this cation and membrane hyperpolarization [122]. Four different classes of K^+ channels have been identified in VSMCs: ATP-sensitive K^+ channels (K_{ATP}), large (big)-conductance Ca^{2+}-activated K^+ channels (BK_{Ca}), voltage-activated K^+ channels(K_V), and inward rectifier K^+ channels (K_{IR}) [266]. In the current study, to investigate the possible involvement of K^+ channels in vasorelaxation induced by kinins, non-selective and selective K^+ channel blockers were applied. The non-selective K^+ channel blocker TEA partially blocked the vasorelaxation induced by BK and des-Arg^9-BK in both B1R- and B2R-TGR aorta. Glibenclamide, the specific K_{ATP} channel blocker, showed no involvement in the relaxation induced by kinins. However, iberiotoxin, the $BKCa^{2+}$blocker, strongly attenuated the vasorelaxation effect induced by kinins in both B1R- and B2R-TGR aorta. This indicates the involvement of $BKCa^{2+}$ in kinin-induced vasorelaxation. Our findings are in agreement with previous in vivo investigations done by Nelson et al. in 2004 demonstrating that des-Arg^9-BK-induced relaxation response was mediated by NO and $BKCa^{2+}$ activation in rat aorta [227]. Vang et al.

in 1994 showed that BK-induced microvasculature vasodilatation in the lung is mediated by hyperpolarization produced by the activation of $BKCa^{2+}$ channels due to endothelial NO liberation [267].

7.4.4 TRPC4 is involved in kinin-induced vasodilatation in B1R- and B2R-TGR aorta via Ca^{2+} influx into endothelial cells

TRP channels are important/crucial modulators of vasoconstriction and vasodilatation signalling pathways initiated by G protein-coupled receptors (GPCR). These channels play an important role in the Ca^{2+} influx into endothelial cells resulting in endothelium-dependent vasodilatation. According to the literature, around 20 family members of diverse TRP channels are expressed in endothelial cells [135], and some of these channels – TRPC1, TRPC3 [145], TRPC4, TRPC5, TRPC6 [146], TRPV1, TRPV3 [147], TRPV4 [148], and TRPA1 [149]- are functional in endothelial cells. Among them, TRPV1, TRPV3, TRPV4, TRPA1, TRPC3, and TRPC4 channels have been reported to be involved in endothelium-dependent vasodilatation [149, 147, 168, 268, 269]. A range of studies has shown that TRP channels are expressed in both smooth muscle and endothelial cells, with a diverse pattern of distribution in different vascular beds and animal species [137]. TRPC3 is predominantly present in human pulmonary artery endothelial cells, but not bovine, whereas TRPC1 is expressed in mouse aortic endothelial cells and is not present in rat [270]. A number of studies which have focused on TRP channels reported that among the TRPC family, TRPC1 and TRPC6 are the most predominant members expressed in vascular smooth muscle cells [271]. TRPC6's main function is regulating vascular tone, especially vasoconstriction and VSMC proliferation [272, 273, 274, 275]. TRP channels participating in endothelium-dependent vasodilatation also vary across the vascular tree. Findings made by Liu et al. in 2006 revealed that BK-induced vasodilatation in rat mesenteric arteries is mediated through TRPC3 [166]. A later study by Senadheera et al. (2012) showed that TRPC3 are present in the endothelium of mesenteric arteries of rat and mouse and play role in endothelium-dependent dilation [168]. Freichel et al. (2000) showed that TRPC4 is involved in endothelium-dependent vasodilation in response to ACh using aortic rings of $TRPC4^{-/-}$ mice [170]. TRPC3 plays a role in the BK-induced NO- and EDHF-type response in males and TRPV4 plays a role in the BK induced NO-mediated response in female porcine isolated coronary arteries [276]. It has been shown that TRPC6 is one of the important channels participating in BK-induced non-CCE (capacitive Ca^{2+} entry) in the mouse heart microvessel endothelial cell line (H5V) [277]. A study performed by Yang et al. (1999) indicated that capsaicin, as an opener of TRPV channels, caused endothelium-dependent relaxation of isolated mesenteric arteries [278]. It is worthwhile to mention that in the present study, we provide evidence for the involvement of TRPC4 in the signalling pathway of des-Arg^9-BK and BK-induced vasodilatation in B1R- and B2R-TGR aorta. The involvement of this TRP channel in kinin signalling has, to our knowledge, not been published so far. We assessed the role of different TRPs (their respective antagonists given in brackets) including TRPC3 (Pyr3), TRPC4 (ML204), TRPC5 (AC1903), TRPC6 (SAR7334 and SHO45), TRPV1 (RN-1734) and TRPV4 (capsazepine) in kinin-induced vasorelaxation. Based on Maier et al., SAR7334 inhibits TRPC6, TRPC3 and TRPC7, while TRPC4 and 5 are not affected by the inhibition [279]. Therefore, a second inhibitor of TRPC6 with higher specificity named SHO45 was assessed in

B1R-TGR aorta and we confirmed that the slight reduction in the vasodilatation effect of des-Arg^{9}-BK (10^{-8} M) in B1R-TGR aorta after blocking by SAR7334 is probably mediated through other TRPCs, maybe TRPC7, and that TRPC6 is not involved in B1R receptor signaling. Our present results demonstrated the involvement of TRPC4 channels in the vasodilatory effect induced by kinins and other TRP channels did not seem to be involved in this pathway; however, we cannot exclude a contribution of TRPC7 in B1R-induced vasorelaxation. To confirm our findings, the TRPC3, TRPC4, TRPC5, TRPC6, TRPV1 and TRPV3 transcripts in aorta isolated from B1R-, B2R-TGR and WT rats were detected and quantified at the level of mRNA. According to the results, all the investigated channels are expressed in both TGR and wildtype rats without any significant differences. Based on our findings, TRPC6 transcript expression is significantly higher than other TRP channels in rat aorta. This can be explained by a series of studies which demonstrated that TRPC6 is predominantly expressed in vascular smooth muscle cells and mainly contributes to vasoconstriction and VSMC proliferation [272, 273, 274, 275]. Nevertheless, in B1R- and B2-TGR aorta, vasodilatation was mediated through TRPC4. So, for the first time, we demonstrated the involvement of TRPC4 in the signalling pathway of des-Arg^{9}-BK and BK-induced vasodilatation in aorta.

7.5 Angioedema induction in rats overexpressing the kinin B2 receptor

7.5.1 Mustard oil acute treatment to induce angioedema

Hereditary angioedema (HAE) is a rare genetic disorder that mostly arises due to an increase in BK [280]. Recent generated HAE mouse models only show increased vascular permeability, but no spontaneous swelling episodes comparable to patient symptoms [214, 281]. Therefore, we aimed to develop and characterize a transgenic rat overexpressing B2R in endothelial cells as an alternative model for HAE and BK-mediated angioedema studies, and to challenge them to develop angioedema episodes similar to HAE in humans. Acute angioedema attacks were induced by applications of mustard oil on the ear and Evans blue (EB) was used to assess the degree of oedema. Mustard oil is a local irritant that induces plasma leakage and inflammation. In the ear where mustard oil was applied, EB extravasation was dramatically higher in B2R-TGR when compared to mustard oil treated WT rats, and also the skin surrounding the region where mustard oil was applied showed higher vascular permeability. In 2002, Han et al. developed C1 inhibitor-deficient mice, which showed no obvious phenotypic abnormality [214]. However, after EB injection, C1 inhibitor-deficient mice revealed increased vascular permeability in comparison with WT littermates in basal conditions. Furthermore, they revealed that extravasations of EB were much more extensive in C1 inhibitor-deficient mice compared to WT after the application of mustard oil to the ears [214]. In the present study, the possible systemic effects induced by mustard oil challenge was evaluated in internal organs/tissues. EB extravasation was significantly higher only in the kidney in male B2R-TGR rats. We assume that this increased vascular permeability remote from

the application site was not related to mustard oil treatment. During the experiments with mustard oil challenge, we noticed that the female B2R-TGR rats also already showed increased vascular permeability under basal conditions in bowel, uterus, liver and kidney when compared to age-matched WT females. This exacerbated vascular permeability in females compared to males supports the potential of the transgenic rat model as a tool to study the influence of sexual hormones on the regulation of the BK-release and HAE. However, additional experiments comparing male and female B2R-TGR rats are necessary to explain this apparent gender difference.

7.5.2 B2R-TGR, a new rat model of HAE mimicking the swelling episodes experienced by humans

We found to our surprise that some B2R-TGR developed strong bowel swelling together with damage in the pancreas. In about 10% percent of B2R-TGR rats, these spontaneous and sporadic abdominal angioedema occurred. Histological investigation of the intestine revealed increased thickness of submucosal tissue and a definite thickening of villi compared to healthy B2R-TGR. The expression of B2R in swollen ileum was not higher than in non-swollen tissues (data not shown). This result showed that the B2R expression in the intestine is not significantly changed during angioedema attacks in the B2R-TGR rats. However, it doesn't mean that B2R never changes/increases in HAE patients during attacks, since this animal model already has a permanent increased expression of the B2R in the B2R-TGR rats [282].

Pancreatic lesions characterized by blood clots spread throughout the tissue were observed in B2R-TGR rats with intestinal swellings. Comparing B2R-TGR pancreas with and without haemorrhagic clots, an increase in the size and amount of Langerhans islets was observed [282]. A great increase in α-cells and decrease in β-cells was detected in pancreas after immunohistochemical analysis when compared to pancreas from non-affected B2R-TGR rats. The pancreatic lesions observed could be due to the pancreatic edema or represent a secondary event to intestinal swelling, which can induce partial or complete ductal obstruction resulting in pancreatitis [283]. The correlation between HAE and pancreatitis is not yet fully understood. More than 20 years ago, a few independent cases were reported among HAE patients developing idiopathic pancreatitis [283, 284]. The haemorrhagic injuries found in our model could correspond to necrotizing haemorrhagic pancreatitis. Haemorrhage can occur in patients with severe necrotizing pancreatitis or as a result of pancreatic pseudoaneurysm rupture, representing a life-threatening emergency in humans. However, through behavioural observations in our rats, we did not find any signs of pancreatitis such as pain or suffering; also, we did not notice any sudden death among these rats. Despite having always observed the pancreatic lesions accompanying the intestinal swellings, we cannot exclude a direct effect of excessive B2R activation causing pancreatic abnormalities in the transgenic rats. Recent studies showed that B2R antagonists exert protective effects in different rodent models of pancreatitis [285, 286], suggesting that B2R is involved in the onset of pancreatic oedema and inflammation, encouraging further studies on the role of B2R in pancreatic physiology.

7.5.3 Vascular permeability analyses after B2 receptor inhibition using Icatibant in B2R-TGR

If BK binding and activation of B2R are mainly responsible for the observed intestinal swellings in B2R-TGR, a B2R antagonist should be efficacious in the treatment of swelling attacks. To investigate whether this hypothesis proves true, we treated the affected rats with the selective B2R antagonist Hoe140 (Icatibant). Icatibant has a high specificity for the B2R and blocks different effects mediated by B2R [287, 288]. Icatibant inhibits increased vascular permeability in C1 esterase inhibitor–knockout mice [289] and blocked the vasodilatation induced by BK in humans [290]. Icatibant exerts significant benefits in patients with HAE having acute attacks. There have been several lines of evidence indicating the importance of B2R blockade in HAE patients. Bork et al. (2014) found that icatibant markedly improved skin swelling and abdominal pain attacks of HAE patients and has a great beneficial effect [288]. A single dose of icatibant showed a noticeable effect in the edemic B2R-TGR group. The EB-extravasations in icatibant-treated edemic rats were decreased in the heart, stomach, rectum, skeletal muscle, skin and submandibular gland compared to the non-edemic B2R-TGR group. However, statistical significance was only reached in the heart, and in other tested organs there was a decrease in extravasation, but without statistical significance, most probably due to the small number of rats per group. In most organs of the icatibant-treated non-edemicB2R-TGR animals - especially stomach, colon, uterus and duodenum, ileum, skin and urinary bladder - EB extravasations were increased unexpectedly when compared to the vehicle-treated B2R-TGR group. Icatibant might have agonistic effect in the absence of BK. A study done by Drube et al. in 2000 showed that in certain tumour cell lines icatibant may act as mitogenic B2R agonist [291].

7.5.4 Enalapril chronic treatment to induce angioedema

Angiotensin-converting enzyme (ACE) inhibitors like enalapril are frequently prescribed drugs for the therapy of hypertension and heart failure. These drugs are believed to prevent high blood pressure and cardiovascular failure [288]. One of the side effects of enalapril is the induction of angioedema and 0.68% of patients treated with enalapril exhibited an angioedema episode [292]. Based on studies, patients with either hereditary or idiopathic angioedema are more prone to ACE inhibitor-induced angioedema [293, 294].

To date, the mechanism of ACE inhibitor-induced angioedema is not fully understood. ACE inhibitors decrease angiotensin II generation by blocking the conversion of angiotensin I to angiotensin II, which leads to reduction in blood pressure. Furthermore, they increase BK, since ACE is one of the most important BK-inactivating enzymes. Increased levels of BK cause vasodilatation and increased vascular permeability, thereby leading to angioedema [295, 294, 296, 297]. In the present study, in the B2R-TGR group which received enalapril for 30 days, the EB extravasations were increased in the stomach, heart, lung, kidney, trachea, tongue, oesophagus, duodenum, colon, brain, eyes and pancreas, but this did not reach statistical significance, most

probably due to the small number of rats per group. In SD control rats treated with enalapril, the EB-extravasation was increased in trachea and significantly in the liver when compared to vehicle-treated SD controls. Thus, our study could not clarify whether B2R-TGR are more susceptible to ACE inhibitor-induced angioedema due to insufficient statistical power.

7.6 Knockout rats lacking carboxypeptidase M

7.6.1 CPM-KO rat generation

Carboxypeptidase M (CPM) is a widely distributed enzyme, present throughout the body in tissues such as lung, placenta, kidney, blood vessels and in various body fluids including amniotic fluid and urine [298, 221, 299, 300]. CPM is a GPI-anchored metallopeptidase that plays an important role in the KKS. BK, as the main product of the KKS, is released from kininogens and exerts its biological activities through B2R. BK is converted to its active metabolite des-Arg^9-BK which binds to B1R. This conversion occurs through the enzymatic action of CPM, which is therefore also known as kininase I [298]. To investigate the role of CPM in KKS and beyond, we decided to generate a rat model lacking CPM globally. The CRISPR/Cas9 technique was applied to introduce mutations in the rat CPM gene. Two lines of CPM-KO were generated, L-38 (with a 6 base pair deletion including the ATG start codon) and L-76 (with a T insertion in the coding sequence). Both lines were functional knockouts and were utilized in the following experiments. Although CP as a widely distributed enzyme was globally knocked out in the rats, none of the KO lines showed any obvious phenotype. They were healthy and bred normally.

7.6.2 Characterization of CPM-KO rats

7.6.2.1 CPM mRNA expression level is strongly decreased in CPM-KO rat

The expression level of the CPM mRNA was quantified in KO and WT heart and lung tissues. CPM is highly expressed in heart and lung of WT rats. In both lines of CPM-KO (L-38 and L-76) the expression levels of CPM mRNA were significantly lower compared to the control group. qPCR data demonstrated that a varying percentage of CPM mRNA was detectable. The reason behind the reduction of mRNA might be due to Nonsense-mediated mRNA decay (NMD), since the open reading frame in the CPM mRNAs of both CPM-KO lines was expected to be disordered. NMD is a protective mechanism, destroying aberrant mRNAs with the potential to encode toxic truncated proteins. Means for creating loss-of-function alleles involve CRISPR/Cas9 and NMD contributes to this process [301]. Most mRNAs produced from CRISPR/Cas9 engineered genes are predicted to be recognized by the NMD pathway and degraded [302].

7.6.2.2 CPM protein is not expressed in CPM KO lungs

The CPM protein expression was analysed in CPM-KO and WT lungs. According to previous studies rhCPM has a lower molecular mass (~50 kDa) than native CPM expressed in human cells and tissues (~62 kDa) [303, 304]. We also observed the same results. A specific band was detected for CPM at approximately 55-65 KDa in WT but not in our CPM KO tissue, as expected. rhCPM yielded a band of about 50 KDa. Since rhCPM is purified from overexpressing cells and lacks the C-terminal GPI anchor, we hypothesized that the difference in molecular mass was due to a different glycosylation state compared to the native CPM. CPM was in fact strongly glycosylated and deglycosylation led to decreased size of about 47KD and to a more distinct shape of the band. This size was even smaller than that of rhCPM, which is not surprising since rhCPM is probably also partially glycosylated. In this study, we observed that CPM protein is not expressed in CPM-KO lungs, although the mRNA did not totally disappear even after the gene was knocked out. In L-38, this is explained by the lack of an ATG start codon, which does not allow for generating a protein from the mRNA. In L-76, the T-insertion leads to a frameshift during translation of the mRNA and a shortened protein with an altered amino acid sequence, which cannot be detected in Western blots. So, the lacking expression of CPM protein confirmed the functional CPM-KO.

7.6.2.3 CPM activity is strongly attenuated in CPM-KO rat

The peptidase activity of CPM was tested in lung tissue at pH 7, which is the optimum pH for CPM activity [305]. Substrate metabolism increased linearly over time in WT lung but not in CPM-KO. We observed a marked reduction in CPM activity in the lung of both CPM-KO lines, confirming the knockout of CPM in our CPM-KO rats. The hydrolysis of Dansyl-Ala-Arg by CPM was inhibited by MERGETPA in both WT and CPM-KO lung tissue, but there was still some activity left, which was equal in transgenic and control rats. This remaining activity could be attributed to other CP enzymes which are present in the tissue and could metabolize the substrate, and are unaffected by MERGETPA. It is known, that there are several CPs in lung, such as CPD, CPE etc. MERGETPA could reduce CP activity also in CPM-KO lungs, indicating that either CPM is not completely ablated or that CPN or another CP, which is inhibited by this compound, is present in the lung. According to findings of Skidgel et al., human pulmonary arterial endothelial cell membranes have high levels of CPM, but no detectable CPN [306].

CPM activity in WT and KO lung was tested with Dansyl-Ala-Arg substrate at pH values ranging from 5 to 8.5. Both lines of CPM-KO show a significant reduction in enzyme activity compared to WT on the whole range of pH tested. In WT, the maximal CP activity was obtained at pH 7, but it still retained about 90% of its activity at pH 7.5 and 70% at pH 8. The activity dropped sharply at acidic pH [307]. In CPM-KO the activity at neutral and basic pH was markedly reduced, but we had still some enzyme activity, mainly at acidic pH. We speculate that this slight activity could not be from CPM or CPN because it does not follow their pH-activity pattern as described in a study done

by Skidgel in 1989 [221], and that what we saw is the activity of other carboxypeptidases like CPD or CPE. These enzymes show their maximum activity in the range of pH 5.0–5.5 and their activity falls off dramatically with increasing pH [307]. Based on these findings we confirmed the mere absence of CPM in our CPM-KO rats.

7.6.2.4 CPM deletion augments chemotactic responses and attenuates mobilization of hematopoietic stem/progenitor cell (HSPC).

CPM is also found in blood vessels and considered as a differentiation-dependent cell surface antigen on white blood cells [37]. Marquez-Curtis et al. (2008) demonstrated the expression of CPM in bone marrow (BM) stromal cells for the first time. They also found CPM transcripts in hematopoietic progenitors, mononuclear cells (MNC), and polymorphonuclear cells (PMN) as well as mature myeloid precursors, mature monocytes and granulocytes [39].

It has been suggested that CPM is acquired early in B lymphoid ontogeny, whereas expression was absent from thymocytes and myeloid progenitors. CPM is expressed in specific stages of B-lymphocyte development [308]. These findings suggest that CPM plays an important role in B lymphopoiesis [309, 310] . The physiological role of CPM has not been fully investigated; however it is known to play a role in the regulation of peptide (kinins, anaphylatoxins, chemokines) generation through their C-terminal lysine or arginine cleavage during inflammation [311, 299]. SDF-1α, or CXCL12, is a chemokine produced by different tissues like BM stromal cells, endothelial cells and fibroblastic cells, and is constitutively expressed in spleen as well. This factor produces a strong retention signal for HSPCs and strongly attracts them into the bone marrow. The retention signal from SDF-1α is mediated via CXCR4 receptors located on HSPCs [299, 40, 312, 313]. SDF-1α has a C-terminal lysine, which renders it a CPM substrate. When SDF-1α is exposed to CPM, it rapidly cleaves the lysine from the C-terminus producing des-lys SDF-1α, thereby reducing the ability of SDF-1 to stimulate chemotaxis and to mediate the retention of HSPC cells in the bone marrow, which block their entry to the blood circulation [314]. Based on these findings we decided to investigate our CPM-KO rats in this regard. Since spleen also harbours some HSPCs in the steady state, we investigated the hematopoietic niche in this organ as well [315, ,316, 317]. Leukocytes were evaluated in BM, spleen and whole blood of WT and CPM-KO rats by fluorescence activated cell sorting (FACS). Our results demonstrated that the number of blood cells per mg spleen did not differ in CPM-KO from the control group, whereas the percentage of non-classical monocytes decreased in CPM-KO spleen and the $CD8^+$ T cell percentage increased compared to the control group. No alteration in the other cell types between CPM-KO and control was found in spleen. In BM the percentage of T cells, $CD8^+$T cells and classical monocytes increased in CPM-KO BM compared to the control.

In the blood of female CPM-KO rats, there was a significant reduction of B cells compared to the control group and no changes in other blood cell types. However, in male CPM-KO rats we saw a general reduction in leukocytes including B-cells, but also other cell types including neutrophils, non-classical monocytes, T cells, T helper cells and cytotoxic T cells. Our results can be explained in that the absence of CPM stabilizes SDF-1α in the BM and spleen, and thereby mediates the retention of HSPC cells in the bone marrow and inhibits the entry of leukocytes into the blood circulation [314].

REFERENCES

1. McCaa R E. Role of the renin-angiotensin-aldosterone and kallikrein-kinin systems in the control of fluid and electrolyte metabolism, renal function, and arterial blood pressure. Clin Exp Hypertens 4, 9–10 (1982).

2. Rhaleb NE, Yang XP, Carretero OA. The Kallikrein-Kinin System as a Regulator of Cardiovascular and Renal Function. Compr Physiol 1, 971–993 (2011).

3. Cagliani R, Forni D, Riva S, Pozzoli U, Colleoni M, Bresolin N, Clerici M, and Sironi M. Evolutionary analysis of the contact system indicates that kininogen evolved adaptively in mammals and in human populations. Mol Biol Evol 30, 1397–1408 (2013).

4. Okamoto H and Greenbaum LM. Pharmacological properties of T-kinin (isoleucyl-seryl-bradykinin) from rat plasma. Biochem Pharmacol 32, 2637–2638 (1983).

5. Gershom ES, Sutherland MR, Lollar P and Pryzdial ELG. Involvement of the contact phase and intrinsic pathway in herpes simplex virus-initiated plasma coagulation. J Thromb Haemost 8, Marie (2010).

6. Merkulov S, Zhang WM, Komar AA, Schmaier AH, Barnes E, Zhou Y, Lu X, Iwaki T, Luo G, McCrae KR. Deletion of murine kininogen gene 1 (mKng1) causes loss of plasma kininogen and delays thrombosis. Blood 111, 1274–81 (2008).

7. Lalmanach G, Naudin C, Lecaille F, Fritz H. Kininogens: More than cysteine protease inhibitors and kinin precursors. Biochimie 92, 1568–1579 (2010).

8. Schachter M. Kallikreins (kininogenases): a group of serine proteases with bioregulatory actions. Pharmacol Rev 3, 1–17 (1980).

9. Moreau ME, Garbacki N, Molinaro G, Brown NJ, Marceau F, Adam A. The Kallikrein-Kinin System: Current and Future Pharmacological Targets. Journal of Pharmacological Sciences 99, 6–38 (2005).

10. Bhoola KD, Figueroa CD and Worthy K. Bioregulation of kinins: Kallikreins, kininogens, and kininases. Pharmacological Reviews 44, 1–80 (1992).

11. Fiedler F. Enzymology of glandular kallikreins. in Bradykinin, Kallidin and Kallikrein. 103–161 (1970).

12. Movat HZ. The plasma kallikrein-kinin system and its interrelationship with other components of blood. Springer-Verlag Berlin 1–89 (1979).

13. Asakai R, Davie EW, Chung DW. Organization of the gene for human Factor XI. Biochemistry 26, 7221–7228 (1987).

14. Yu H, Bowden DW, Spray BJ, Roch SS and Freedman BI. Identification of human plasma kallikrein gene polymorphisms and evaluation of their role in end-stage renal disease. Hypertension 31, 906–911 (1998).

15. Regoli D, Rhaleb N-E, Drapeau G, Dion S, Tousignant C, D'Orléans-Juste P and Devillier P. Basic pharmacology of kinins: pharmacologic receptors and other mechanisms. Advances in Experimental Medicine and Biology 247A, 399–407 (1989).

16. Maas C. Plasminflammation—An Emerging Pathway to Bradykinin Production. Frontiers in Immunology. Frontiers in Immunology 10, (2019).

17. Yousef GM and Diamandis EP. The expanded human kallikrein gene family: locus characterization and molecular cloning of a new member KLK-L3. Genomics 65, 184–194 (2000).

18. Clements JA. The molecular biology of the kallikreins and their roles in inflammation. In: Farmer SG (ed) The Kinin System. Academic Press 71–97 (1997).

19. Black MH and Diamandis EP. The diagnostic and prognostic utility of prostate specific antigen for diseases of the breast. Breast Cancer 59, 1–14 (2000).

20. Chao J, Buse J, Shimamoto K, Margolius HS. Kallikrein-induced uterine contraction independent of kinin formation. Proc Natl Acad Sci USA 78, 6154–6157 (1981).

21. Biyashev D, Tan F, Chen Z. Kallikrein activates bradykinin B2 receptors in absence of kininogen. Am J Physiol Heart Circ Physiol 290, ron (2006).

22. Regoli D and Gobeil F. Critical insights into the beneficial and protective actions of the kallikrein–kinin system. Vascul Pharmacol 64, 1–10 (2015).

23. Jin R, Liu L, Zhang SH, Nanda A, Li G. Role of inflammation and its mediators in acute ischemic stroke. J Cardiovasc Transl Res 6, 834–851 (2013).

24. Campbell DJ. Towards understanding the kallikrein-kinin system: insights from measurement of kinin peptides. Brazilian Journal of Medical and Biological Research 33, 665–677 (2000).

25. Ramachandran R, Altier C, Oikonomopoulou K, and Hollenberg MD. Proteinases, Their Extracellular Targets, and Inflammatory Signaling. Pharmacol Rev 68, 1110–1142 (2016).

26. Duncan John Campbell. Neprilysin inhibitors and bradykinin. Frontiers in Medicine 5, (2018).

27. Dobrovolsky AB and Titaeva EV. The fibrinolysis system: regulation of activity and physiologic functions of its main components. Biochemistry 67, 99–108 (2002).

28. Molinaro G, Gervais N and Adam A. Biochemical basis ofangioedema associated with recombinant tissue plasminogen activator treatment: an in vitro experimental approach. Stroke 33, 1712–1716 (2002).

29. Breen P. Basics of coagulation pathways. Int Anesthesiol Clin 42, 1–9 (2004).

30. Levi M, Hack CE, de Boer JP, Brandjes DP, Büller HR and Ten Cate JW. Contact system dependent fibrinolytic activity in vivo: observations in healthy subjects and factor XII deficient patients. Agents Actions 38, 292–8 (1992).

31. Kahn R, Hellmark T, Leeb-Lundberg LM, Akbari N, Todiras M, Olofsson T, Wieslander J, Christensson A, Westman K, Bader M, Müller-Esterl W, Karpman D. Neutrophil-derived proteinase 3 induces kallikrein-independent release of a novel vasoactive kinin. J Immunol 182, 7906–7915 (2009).

32. López-Otín C and Overall CM. Protease degradomics: a new challenge for proteomics. Nature reviews. Molecular cell biolog. Molecular cell biology 3, 509–519 (2002).

33. Turk B. Targeting proteases: successes, failures and future prospects. Nature reviews. Drug discovery 5, 785–799 (2006).

34. Rawlings, N D and Barrett A J. Evolutionary families of metallopeptidases. Methods in Enzymology. Methods in Enzymology 248, 183–228 (1999).

35. Reznik SE and Fricker LD. Carboxypeptidases from A to Z: implications in embryonic development and Wnt binding. Cell Mol Life Sci 58, 1790–1804 (2001).

36. Arolas JL, Vendrell J, Aviles FX and Fricker LD. Metallocarboxypeptidases: emerging drug targets in biomedicine. Curr Pharm 13, 349–366 (2007).

37. Skidgel R A. Carboxypeptidase M. in Handbook of Proteolytic Enzymes 1347–1349 (Barrett A. J., Rawlings N. D. and Woessner J. F., 1998).

38. Auld D S. Carboxypeptidase A2. in In: Handbook of Proteolytic Enzymes 1326–1328 (Barrett A J, Rawlings N D and Woessner J F., 1998).

39. Marquez-Curtis L, Jalili A, Deiteren K, Shirvaikar N, Lambeir AM and Janowska-Wieczorek A. Carboxypeptidase M expressed by human bone marrow cells cleaves the C-terminal lysine of stromal cell-derived factor-1alpha: another player in hematopoietic stem/progenitor cell mobilization? stem cells 26, 1211–20 (2008).

40. Aiuti A, Webb IJ, Bleul C. The chemokine SDF-1 is a chemoat-tractant for human CD34(⩽) hematopoietic progenitor cells and providesa new mechanism to explain the mobilization of CD34(⩽) progenitors toperipheral blood. J Exp Med 185, 111–120 (1997).

41. Levin Y, Skidgel RA and Erdos EG. Isolation and characterization of the subunits of human plasma carboxypeptidase N (kininase i). Proc. Natl. Acad. Sci 79, 4618–4622 (1982).

42. Gebhard W, Matthias S and Eulitz M. cDNA cloning and complete primary structure of the small, active subunit of human carboxypeptidase N. Eur. J. Biochem. 178, 603 (1989).

43. Riley D A, Tan F, Miletich D J and Skidgel R A. Chromosomal localization of the genes for human carboxypeptidase D (CPD) and the active 50-kilodalton subunit of human carboxypeptidase N (CPN1). Genomics 50, 105 (1998).

44. Tsukahara Y, Itakura A, Ohno Y, Ando H and Mizutani S. Umbilical plasma kininase I activity in fetal hypoxia. Horm Metab Res 35, 583–587 (2003).

45. Ito Y, Mizutani S, Kurauchi O, Kasugai M, Narita O and Tomoda Y. Purification and properties of microsomal carboxypeptidase N (kininase I) in human placenta. Enzyme 42, 8–14 (1989).

46. Nagae A, Abe M, Becker RP, Deddish PA, Skidgel RA and Erdös EG. High concentration of carboxypeptidase M in lungs: presence of the enzyme in alveolar type I cells. Am J Respir Cell Mol Biol 9, 221–229 (1993).

47. Leeb-Lundberg LM, Marceau F, Muller-Esterl W, Pettibone DJ and Zuraw BL. International union of pharmacology. XLV. Classification of the kinin receptor family: from molecular mechanisms to pathophysiological consequences. Pharmacol Rev 57, 27–77 (2005).

48. Marceau F, Hess JF and Bachvarov DR. The B1 receptors for kinins. Pharmacol Rev 50, 357–386 (1998).

49. Regoli D, Rhaleb N E, Dion S and Drapeau G. New selective bradykinin receptorantagonists and bradykinin B2 receptor characterization. Trends.Pharmacol.Sci 11, 156-161 (1990).

50. Kammerer S, Braun A, Arnold N and Roscher AA. The human bradykinin B2 receptor gene: full length cDNA, genomic organization and identification of the regulatory region. Biochem. Biophys. Res. Commun 211, 226–233 (1995).

51. Bachvarov DR, Hess JF, Menke JG, Larrivee JF and Marceau F. Structure and genomic organization of the human B1 receptor gene for kinins (BDKRB1). Genomics 33, 374–381 (1996).

52. Austin KE, Faussner A, Robinson HE, Chakravarty S, Kyle DJ, Bathon JM and Proud D. Stable expression of the kinin B1 receptor in Chinese hamster ovary cells. Journal of Biological Chemistry 271, 11420–11425 (1997).

53. McIntyre P, Phillips E, Skidmore E, Brown M, DimWebb M. Cloned murine bradykinin receptor exhibits a mixed B1 andB2 pharmacological selectivity. Mol. Pharmacol 44, 346–355 (1993).

54. Wang DZ, Ma JX, Chao L and Chao J. Molecular cloning and sequence analysis of rat bradykinin B2 receptor gene. Biochim. Biophys. Acta 1219, 171–174 (1994).

55. Bachvarov DR, Saint-Jacques E, Larrivee JF, Levesque L. Cloning and pharmacological characterization of the rabbit bradykinin B2 receptor. J. Pharmacol. Exp. Ther 275, 1623–1630 (1995).

56. Regoli D and Barabe J. Pharmacology of bradykinin and ´ related kinins. Pharmacol. Rev 32, 1–46 (1980).

57. Tschöpe C, Heringer-Walther S, Koch M, Spillmann F, Wandorf M, Leitner E, Schultheiss H P and Walther T. Upregulation of bradykinin B1-receptorexpressions after myocardial infarction. Br. J. Pharmacol 129, 1537-1538 (2000).

58. Calixto JB, Medeiros R, Fernandes ES, Ferreira J, Cabrini DA and Campos MM. Kinin B1 receptors: key G-protein-coupled receptors and their role in inflammatory and painful processes. Br J Pharmacol 143, 803–818 (2004).

59. Marceau F and Regoli D. Bradykinin receptor ligands: therapeutic perspectives. Nat Rev Drug Discov 3, 845–852 (2004).

60. Huang H and Player MR. Bradykinin B1 receptor antagonists as potential therapeutic agents for pain. J Med Chem 53, 5383–5389 (2010).

61. Wothersponn G and Winter J. Bradykinin B1 receptor is constitutively expressed in the rat sensory nervous system. Neurosci Lett 294, 175–178 (2000).

62. Schanstra JP, Bataelle E, Castano M E M, Barascud Y, Hirtz C, Pesquero JB, Pecher C, Guathier F, Girolami J P and Bascands JL. The B1 -agonist [des-Arg10]-kallidin activates transcription factor NF-κB and induces homologous up-regulation of the bradykinin B1-receptor in cultured human lung fibroblasts. J. Clin. Invest 101, 2080–2091 (1998).

63. Angers, Drouin R, Bachvarova M, Paradis I., Maraceau F and Bachvarova DR. In vivo protein-DNA interactions at the kinin B1 receptor gene promoter: no modification on interleukin-1 beta or lypopolysaccharide induction. J. Cell. Biochem 78, 278–296 (2000).

64. Medeiros R, Cabrini D A, Ferreira J, Fernandes E S, Mori M A, Pesquero JB, Bader M, Avellar M C, Campos M and Calixto J B. Bradykinin B1 receptor expression induced by tissue damage in the rat portal vein. A critical role for mitogen-activated protein kinase and nuclear factor-κB signaling pathways. Circ. Res 94, 1375–1382 (2004).

65. Medeiros R, Cabrini D A and Calixto J B. The in vivo and ex vivo roles of cyclooxygenase-2, nuclear factor-κB and protein kinases pathways in the up-regulation of B1 receptor mediated contraction of the rabbit aorta. Regul. Pept 97, 121–130 (2001).

66. Cayla C, Merino VF, Cabrini DA, Silva JA Jr, Pesquero JB and Bader M. Structure of the mammalian kinin receptor gene locus. Int Immunopharmacol 2, 1721–1727 (2002).

67. Pesquero JB, Lindsey CJ, Zeh K, Paiva AC. Molecular structure and expression of rat bradykinin B2 receptorgene. Evidence for alternative splicing. J. Biol. Chem 269, 26920–26925 (1994).

68. Couture R, Harrisson M, Vianna RM and Cloutier F. Kinin receptors in pain and inflammation. Eur J Pharmacol 429, 161–176 (2001).

69. Hall J M. Bradykinin receptors. Gen. Pharmac 28, 1-6 (1997).

70. Praddaude F, Tack I, Emond C, Bascands JL, Girolami JP, Tran-Van T, Regoli D and Ader JL. In vivo and in vitro homologous desensitization of rat glomerular bradykinin B2 receptors. European Journal of Pharmacology 294, 173–182 (1995).

71. Blaukat A, Abdulla S, Lohse MJ and Müller-Esterl W. Ligand-induced phosphorylation/dephosphorylation of the endogenous bradykinin B2 receptor from human fibroblasts. Journal of Biological Chemistry 271, 32366–32374 (1996).

72. de Weerd WF and Leeb-Lundberg LM. Bradykinin sequesters B2 bradykinin receptors and the receptor-coupled G subunits Gq and Gi in caveolae in DDT1 MF-2 smooth muscle cells. J Biol Chem 272, 17858–17866 (1997).

73. Leeb-Lundberg LM, Marceau F, Muller-Esterl W, Pettibone DJ and Zuraw BL. Classification of the kinin receptor family: from molecular mechanisms to pathophysiological consequences. Pharmacol Rev 57, 27–77 (2000).

74. Busse R and Fleming I. Molecular responses of endothelial tissue to kinins. Diabetes 45, S8–S13 (1996).

75. Van Iwaarden F, De Groot PG, Sixma JJ, Berrettini M and Bouma BN. High molecular weight kininogen is present in cultured human endothelial cells. Blood 71, 1268–1276 (1988).

76. Costerousse O, Jaspard E, Wei L, Corvol P and Alhenc-Gelas F. The angiotensin I-converting enzyme kininase II: Molecular organisation and regulation of its expression in humans. J. Cardiovasc. Pharmacol 20, S10-15 (1992).

77. Mombouli J V and Vanhoutte PM. Kinins mediate kallikrein-induced endothelium-dependent relaxations in isolated cananine coronary arteries. Biophys 185, 186 (1992).

78. Zhu P, Beny J L, Flammer L, Lucher T F and Hafflieger I O. Relaxation by bradykinin in porcine ciliary artery. Role of nitric oxide and K+-channels. Invest. Ophthalmol. Vis. Sci 38, 1761–1767 (1997).

79. Persson K and Andersson R G. Biphasic response to bradykinin in isolated porcine iliac arteries is mediated by bradykinin B1 and B2 receptors. J Cardiovasc Pharmacol 31, 306–313 (1998).

80. Oleson SP. Regulation of ion permeability in frog brain venules, significance of calcium, cyclic nucleotides and protein kinase C. J. Physiol. 387, 59–68 (1987).

81. Wiemer G, Popp R, Scholkens B A and Gogelein H. Enhancement of cytosolic calcium, prostacyclin and nitric oxide by bradykinin and the ACE inhibitor ramiprilat in porcine brain capillary endothelial cells. Brain Res 638, 261–266 (1994).

82. Tsutsui M, Onoue H, Iida Y, Smith L, O'Brien T, and Katusic Z S. B1 and B2 bradykinin receptors on adventitial fibroblasts of cerebral arteries are coupled to recombinant eNOS. Am J Physiol Heart Circ Physiol 278, H367–H372 (2000).

83. Felipe S A, Rodrigues E S, Martin R P, Paiva A C M, Pesquero J B and Shimuta S I. Functional expression of kinin B1 and B2 receptors in mouse abdominal aorta. J Med Biol Res 40, 649–655 (2007).

84. Blum-Johnston C, Blood Q, Wee C, Wilson R, Blood AB, Longo LD, Wilson SM. Bradykinin-induced pulmonary vasorelaxation is modified by long-term hypoxia and postnatal maturation in sheep. The FASEB Journal 27, 1140–7 (2013).

85. Kuga T, Mohri M, Egashira K, Hirakawa Y,Tagawa T, Shimokawa H,Takeshita A. Bradykinin-induced vasodilation of human coronary arteries in vivo: role of nitric oxide and angiotensin-converting enzyme. Journal of the American College of Cardiology 30, THE (1997).

86. Thebault S, González C, García C, David Zamarripa AD, Nava G, Vaca L, Casillas F, Gonzales S, Escalera M, Clapp C. Vasoinhibins prevent bradykinin-stimulated endothelial cell proliferation by inactivating eNOS via reduction of both intracellular Ca2+ levels and eNOS phosphorylation at Ser1179. Pharmaceuticals 4, 1052–69 (2011).

87. Klabunde. in Cardiovascular Physiology Concepts (Wolters Kluwer, 2021).

88. Vanhoutte PM. Cellular signaling and NO production. Pflugers Arch 459, 807–816 (2010).

89. Lamattina L, Garc´ıa-Mata C, Graziano M, and Pagnussat G. NITRIC OXIDE: The Versatility of an Extensive Signal MoleculE. Annu. Rev. Plant Biol. 54, 109–36 (2003).

90. Bae SW, Kim HS, Cha YN, Park YS, Jo SA, Jo I. Rapid increase in endothelial nitric oxide production by bradykinin is mediated by protein kinase A signaling pathway. Biochemical and Biophysical Research Communications 306, 981–87. (2003).

91. Lal MA, Kennedy CR, Proulx PR. Bradykinin-stimulated cPLA2 phosphorylation is protein kinase C dependent in rabbit CCD cells. Am JPhysiol 273, F907–F915 (1997).

92. Kennedy C, Proulx PR and Hebert RL. Bradykinin-induced translocation of cytoplasmic phospholipase A2 in MDCK cells. J Physiol Pharmacol 75, 563–567 (1997).

93. Líbano-Soares J, Gomes-Quintana H K, Melo E P, Queiroz-Madeira R G, Roubach A G, Lopes C, Caruso-Neves. B2 receptor-mediated dual effect of bradykinin on proximal tubule Na+-ATPase: Sequential activation of the phosphoinositide-specific phospholipase Cβ/protein kinase C and Ca2+-independent phospholipase A2 pathways. Biochimica et Biophysica Acta (BBA) - Biomembranes 1778, 1316–1323 (2008).

94. Rodriguez JA, De la Cerda P, Collyer E, Decap V, Vio CP, Velarde V. Cyclooxygenase-2 inductionby bradykinin in aortic vascular smooth muscle cells. J Physiol Heart Circ Physiol 290, H30–H36 (2006).

95. Welsh C, Dubyak G and Douglas JG. Relationship between phospholipase Cactivation and prostaglandin E2 and cyclic adenosine monophosphate production in rabbit tubular epithelial cells. Effects of angiotensin, bradykinin, and arginine vasopressin. J Clin Invest 81, 710–719 (1988).

96. Liao JK and Homcy CJ. The G proteins of the G alpha i and G alpha q familycouple the bradykinin receptor to the release of endothelium-derived relaxing factor. J Clin Invest 92, 2168–2172 (1993).

97. Feletou M, Germain M, Thurieau C, Fauchere J L, Canet E. Agonistic and antagonistic properties of the bradykinin B2 receptor antagonist, Hoe 140, in isolated blood vessels from different species. Br J Pharmacol 112, 683–689 (1994).

98. Busse R, Edwards G, Feletou M, Fleming I, Vanhoutte PM and Weston AH. EDHF: bringing the concepts together. Trends in Pharmacological Sciences 23, 374–380 (2002).

99. Godo S, Sawada A, Saito H, Ikeda S, Enkhjargal B, Suzuki K, Tanaka S, Shimokawa H. Disruption of physiological balance between nitric oxide and endothelium-dependent hyperpolarization impairs cardiovascular homeostasis in mice. Arterioscler Thromb Vasc Biol 36, 97 107 (2016).

100. Wu Y, Huang A, Sun D, Falck JR, Koller A and Kaley G. Gender-specific compensation for the lack of NO in the mediation of flow-induced arteriolar dilation. American Journal of Physiology 280, H2456–H2461 (2001).

101. Scotland RS, Madhani M, Chauhan S. Investigation of vascular responses in endothelial nitric oxide synthase/cyclooxygenase-1 double-knockout mice: key role for endothelium-derived hyperpolarizing factor in the regulation of blood pressure in vivo. Circulation 111, 796–803 (2005).

102. Fleming I and Busse R. Endothelium-derived epoxyeicosatrienoic acids and vascular function. Hypertension 47, 629–633 (2006).

103. Ozkor MA and Quyyumi AA. Endothelium-Derived Hyperpolarizing Factor and Vascular Function. Cardiology Research and Practice (2011) doi:10.4061/2011/156146.

104. Luckhoff A, Zeh R and Busse R. Desensitization of the bradykinin-induced rise in intracellular free calcium in cultured endothelial cells. Pflugers Archiv 412, 654–658 (1988).

105. Chen G, Suzuki H, Weston AH. Acetylcholine releases endothelium-derived hyperpolarizing factor and EDRF from rat blood vessels. British Journal of Pharmacology 95, 1165–1174 (1988).

106. Dawes M, Sieniawska C, Delves T, Dwivedi R, Chowienczyk PJ and Ritter JM. Barium reduces resting blood flow and inhibits potassium-induced vasodilation in the human forearm. Circulation 105, 1323–1328 (2002).

107. Quingnard JF, Feletou M, Edwards G, Duhault J, Weston AH, Vanhoutte PM. Role of endothelial cell hyperpolarization in EDHF-mediated responses in the guinea-pig carotid artery. Br. J. Pharmacol 129, 1103–1112 (2000).

108. Dong H, Jiang Y, Cole WC, Triggle CR. Comparison of the pharmacological properties of EDHF-mediated vasorelaxation in guinea-pig cerebral and mesenteric resistance vessels. Br. J. Pharmacol. 130, 1983–1991 (2000).

109. Li PL, Chen CL, Bortell R and Campbell WB. 11,12-epoxyeicosatrienoic acid stimulates endogenous mono-ADP-ribosylation in bovine coronary arterial smooth muscle. Circulation Research 85, 349–356 (1999).

110. Fissithaler B, Popp R, Kiss L, Potente M, Harder DR, Fleming L, Busse R. Cytochrome P450 2C is an EDHF synthase in coronary arteries. Nature 401, 493–497 (1999).

111. Archer SL, Gragasin FS, Wu X, Wang S, McMurtry S, Kim DH, Platonov M, Koshal A, Hashimoto K, Campbell WB Falck JR, Michelakis ED. Endothelium-derived hyperpolarizing factor in human internal mammary artery is 11,12-epoxyeicosatrienoic acid and causes relaxation by activating smooth muscle BKCa channels. Circulation 107, (2003).

112. Bellien J, Joannides R, Iacob M, Arnaud P and Thuillez C. Evidence for a basal release of a cytochrome-related endothelium-derived hyperpolarizing factor in the radial artery in humans. American Journal of Physiology 290, H1347–H1352 (2006).

113. Matoba T, Shimokawa H, Nakashima M, Hirakawa Y, Mukai Y, Hirano K, Kanaide H, Takeshita A. Hydrogen peroxide is an endothelium-derived hyperpolarizing factor in mice. Journal of Clinical Investigation 106, 1521–1530 (2002).

114. Beny JL and von der Weid PY. Hydrogen peroxide: an endogenous smooth muscle cell hyperpolarizing factor. Biochemical and Biophysical Research Communications 176, 378–384 (1991).

115. Matoba T, Shimokawa H, Nakashima M, Hirakawa Y, Mukai Y, Hirano K, Kanaide H, Takeshita A. Hydrogen peroxide is an endothelium-derived hyperpolarizing factor in mice. Journal of Clinical Investigation. Journal of Clinical Investigation 106, 1521–1530 (2000).

116. Miura H, Bosnjak JJ, Ning G, Saito T, Miura M and Gutterman DD. Role for hydrogen peroxide in flow-induced dilation of human coronary arterioles. Circulation research 92, 31–40 (2003).

117. Gilligan DM, Panza JA, Kilcoyne CM, Waclawiw MA, Casino PR and Quyyumi AA. Contribution of endothelium-derived nitric oxide to exercise-induced vasodilation. Circulation 90, 2853–2858 (1994).

118. Quyyumi AA, Dakak N, Andrews NP, Gilligan DM, Panza JA, Cannon RO. Contribution of nitric oxide to metabolic coronary vasodilation in the human heart. Circulation 92, 320–326 (1995).

119. Griffith TM. Endothelium-dependent smooth muscle hyperpolarization: do gap junctions provide a unifying hypothesis? British Journal of Pharmacology 141, 881–903 (2004).

120. Sandow SL and Hill CE. Incidence of myoendothelial gap junctions in the proximal and distal mesenteric arteries of the rat is suggestive of a role in endothelium-derived hyperpolarizing factor-mediated responses. Circulation Research 86, 341–346 (2000).

121. Shimokawa H, Yasutake H, Fujii K. The importance of the hyperpolarizing mechanism increases as the vessel size decreases in endothelium-dependent relaxations in rat mesenteric circulation. Journal of Cardiovascular Pharmacology 28, 703–711 (1996).

122. Nelson MT and Quayle JM. Physiological roles and properties of potassium channels in arterial smooth muscle. Am J Physiol 268, 799–822 (1995).

123. Edwards G, Dora K A, Gardener MJ, Garland CJ and Weston AH. K+ is an endothelium-derived hyperpolarizing factor in rat arteries. Nature 396, 269–272 (1998).

124. Samanta A, Hughes TEE and Moiseenkova-Bel VY. Transient Receptor Potential (TRP) Channels. Subcell Biochem 87, 141–165 (2018).

125. Latorre R, Zaelzer C and Brauchi S. Structure-function intimacies of transient receptor potential channels. Rev Biophys 42, 201–46 (2009).

126. Ramsey I S, Delling M and Clapham D E. An introduction to TRP channels. Annu Rev Physiol 68, 619–47 (2006).

127. Lanitis E, Irving M and Coukos G. Targeting the tumor vasculature to enhance T cell activity. Curr Opin Immunol 33, 55–63 (2015).

128. Sacharidou A, Stratman AN and Davis GE. Molecular mechanisms controlling vascular lumen formation in three-dimensional extracellular matrices. Cells Tissues Organs 195, 122–143 (2012).

129. Kim HR, Appel S, Vetterkind S, Gangopadhyay SS and Morgan KG. Smooth muscle signalling pathways in health and disease. J Cell Mol Med 12, 2165–2180 (2008).

130. Verma S and Anderson T J. Fundamentals of endothelial function for the clinical cardiologist. Circulation 105, 546–549 (2002).

131. Verma S, Buchanan M R and Anderson T G. Endothelial function testing as a biomarker of vascular disease. Circulation 108, 2054–2059 (2003).

132. Dietrich A, Chubanov V, Kalwa H, Rost BR and Gudermann T. Cation channels of the transient receptor potential superfamily: their role in physiological and pathophysiological processes of smooth muscle cells. Pharmacol Ther 112, 744–760 (2006).

133. Dietrich A, Kalwa H and Gudermann T. TRPC channels in vascular cell function. Thromb Haemost 103, 262–270 (2010).

134. Hill-Eubanks DC, Gonzales AL, Sonkusare SK and Nelson MT. Vascular TRP channels: performing under pressure and going with the flow. Physiology 29, 343–360 (2014).

135. Sullivan MN and Earley S. TRP channel Ca2+ sparklets: fundamental signals underlying endothelium-dependent hyperpolarization. Am J Physiol Cell Physiol 305, C999–C1008 (2013).

136. Yao J and Qin F. Interaction with phosphoinositides confers adaptation onto the TRPV1 pain receptor. PLoS biology 7, (2009).

137. Earley S and Brayden JE. Transient receptor potential channels in the vasculature. Physiol Rev 95, 645–690 (2015).

138. Lee MW and Severson DL. Signal transduction in vascular smooth muscle: diacylglycerol second messengers and PKC action. Am J Physiol 267, C659-78 (1994).

139. Berridge MJ, Lipp P and Bootman MD. The versatility and universality of calcium signalling. Nat Rev Mol Cell Biol 1, 11–21 (2000).

140. Putney JW Jr. A model for receptor-regulated calcium entry. Cell Calcium 7, 1–12 (1986).

141. Chen XL and Rembold CM. Phenylephrine contracts rat tail artery by one electromechanical and three pharmacomechanical mechanisms. Am J Physiol 268, H74-81 (1995).

142. Nelson MT, Huang Y, Brayden JE, Hescheler J and Standen NB. Arterial dilations in response to calcitonin gene related peptide involve activation of K+ channels. Nature 344, 770–773 (1990).

143. Michiel C. Endothelial cell function. J. Cell. Physiol 196, 430–443 (2003).

144. Nilius B, Droogmans G and Wondergem R. Transient receptor potential channels in endothelium: solving the calcium entry puzzle? Endothelium 10, 5–15 (2003).

145. Chang AS, Chang SM, Garcia RL and Schilling WP. Concomitant and hormonally regulated expression of trp genes in bovine aortic endothelial cells. FEBS Lett 415, 335–340 (1997).

146. Garcia RL and Schilling WP. Differential expression of mammalian TRP homologues across tissues and cell lines. Biochem Biophys Res Commun 239, 279–283 (1997).

147. Earley S, Gonzales AL and Garcia ZI. A dietary agonist of transient receptor potential cation channel V3 elicits endothelium-dependent vasodilation. Mol Pharmacol 77, 612–620 (2010).

148. Wissenbach U, Bodding M, Freichel M and Flockerzi V. a novel Trp related protein from kidney. FEBS Lett 485, 127–134 (2000).

149. Earley S, Gonzales AL and Crnich R. Endothelium-dependent cerebral artery dilation mediated by TRPA1 and Ca2+-Activated K+ channels. Circ Res 104, 987–994 (2009).

150. Caterina MJ, Schumacher MA, Tominaga M, Rosen TA, Levine JD and Julius D. The capsaicin receptor: a heat-activated ion channel in the pain pathway. Nature 389, 816–824 (1997).

151. Poblete IM, Orliac ML, Briones R, Adler-Graschinsky E and Huidobro-Toro JP. Anandamide elicits an acute release of nitric oxide through endothelial TRPV1 receptor activation in the rat arterial mesenteric bed. J Physiol 568, 539–551 (2005).

152. Peier AM, Reeve AJ, Andersson DA, Moqrich A, Earley TJ, Hergarden AC, Story GM, Colley S, Hogenesch JB, McIntyre P, Bevan S, Patapoutian A. A heat-sensitive TRP channel expressed in keratinocytes. Science 296, 2046–2049 (2002).

153. Xu H, Delling M, Jun JC and Clapham DE. Oregano, thyme and clove-derived flavors and skin sensitizers activate specific TRP channels. Nature Neurosci 9, 628–635 (2006).

154. Watanabe H, Vriens J, Suh SH, Benham CD, Droogmans G and Nilius B. Heat-evoked activation of TRPV4 channels in a HEK293 cell expression system and in native mouse aorta endothelial cells. J Biol Chem 277, 47044–47051 (2002).

155. Liedtke W, Choe Y, Marti-Renom MA, Bell AM, Denis CS, Sali A, Hudspeth AJ, Friedman JM and Heller S. Vanilloid receptor-related osmotically activated channel (VR-OAC), a candidate vertebrate osmoreceptor. Cell 103, 525–535 (2000).

156. Watanabe H, Vriens J, Prenen J, Droogmans G, Voets T and Nilius B. Anandamide and arachidonic acid use epoxyeicosatrienoic acids to activate TRPV4 channels. Nature 424, 434–438 (2003).

157. Macpherson LJ, Geierstanger BH, Viswanath V, Bandell M, Eid SR, Hwang S and Patapoutian A. The pungency of garlic: activation of TRPA1 and TRPV1 in response to allicin. Curr Biol 15, 929–934 (2005).

158. Bandell M, Story GM, Hwang SW, Viswanath V, Eid SR, Petrus MJ, Earley TJ and Patapoutian A. Noxious cold ion channel TRPA1 is activated by pungent compounds and bradykinin. Neuron 41, 849–857 (2004).

159. Andre E, Campi B, Materazzi S, Trevisani M, Amadesi S, Massi D. Cigarette smoke-induced neurogenic inflammation is mediated by alpha,beta-unsaturated aldehydes and the TRPA1 receptor in rodents. J Clin Invest 118, 2574–2582 (2008).

160. Talavera K, Gees M, Karashima Y, Meseguer V M, Vanoirbeek J A, Damann, N. Nicotine activates the chemosensory cation channel TRPA1. Nat Neurosci 12, 1293–1299 (2009).

161. Leffler A, Lattrell A, Kronewald S, Niedermirtl F and Nau C. Activation of TRPA1 by membrane permeable local anesthetics. Mol. Pain 7, 62 (2011).

162. Woll K A, Skinner K A, Gianti E, Bhanu N V, Garcia B A, Carnevale V, Eckenhoff RG, Gaudet R. Sites Contributing to TRPA1 Activation by the Anesthetic Propofol Identified by Photoaffinity Labeling. Biophys J 113, 2168–2172 (2017).

163. Karashima Y, Prenen J, Talavera K, Janssens A, Voets T and Nilius B. Agonist-induced changes in Ca2+ permeation through the nociceptor cation channel TRPA1. Biophys J 98, 773–783 (2010).

164. Kamouchi M, Philipp S, Flockerzi V, Wissenbach U, Mamin A, Raeymaekers L, Eggermont J, Droogmans G and Nilius B. Properties of heterologously expressed hTRP3 channels in bovine pulmonary artery endothelial cells. J Physiol 518, 345–358 (1999).

165. Lichtenegger M, Tiapko O, Svobodova B, Stockner T, Glasnov T N, Schreibmayer W, Platzer D, Cruz G G, Krenn S and Schober R. An optically controlled probe identifies lipid-gating fenestrations within the TRPC3 channel. Nat Chem Biol 14, 1–9 (2018).

166. Liu CL, Huang Y, Ngai CY, Leung YK and Yao XQ. TRPC3 is involved in flow- and bradykinin-induced vasodilation in rat small mesenteric arteries. Acta Pharmacol Sin 27, 981–990 (2006).

167. Huang JH, He GW, Xue HM, Yao XQ, Liu XC, Underwood MJ and Yang Q. TRPC3 channel contributes to nitric oxide release: significance during normoxia and hypoxia-reoxygenation. Cardiovasc Res 91, 472–482 (2011).

168. Senadheera S, Kim Y, Grayson TH, Toemoe S, Kochukov MY, Abramowitz J, Housley GD, Bertrand RL, Chadha PS, Bertrand PP, Murphy TV, Tare M, Birnbaumer L, Marrelli SP and Sandow SL. Transient receptor potential canonical type 3 channels facilitate endothelium-derived hyperpolarization-mediated resistance artery vasodilator activity. Cardiovasc Res 95, 439–447 (2012).

169. Freichel M, Tsvilovskyy V and Camacho-London˜ o JE. Intracellular spermine blocks TRPC4 channel via electrostatic interaction with C-terminal negative amino acids. European Journal of Physiology 468, 551–561 (2016).

170. Freichel M, Suh SH, Pfeifer A, Schweig U, Trost C, Weissgerber P, Biel M, Philipp S, Freise D, Droogmans G, Hofmann F, Flockerzi V and Nilius B. Lack of an endothelial store-operated Ca2+ current impairs agonist-dependent vasorelaxation in TRP4−/− mice. Nature Cell Biol 3, 121–127 (2001).

171. Zisman LS. Inhibiting tissue angiotensin-converting enzyme: a pound of flesh without the blood. Circulation 98, 2788–2790 (1998).

172. Cugno M, Nussberger J and Cicardi M. Bradykinin and the pathology of angioedema. IntImmunopharmacol 3, 311–317 (2003).

173. Regoli D, Plante G E and Gobeil F Jr. Impact of kinins in the treatment of cardiovascular diseases. Pharmacol Ther 135, 94–111 (2012).

174. Ribeiro S A, Corrado A P and Graeff FG. Antinociceptive action of intraventricular bradykinin. Neuropharmacology 10, 725–731 (1971).

175. Ribeiro S A, Rocha E and Silva M. Antinociceptive action of bradykinin and related kinins of larger molecular weights by the intraventricular route. Br J Pharmacol 47, 517–528 (1973).

176. Laneuville O, Reader T A and Couture R. Intrathecal bradykinin acts presynaptically on spinal noradrenergic terminals to produce antinociception in the rat. Eur. J. Pharmacol 159, 273–283 (1989).

177. Dray A. Kinins and their receptors in hyperalgesia. Can J Physiol Pharmacol 75, 704–712 (1997).

178. Yusuf S, Sleight P, Pogue J, Bosch J, Davies R and Dagenais G. Effects of an angiotensin-converting-enzyme inhibitor, ramipril, on cardiovascular events in high-risk patients. N Engl J Med 342, 145–153 (2000).

179. Phagoo SB, Yaqoob M, McIntyre P, Jones C and Burgess GM. Cytokines increase B1 bradykinin receptor mRNA and protein levels in human lung fibroblasts. Biochem Soc Trans 25, 43S (1997).

180. Cruwys SC, Garrett NE, Perkins MN, Blake DR and Kidd BL. The role of bradykinin B1 receptors in the maintenance of intraarticular plasma extravasation in chronic antigen-induced arthritis. Br J Pharmacol 113, 940–944 (1994).

181. Pesquero JB, Araujo RC, Heppenstall PA, Stucky CL, Silva JA Jr, Walther T. Hypoalgesia and altered inflammatory responses in mice lacking kinin B1 receptors. Proc Natl Acad Sci U S A. 97, 8140-8145. (2000).

182. Dray A and Perkins M N. Bradykinin and inflammatory pain. Trends Neurosci 16, 13–18 (1993).

183. Munoz C M and Leeb-Lundberg L. Receptor-mediated internalization of bradykinin DDT1 MF-2 smooth muscle cells process internalized bradykinin via multiple degradative pathways. J Biol Chem 267, 303–309 (1992).

184. Munoz C M, Cotecchia S and Leeb-Lundberg L M F. B2 kinin receptor-mediated internalization of bradykinin in DDT1 MF-2 smooth muscle cells is paralleled by sequestration of the occupied receptors. Arch Biochem Biophys 301, 336–344 (1993).

185. Mathis S A, Criscimagna N L and Leeb-Lundberg L M F. B2 and B1 kinin receptors mediate distinct patterns of intracellular Ca2q2 signalling in single cultured vascular smooth muscle cells. Mol.Pharmacol 50, 128–139 (1996).

186. Phagoo S B, Poole S and Leeb-Lundberg L M F. Autoregulation of bradykinin receptors: agonists in the presence of interleukin-1bshift the repertoire of receptor subtypes from B to B in human lung 21 fibroblasts. Mol. Pharmacol 56, 325–333 (1999).

187. Faussner A, Bathon JM and Proud D. Comparison of the responses of B and B kinin receptors to agonist stimulation. Im munopharmacology 45, 13–20 (1999).

188. Britos J and Nolly H L. Kinin-forming enzyme of rat cardiac tissue. Subcellular distribution and biochemical properties. Hypertension 3, 42–55 (1981).

189. Sharma J N, Uma K, and Noor A R. Blood pressure regulation by the kallikrein-kinin system. Gen. Pharmacol 27, 55–63 (1996).

190. Vegh A, Szekeres L, and Parratt J R. Local intracoronary infusions of bradykinin profoundly reduce the severity of ischaemia-induced arrhythmia in anaesthetized dogs. Br J Pharmacol 104, 294–295 (1991).

191. Linz W, Wiemer G, and Scholkens B A. Bradykinin prevents left ventricular hypertrophy in rats. Hypertens 11, S96–S97 (1993).

192. Scholkens B A. Kinins in the cardiovascular system. Immunopharmacology 33, 209–217 (1996).

193. Madeddu P, Milia A F, Salis M B, Gaspa L, Gross W, Lippoldt A and Emanueli G. Renovascular hypertension in bradykinin B2-receptor knockout mice. Hypertension 23, 305–509 (1998).

194. Whalley ET, Soomon JA, and Modafferi DM. A novel potent bradykinin antagonist increases survival in rat and rabbit model of endotoxin shock. Agents Actions 38, 431–420 (1992).

195. Walls T M, Sheehy R and Hartman J C. Role of bradykinin in myocardial preconditioning. J Pharmacol Exp Ther 270, 681–689 (1994).

196. Marketou ME and Vardas PE. Bradykinin in arterial hypertension therapy. Enemy or Ally? Hellenic J Cardiol 52, 269–272 (2011).

197. Sharma J N. Role of tissue kallikrein-kininogen-kinin pathways in the cardiovascular system. Arch Med Res 37, 299–306 (2006).

198. De Freitas F M, Farraco E Z, and De Azevedo DF. General circulatory alterations induced by intravenous infusion of synthetic bradykinin in man. Circulation 29, 66–70 (1964).

199. Webster M E and Gilmore J P. Influence of kallidin-10 on renal function. Am J Physiol 206, 714–718 (1964).

200. Kaplan AP. Drug induced angioedema. J Angioedema 1, 14–22 (2011).

201. Lazarovich M. Urticaria and angioedema.ImmunologiaKliniczna (Clinical Immunology). Mediton 59, 257–272 (2000).

202. Cicardii M, Zingale LC, Pappalardo E. Autoantibodies and lymphoproliferative diseases in acquired inhibitor deficiences. Medicine 82, 274–281 (2003).

203. Quincke H. Über akutes umschriebenes H autödem. Monatsschr Prakt Dermatol 1, 129–131 (1882).

204. Osler W. Hereditary angioneurotic oedema. Am J Med Sci 95, 362–367 (1888).

205. Donaldson VH and Evans RR. A biochemical abnormality in hereditary angioneurotic edema. Am J Med 35, 37–44 (1963).

206. Cicardi M and Johnston DT. Hereditary and Acquired Complement Component 1 Esterase Inhibitor Deficiency: A Review for the Hematologist. Acta Haematol 127, 208–220 (2012).

207. Busse PJ and Buckland MS. Non-histaminergic angioedema: focus on bradykinin-mediated angioedema. Clin Exp Allergy 43, 385–94 (2013).

208. Ricklin D, Hajishengallis G, Yang K and Lambris JD. Complement: a key system for immune surveillance and homeostasis. Nat Immunol 11, 785–97 (2010).

209. Sainz IM, Pixley RA and Colman RW. Fifty years of research on the plasma kallikrein-kinin system: from protein structure and function to cell biology and in-vivo pathophysiology. Thromb Haemos 98, 785–97 (2007).

210. Joseph K, Tholanikunnel BG and Kaplan AP. Factor XII–independent cleavage of high-molecular-weight kininogen by prekallikrein and inhibition by C1 inhibitor. J Allergy Clin Immunol 124, 143–9 (2009).

211. Chen LM, Chung P, Chao S, Chao L, Chao Jet al. Differential regulation of kininogen gene expression by estrogen and progesterone in vivo. Biochim Biophys Acta 1131, 145–51 (1992).

212. Misiti CS, Felici A, Farsetti A, Pontecorvi A and Fantoni A. Estrogen induction and contact phase activation of human factor XII. Steroids 61, 270–6 (1996).

213. Madeddu P, Emanueli C, Vittoria M, Maria V, Demontis P, Anania V, Glorioso N and Chao J. Regulation of bradykinin B2-receptor expression by oestrogen. Br J Pharmacol 121, 1763–9 (1997).

214. Han ED, MacFarlane RC, Mulligan AN, Scafidi J and Davis AE. Increased vascular permeability in C1 inhibitor-deficient mice mediated by the bradykinin type 2 receptor. J Clin Invest 108, 1057–63 (2002).

215. Merino VF, Todiras M, Campos LA, Saul V, Popova E, Baltatu OC, Pesquero JB and Bader M. Increased susceptibility to endotoxic shock in transgenic rats with endothelial overexpression of kinin B1 receptors. J Mol Med 86, 791–798 (2008).

216. Popova E, Krivokharchenko A, Ganten D and Bader M. Mol Reprod Dev. 63, 177–82 (2002).

217. Nishimura Y and Susuki A. Relaxant effects of vasodilator peptides on isolated basilar arteries from stroke-prone spontaneously hypertensive rats. Clin Exp Pharmacol Physiol 24, 157 ± 161 (1997).

218. Whalley E T, Amure Y O and Lye R H. Analysis of the mechanism of action of bradykinin on human basilar artery in vitro. Pharmacol 335, 433 ± 437 (1987).

219. Ihara E, Hirano K, Derkach DN, Nishimura J, Nawata H and Kanaide H. The mechanism of bradykinin-induced endothelium-dependent contraction and relaxation in the porcine interlobar renal artery. British Journal of Pharmacology 129, 943–952 (2000).

220. Skidgel R A, Barrett A J, Rawlings N D and Woessner J F. Carboxypeptidase M. in: Handbook of proteolytic enzymes. 1347–1349 (1998).

221. Skidgel R A, David RM and Tan F. Human Carboxypeptidase M. The Journal of Biological Chemistry 264, 2236–2241 (1989).

222. Ratajczak MZ, Kim CH, Abdel-Latif A, Schneider G, Kucia M, Morris A J, Laughlin M J and Ratajczak J. A novel perspective on stem cell homing and mobilization: review on bioactive lipids as potent chemoattractants and cationic peptides as underappreciated modulators of responsiveness to SDF-1 gradients. Leukemia 26, 63–72 (2012).

223. Cicardi M, Bork K, Caballero T. Evidence-based recommendations for the therapeutic management of angioedema owing to hereditary C1 inhibitor deficiency. Allergy 67, 147–157 (2011).

224. Popova E, Bader M and Krivokharchenko A. Production of transgenic models in hypertension. Methods Mol Med 108, 33–50 (2005).

225. Sangsree S, Brovkovych V, Minshall RD and Skidgel RA. Kininase I-type carboxypeptidases enhance nitric oxide production in endothelial cells by generating bradykinin B1 receptor agonists. J Physiol Heart Circ Physiol 248, 1959–1968 (2003).

226. Ignjatovic T, Tan F, Brovkovych V, Skidgel RA and Erdös EG. Novel mode of action of angiotensin I converting enzyme inhibitors. J Biol Chem 277, 16847–16852 (2002).

227. Farias NC, Feres T, Paiva AC and Paiva TB. Lys-[Leu8,desArg9]-bradykinin blocks lipopolysaccharide-induced SHR aorta hyperpolarization by inhibition of Ca(++)- and ATP-dependent K+ channels; hyperpolarization by inhibition of Ca++- and ATP-dependent K+ channels. Eur J Pharmacol 498, 163–169 (2004).

228. Liesmaa I, Kuoppala A, Shiota N, Kokkonen JO, Kostner K, Mayranpaa M, Kovanen PT and Lindstedt KA. Increased expression of bradykinin type-1 receptors in endothelium of intramyocardial coronary vessels in human failing hearts. Am J Physiol Heart Circ Physiol 288, 2317–2322 (2005).

229. McLean PG. Inducible expression of the kinin B1 receptor in the endotoxemic heart: mechanisms of des-Arg9bradykinin-induced coronary vasodilation. Br J Pharmacol 128, 275–282 (1999).

230. Raidoo DM, Ramsaroop R, Naidoo S, Müller-Esterl W and Bhoola KD. Kinin receptors in human vascular tissue: their role in atheromatous disease. Immunopharmacology 36, 153–160 (1997).

231. Lagneux C, Innocenti-Francillard P, Godin-Ribuot D, Bader M and Ribuot C. Heat stress-induced B1 receptor synthesis in the rat: an ex vivo study. Br J Pharmacol 125, 812–816 (1998).

232. Bouthillier J, Deblois D and Marceau F. Studies on the induction of receptor sequestration, ligand internalization, and signal transduc9 pharmacological responses to des-Arg -bradykinin in vitro and in tion. J Biol Chem 20, 2617–2623 (1998).

233. Schanstra JP, Bataillé E, Marin Castaño ME, Barascud Y, Hirtz C Pesquero JB, Pecher CH, Gauthier F, Girolami JP, and Bascands JL,. The B1-agonist [des-Arg10]-kallidin Activates Transcription Factor NF-kB and Induces Homologous Upregulation of the Bradykinin B1–receptor in Cultured Human Lung Fibroblasts. J Clin Invest 101, 2029–2296 (1998).

234. Duka I, Kintsurashvil E, Gavras I, Johns C Bresnahan M and Gavras H. Vasoactive potential of the b(1) bradykinin receptor in normotension and hypertension. Circ Res 88, 75–81 (2001).

235. Kintsurashvili E, Duka I, Gavras I, Johns C, Farmakiotis D and Gavras H. Effect of ANG II on bradykinin receptor gene expression in cardiomyocytes and vascular smooth muscle cells. Am J Physiol Heart Circ Physiol 281, 78–83 (2001).

236. Marcon R, Claudino RF, Dutra RC, Bento AF, Schmidt EC, Bouzon ZL, Sordi R, Morais RLT, Pesquero JB and Calixto JB. Exacerbation of DSS-induced colitis in mice lacking kinin B1 receptor through compensation of up-regulation of kinin B2 receptors: the role of tight junction and intestinal homeostasis. Br J Pharmacol 183, 389–402 (2013).

237. McLean PG, Perretti M and Ahluwalia A. Kinin B(1) receptors and the cardiovascular system: regulation of expression and function. Cardiovasc Res 48, 194–210 (2000).

238. Shirasaki H, Kanaizumi E and Himi T. Immunohistochemical localization of the bradykinin B1 and B2 receptors in human nasal mucosa. Mediators Inflamm 2009, (2009).

239. Morand-Contant M, Anand-Srivastava MB and Couture R. Kinin B1 receptor upregulation by angiotensin II and endothelin-1 in rat vascular smooth muscle cells: receptors and mechanisms. Am J Physiol Heart Circ Physiol 299, 1625–1632 (2010).

240. Duchene J and Ahluwalia A. The kinin B(1) receptor and inflammation: new therapeutic target for cardiovascular disease. Curr Opin Pharmacol 9, 125–131 (2009).

241. Tschope C, Heringer-Walther S, Koch M, Spillmann F, Wendorf M, Leitner E, Schultheiss HP and Walther T. Upregulation of bradykinin B1-receptor expression after myocardial infarction. Br J Pharmacol 129, 1537–1538 (2000).

242. Barki-Harrington L, Bookout AL, Wang G, Lamb ME, Leeb-Lundberg LM and Daaka Y. Requirement for direct cross-talk between B1 and B2 kinin receptors for the proliferation of androgen-insensitive prostate cancer PC3 cells. Biochem J 371, 581–587 (2003).

243. Chee J, Naran A, Misso NL, Thompson PJ and Bhoola KD. Expression of tissue and plasma kallikreins and kinin B1 and B2 receptors in lung cancer. Biol Chem 389, 1225–1233 (2008).

244. Dlamini Z and Bhoola KD. Upregulation of tissue kallikrein, kinin B1 receptor, and kinin B2 receptor in mast and giant cells infiltrating oesophageal squamous cell carcinoma. J Clin Pathol 58, 915–922 (2005).

245. Ni A, Yin H, Agata J, Yang Z, Chao L, and Chao J. Overexpression of Kinin B1 Receptors Induces Hypertensive Response to Des-Arg9 -bradykinin and Susceptibility to Inflammation. J Biol Chem 278, 219–25 (2003).

246. Siltari A, Korpela R and Vapaatalo H. Bradykinin -induced vasodilatation: Role of age, ACE1-inhibitory peptide, mas- and bradykinin receptors. Peptides 85, 46–55 (2016).

247. Mahyan, W.G. Impairment of endothelium-dependent dilatation of basilar artery during chronic hypertension. Am. J. Physiol 259, H1455 ± H1462 (1990).

248. Furchgott RF and Zawadzki. The obligatory role of endothelial cells in the relaxation of arterial smooth muscle by acetylcholine. Nature 288, 373–376 (1980).

249. Altura BM and Chand N. Bradykinin-induced relaxation of renal and pulmonary arteries is dependent upon intact endothelial cell. British Journal of Pharmacology 74, 10–11 (1981).

250. Cherry P D, Furchgott R F, Zawadzki J V, and Jothianandan D. Role of endothelial cells in relaxation of isolated arteries by bradykinin. PNAS 2106–2110 (1982).

251. Furchgott RF and Vanhoutte PM. Endothelium-derived relaxing and contracting factors. FASEB Journal 3, 2007–2018 (1989).

252. Feletou M and Vanhoutte P. Endothelium-derived hyperpolarising factor. Clin Exp Pharmacol Physiol 23, 1082–1090 (1996).

253. De Mey JG, Claeys M and Vanhoutte PM. Endothelium-dependent inhibitory effects of acetylcholine, adenosine triphosphate, thrombin and arachidonic acid in the canine femoral artery. J Pharmacol Exp Ther 222, 166–73 (1982).

254. Tomioka H, Hattori Y, Fukao M, Sato A, Liu M, Sakuma I, Kitabatake A, Kanno M. Relaxation in different-sized rat blood vessels mediated by endothelium-derived hyperpolarizing factor: importance of processes mediating precontractions. J Vasc Res 36, 311–320 (1999).

255. Tirapelli, CR, Bonaventura D Tirapelli LF, Oliveira AM. Mechanisms underlying the vascular actions of endothelin 1, angiotensin II and bradykinin in the rat carotid. Pharmacology 84, 111–26 (2009).

256. Richard V, Tanner F,Tschudi M, Lüscher T F. Different activations of l-arginine pathway by bradykinin, serotonin, and clonidine in coronary arteries. Am J Physiol 350, 1433–1439 (1990).

257. Tschudi M, Richard V, Bühler F R, Lüscher T F. Importance of endothelium-derived nitric oxide in porcine coronary resistance arteries. Am J Physiol 260, H13 (1991).

258. Pelc LR, Gross GJ, Warltier D. Mechanisms of coronary vasodilation produced by bradykinin. Circulation 83, 2048–2056 (1991).

259. Mombouli J V, Vanhutte P M. Endothelium-derived hyperpolarizing factor(s): updating the unknown. Trends Pharmacol Sci 18, 252–256 (Tschudi).

260. Fisslthaler B, Popp R, Kiss L, Potente M, Harder D R, Fleming I, Busse R. Cytochrome P450 2C is an EDHF synthase in coronary arteries. Nature 401, 493–497 (1999).

261. Calixto JB and Medeiror YS. Effect of protein kinase C and calcium on bradykinin-mediated contractions of rabbit vessels. Hypertension 19, I187–I193 (1992).

262. Gaudreau P, Barabe J, Stpierre S and Regoli D. Pharmacological studies of kinins in venous smooth muscles. Canadian Journal of Physiology and Pharmacology 59, 371–379 (1981).

263. Regoli D., Barabe J., Park W.K. Receptors for bradykinin in rabbit aortae. Can J Physiol Pharmacol 55, 855–867 (1977).

264. Ihara E, Hirano K, Derkach DN, Nishimura J, Nawata H and Kanaide H. The mechanism of bradykinin-induced endothelium-dependent contraction and relaxation in the porcine interlobar renal artery. Br J Pharmacol 29, 943–952 (2000).

265. Bolton TB, Gordienko DV, Pucovsky V, Parsons S and Povstyan O. Calcium release events in excitation-contraction coupling in smooth muscle. Novartis Found Symp 246, 154–168 (2000).

266. Jackson WF. Potassium channels and regulation of the microcirculation. Microcirculation 5, 85–90 (1998).

267. Alexander V, Jeffrey M, Brian C and Gaurav C. Activation of endothelial BKCa channels causes pulmonary vasodilation. Vascul Pharmacol 5, 122–129 (2010).

268. Zhang DX, Mendoza SA, Bubolz AH, Mizuno A, Ge ZD, Li R, Warltier DC, Suzuki M, Gutterman DD. Transient receptor potential vanilloid type 4-deficient mice exhibit impaired endothelium-dependent relaxation induced by acetylcholine in vitro and in vivo. Hypertension 53, 532–538 (2009).

269. Zhang DX, Gutterman DD. Transient receptor potential channel activation and endothelium-dependent dilation in the systemic circulation. J Cardiovasc Pharmacol 57, 133–139 (2011).

270. Moccia F, Berra-Romani R, Tanzi F. Update on vascular endothelial Ca2+ signalling: a tale of ion channels, pumps and transporters. World J Biol Chem 3, 127–158 (2012).

271. Inoue R, Jensen L J, Shi J, Morita H, Nishida M, Honda A,. Transient receptor potential channels in cardiovascular function and disease. Circ Res 99, 119–131 (2006).

272. Albert AP, Saleh SN, Large WA. Identification of canonical transient receptor potential (TRPC) channel proteins in native vascular smooth muscle cells. Curr Med Chem 16, 1158–1165 (2009).

273. Jung S, Strotmann R, Schultz G, Plant TD. TRPC6 is a candidate channel involved in receptor-stimulated cation currents in A7r5 smooth muscle cells. Am J Physiol Cell Physiol 282, C347–C359 (2002).

274. Sweeney M, Yu Y, Platoshyn O, Zhang S, McDaniel SS, Yuan JX. Inhibition of endogenous TRP1 decreases capacitative Ca2+ entry and attenuates pulmonary artery smooth muscle cell proliferation. Am J Physiol Lung Cell Mol Physiol 283, L144–L155 (2002).

275. Welsh DG, Morielli AD, Nelson MT and Brayden JE. Transient receptor potential channels regulate myogenic tone of resistance arteries. Circ Res 90, 248–250 (2002).

276. Wong P S, Roberts R E, Randall M D. Sex differences in the role of transient receptor potential (TRP) channels in endothelium-dependent vasorelaxation in porcine isolated coronary arteries. Eur J Pharmacol 750, 108–117 (2015).

277. Leung P, Cheng K T, Liu C, Cheung W, Kwan H Y, Lau KL, Huang Y and Yao X. Mechanism of non-capacitative Ca2+ influx in response to bradykinin in vascular endothelial cells. J Vasc Res 43, 367–376 (2006).

278. Yang D, Luo Z, Ma S, Wong WT, Ma L, Zhong J, He H, Zhao Z, Cao T, Yan Z, Liu D, Arendshorst W, Huang Y, Tepel M, Zhu Z. Activation of TRPV1 by dietary capsaicin improves endothelium-dependent vasorelaxation and prevents hypertension. Cell Metab 12, 130–141 (2010).

279. Maier T, Follmann M, Hessler G, Kleemann HW , Hachtel S, Fuchs B, Weissmann N, Linz W, Schmidt T, Löhn M, Schroeter K , Wang L, Rütten H, Strübing C. Discovery and pharmacological characterization of a novel potent inhibitor of diacylglycerol-sensitive TRPC cation channels. Br J Pharmacol 172, 3650–3660 (2015).

280. De Maat S, Hofman ZLM and Maas C. Hereditary angioedema: the plasma contact system. J Thromb Haemost 16, 1674–1685 (2018).

281. Qiu T, Chiuchiolo MJ, Whaley AS, Russo AR, Sondhi D, Kaminsky SM, Crystal RG,. Gene Therapy for C1 Esterase Inhibitor Deficiency in a Murine Model of. Allergy 74, 1081–1089 (2018).

282. Veronez CL, Maghsodi S, Todiras M, Popova E, Rodrigues AF, Qadri F, Pesquero JB, Bader M. Endothelial B2-receptor overexpression as an alternative animal model for hereditary angioedema. Allergy 74, 1998–2002 (2019).

283. Czaller I, Molnár K, Csuka D, Varga L and Farkas H. Successful outcome using C1 concentrate in acute pancreatitis caused by hereditary angioedema. Gastroenterol Nurs 34, 60–63 (2011).

284. Brickman CM, Tsokos GC, Balow JE, Lawley TJ, Santaella M, Hammer CH, Frank MM. Immunoregulatory disorders associated with hereditary angioedema. I. Clinical manifestations of autoimmune disease. J Allergy Clin Immunol 77, 749–757 (1986).

285. Chen Q, Vera, Portocarrero LP, Ossipov MH, Vardanyan M, Lai J and Porreca F. Attenuation of persistent experimental pancreatitis pain by a bradykinin b2 receptor antagonist. Pancreas 39, 1220–1225 (2010).

286. Hirata M, Hayashi I, Yoshimura K, Ishii K, Soma K, Ohwada T, Kakita A, Majima M. Blockade of bradykinin B (2) receptor suppresses acute pancreatitis induced by obstruction of the pancreaticobiliary duct in rats. Br J Pharmacol 135, 29–36 (2002).

287. Wirth KJ, Heitsch H, Scholkens BA. Kinin receptor antagonists: unique probes in basic and clinical research. Can J Physiol Pharmacol 73, 797–804 (1995).

288. Wirth K, Hock FJ, Albus U, Linz W, Alpermann HG, Anagnostopoulos. Hoe 140 a new potent and long acting bradykinin antagonist in vivo studies. Br J Pharmacol 102, 774–7 (1991).

289. Davis AE III. Mechanism of angioedema in first complement component inhibitor deficiency. Immunol Allergy Clin North Am 26, 633–651 (2006).

290. Han ED, MacFarlane RC, Mulligan AN, Scafidi J, Davis AE III. Increased vascular permeability in C1 inhibitor-deficient mice mediated by the bradykinin type 2 receptor. J Clin Invest 109, 1057–1063 (2002).

291. Drube S, Liebmann C. In various tumour cell lines the peptide bradykinin B (2) receptor antagonist, Hoe 140 (Icatibant), may act as mitogenic agonist. Br J Pharmacol. 131, 1553–1560 (2000).

292. Bork K, Frank J, Grundt B, Schlattmann P. Treatment of acute edema attacks in hereditary angioedema with a bradykinin receptor-2 antagonist (Icatibant). J Allergy Clin Immunol 119, 1497–503 (2007).

293. Banerji AS, Blanda CM, LoVecchio F, Snyder B and Camargo CA. Multicenter study of patients with angiotensin converting enzyme inhibitor-induced angioedema who present to the emergency department. Annals of Allergy 100, 327–332 (2008).

294. Israili Z H and Hall W. Cough and angioneurotic edema associated with angiotensin-converting enzyme inhibitor therapy. A review of the literature and pathophysiology. Annals of Internal Medicine 117, 234–242 (1992).

295. Sondhi D, Lippmann M and Murali G. "Airway compromise due to angiotensin-converting enzyme inhibitor-induced angioedema: clinical experience at a large community teaching hospital. Chest 126, 400–404 (2004).

296. Nikpoor B, Duan Q L and Rouleau G A. Acute adverse reactions associated with angiotensin-conventing enzyme inhibitors: genetic factors and therapeutic implications. Expert Opinion on Pharmacotherapy 3, 1851–1856 (2005).

297. Adam A, Cugno M, Molinaro G, Perez M and Lepage Y. Aminopeptidase P in individuals with a history of angio-oedema on ACE inhibitors. The Lancet 359, 2088–2089 (2002).

298. Nagae A, Deddish PA, Becker RP, Anderson CH, Abe M, Tan F, Skidgel RA, Erdös EG. Carboxypeptidase M in Brain and Peripheral Nerves. J Neurochem 59, 2201–12 (1992).

299. Skidgel RA , McGwire GB and Li XY. Membrane anchoring and release of carboxypeptidase M: implication for extracellular hydrolysis of peptide hormones. Immunopharmacology 32, 48–52 (1996).

300. McGwire GB and Skidgel RA. Extracellular Conversion of Epidermal Growth Factor (EGF) to des-Arg Graphic-EGF by Carboxypeptidase M. J Biol Chem 270, 17154–17158 (1995).

301. Smith JE and Baker KE. Smith JE, Baker KE. Bioessays 37, 612–23 (2015).

302. Karousis ED, Nasif S and Muhlemann O. Nonsense-mediated mRNA decay: novel mechanistic insights and biological impact. Wiley Interdiscip Rev RNA 7, 661–682 (2016).

303. Reverter D, Maskos K, Tan F, Skidgel R A and Bode W. Crystal structure of human carboxypeptidase M, a membrane-bound enzyme that regulates peptide hormone activity. J. Mol. Biol 338, 257–269 (2004).

304. Tan F, Balsitis S, Black JK, Blöchl A, Mao JF, Becker RP, Schacht D and Skidgel RA. Effect of mutation of two critical glutamic acid residues on the activity and stability of human carboxypeptidase M and characterization of its signal for glycosylphosphatidylinositol anchoring. Biochem J 370, 567–578 (2003).

305. Zhang X, Tan F, Zhang Y and Skidgel RA. Carboxypeptidase M and kinin B1 receptors interact to facilitate efficient B1 signaling from B2 agonists. J Biol Chem 12, 7994–8000 (2008).

306. Skidgel RA and Erdös EG. Structure and function of human plasma carboxypeptidase N, the anaphylatoxin inactivator. International immunopharmacology 7, 1888–99 (2007).

307. Fricker, LD. Handbook of Proteolytic Enzymes (Second Edition). 1, 2004.

308. de Saint-Vis B, Cupillard L, Pandrau-Garcia D, Ho S, Renard N, Grouard G, Duvert V, Thomas X, Galizzi JP, Banchereau J. Distribution of carboxypeptidase M on lymphoid and myeloid cells parallels the other zinc-dependent proteases CD10 and CD13. Blood 86, 1098–105 (1995).

309. Salles G, Chen C-Y, Reinherz EL and Shipp MA. CD7IO NEP is expressed on Thy-lM B220+ murine B-cell progenitors and functions to regulate stromal cell-dependent lymphopoiesis. Blood 80, 2021 (1992).

310. Salles G, Rodewald H-R, Chin BS, Reinhen EL and Shipp MA. Inhibition of CDlOl mutral endopeptidase 24.11 promotes B-cell reconstitution and maturation in vivo. Roc Natl Acad Sci USA 90, 7618 (1993).

311. Bokisch V and Müller-Eberhard H. Anaphylatoxin inactivator of human plasma: Its isolation and characterization as a carboxypeptidase. J Clin Invest 49, 2427–2436 (1970).

312. Bleul C, Fuhlbrigge RC, Casasnovas JM, Aiuti A, Springer TA. A highly efficacious lymphocyte chemoattractant, stromal cell-derived factor 1 (SDF-1). Exp Med 184, 1101–1109 (1996).

313. Tashiro K, Tada H, Heilker R, Shirozu M and Nakano. T. Signal sequence trap: a cloning strategy for secreted proteins and type I membrane. Science 261, 600–603 (1993).

314. De La Luz Sierra MD, Yang FQ, Narazaki M, Salvucci O, Davis D, Yarchoan R, Zhang H, Fales H, Tosato G. Differential processing of stromal-derived factor-1 alpha and stromal-derived factor-1 beta explains functional diversity. Blood 103, 2452–2459 (2004).

315. Sugiyama T, Kohara H, Noda M and Nagasawa T. Maintenance of the hematopoietic stem cell pool by CXCL12-CXCR4 chemokine signaling in bone marrow stromal cell niches. j immuni 25, 977–988 (2006).

316. Ding L and Morrison S J. Haematopoietic stem cells and early lymphoid progenitors occupy distinct bone marrow niches. Nature 495, 231–235 (2013).

317. Robbins C S, Chudnovskiy A, Rauch P J, Figueiredo J L, Iwamoto Y, Gorbatov R, Etzrodt M, Weber G F, Ueno T, van Rooijen N, et al. Extramedullary hematopoiesis generates Ly-6C(high) monocytes that infiltrate atherosclerotic lesions. Circulation 125, 364–374 (20312).

Eidesstattliche Versicherung

Ich, [Sara Maghsodi], versichere an Eides statt durch meine eigenhändige Unterschrift, dass ich die vorgelegte Dissertation mit dem Thema: [Functional analysis of components of the kallikrein-kinin system in genetically altered rat models], [Funktionsanalyse von Komponenten des Kallikrein-Kinin-Systems in genetisch veränderten Rattenmodellen] selbstständig und ohne nicht offengelegte Hilfe Dritter verfasst und keine anderen als die angegebenen Quellen und Hilfsmittel genutzt habe.

Alle Stellen, die wörtlich oder dem Sinne nach auf Publikationen oder Vorträgen anderer Autoren/innen beruhen, sind als solche in korrekter Zitierung kenntlich gemacht. Die Abschnitte zu Methodik (insbesondere praktische Arbeiten, Laborbestimmungen, statistische Aufarbeitung) und Resultaten (insbesondere Abbildungen, Graphiken und Tabellen) werden von mir verantwortet. [Für den Fall, dass Sie die Forschung für Ihre Promotion ganz oder teilweise in Gruppenarbeit durchgeführt haben:] Ich versichere ferner, dass ich die in Zusammenarbeit mit anderen Personen generierten Daten, Datenauswertungen und Schlussfolgerungen korrekt gekennzeichnet und meinen eigenen Beitrag sowie die Beiträge anderer Personen korrekt kenntlich gemacht habe (siehe Anteilserklärung). Texte oder Textteile, die gemeinsam mit anderen erstellt oder verwendet wurden, habe ich korrekt kenntlich gemacht.

Meine Anteile an etwaigen Publikationen zu dieser Dissertation entsprechen denen, die in der untenstehenden gemeinsamen Erklärung mit dem/der Erstbetreuer/in, angegeben sind. Für sämtliche im Rahmen der Dissertation entstandenen Publikationen wurden die Richtlinien des ICMJE (International Committee of Medical Journal Editors; www.icmje.og) zur Autorenschaft eingehalten. Ich erkläre ferner, dass ich mich zur Einhaltung der Satzung der Charité – Universitätsmedizin Berlin zur Sicherung Guter Wissenschaftlicher Praxis verpflichte.

Weiterhin versichere ich, dass ich diese Dissertation weder in gleicher noch in ähnlicher Form bereits an einer anderen Fakultät eingereicht habe.

Die Bedeutung dieser eidesstattlichen Versicherung und die strafrechtlichen Folgen einer unwahren eidesstattlichen Versicherung (§§156, 161 des Strafgesetzbuches) sind mir bekannt und bewusst.“

Datum Unterschrift

Anteilserklärung an den erfolgten Publikationen

[Die Anteile an der/n jeweiligen Publikation/en sind so deutlich und detailliert zu erklären, dass es der Promotionskommission und den wissenschaftlichen Gutachtern ohne Probleme möglich ist zu erkennen, was Sie selbst dazu beigetragen haben. Wünschenswert wäre ein konkreter Bezug zur Publikation wie z. B.: „aus meiner statistischen Auswertung sind die Tabellen 1, 4, 47 und 60 entstanden."

Sara Maghsodi hatte folgenden Anteil an der folgenden Publikation:

Publikation 1: Camila Lopes Veronez*, Sara Maghsodi*, Mihail Todiras, Elena Popova, André Felipe Rodrigues, Fatimunnisa Qadri, João Bosco Pesquero, Michael Bader], [Endothelial B2-receptor overexpression as an alternative animal model for hereditary angioedema, Allergy 74(10):1998-2002 (2019)

*geteilte Erstautorenschaft

Beitrag im Einzelnen (bitte ausführlich ausführen):

Frau Maghsodi war maßgeblich an allen Experimenten beteiligt und hat insgesamt einen sehr großen Beitrag zu dem Projekt geleistet, weshalb sie als eine Erstautorin gelistet ist. Die zweite Erstautorin, Camila Veronez, hat die transgene Ratte mit der Überexpression des Bradykinin B2 Rezeptors (zusammen mit Elena Popova) generiert (Fig. S1A) und erste Experimente zur Vasopermeabilität (unterstützt von Mihail Todiras und andre Rodrigues) und zur Angioödem-Bildung (unterstützt durch Fatimunnisa Qadri) in diesen Ratten (Fig. 1 und 2) durchgeführt. Daran war Frau Maghsodi schon maßgeblich beteiligt. Sie hat darüber hinaus Genexpressions-Studien (Fig. S1B-D), alle Experimente mit isolierten Gefässen (Fig. S2) und pharmakologische Behandlungen der Tiere durchgeführt (Fig. S3). Joao Pesquero und Michael Bader waren für die Drittmitteleinwerbung verantwortlich und an der Entwicklung der Fragestellung, der Analyse und Interpretation der Ergebnisse und dem Schreiben der Publikation beteiligt.

_____

Unterschrift, Datum und Stempel des/des erstbetreuenden Hochschullehrers/in

_____

Unterschrift des Doktoranden/der Doktorandin

Publications

Maghsodi S, Gol A, Dabiri S, Javadi A. Preventive Effect of Ginger (Zingiber officinale) Pretreatment on Renal Ischemia-Reperfusion in Rats. *European Surgical Research* **46**, 45-51 (2011).

Veronez CL*, **Maghsodi S***, Todiras M, Popova E, Rodrigues AF, Qadri F, Pesquero JB, Bader M. Endothelial B2-receptor overexpression as an alternative animal model for hereditary angioedema. *Allergy* **74**, 1998–2002 (2019). *joined first authors

Ercu M, Markó L, Schächterle C, Tsvetkov D, Cui Y, **Maghsodi S,** Bartolomaeus TUP, Maass PG, Zühlke K, Gregersen N, Hübner N, Hodge R, Mühl A, Pohl B, Illas RM, Geelhaar A, Walter S, Napieczynska H, Schelenz S, Taube M, Heuser A, Anistan YM, Qadri F, Todiras M, Plehm R, Popova E, Langanki R, Eichhorst J, Lehmann M, Wiesner B, Russwurm M, Forslund SK, Kamer I, Müller DN, Gollasch M, Aydin A, Bähring S, Bader M, Luft FC, Klussmann E. Phosphodiesterase 3A and Arterial Hypertension. *Circulation* **142**, 133-149 (2020).

Maghsodi S, Qadri F, Bader M, Receptors | Bradykinin Receptors. Editor: Jez J, *Encyclopedia of Biological Chemistry III*, Elsevier, 126-131 (2021)

Maghsodi S, Veronez CL, Todiras M, Popova E, Qadri F, Pesquero JB, Gollasch M, Bader M. TRPC4 mediates vasodilatation induced by kinin B1 and B2 receptors. in preparation

Acknowledgements

First of all, I gratefully acknowledge Prof. Dr. Michael Bader for an amazing opportunity and his supervision. I am particularly grateful for his excellent supervision of my work and having the first-class working conditions in his laboratory, giving me freedom in this project, making everything possible, and for his nice and calm character.

Furthermore, my special thanks go to Prof. Dr. Maik Gollasch from Charite as the second supervisor of this project. I am grateful for having the opportunity to work on my dissertation in his amazing group as a part of an exciting project.

I do not know where I would be without Dr. Fatimunnisa (Sayeeda) Qadri. There is simply no way to measure the profound knowledge, expertise and kindness in which she helped me, for the good atmosphere and the many fun hours in and outside the laboratory, and for the tireless support with all my questions.

I want to thank the animal caretakers Annegret Dahlke, Monique Bergemann and Franziska Kratz for the excellent care of the laboratory animals.

I would like to thank the rest of the lab members for creating a unique working atmosphere in this lab, including Alex, Anne, André, Andrea, Andrei, Anthony, Benjamin, Berni, Boyka, Camila, Conny, Charly, Dani, Daniel, Elena, Fernanda, Franz, Fred, Gabriel, Helena, Iris, Karolina, Katrin, Laura, Leandro, Lisa, Lena, Lorena, Lucas, Luiza, Madeleine, Marcos, Marike, Markus, Masha, Megha, Mihail, Mike, Naozumi, Natasha, Nina, Olga, Paula, Polina, Priya, Rike, Rogerio, Stijn, Sabine, Susann, Susi, Talita, Tina, Thaìs, Thorsten, Valeria, Vivien, Yasmine, Yunqing and Zeynep.

I would like to thank Cathrin and Andrea for their excellent technical assistance, who helped me with their expertise.

I want to thank DZHK for financing the first three years, the Graduate School TransCard and the PhD office for support.

I want to thank the committee members Prof. Dr. Michael Bader, Prof. Dr. Maik Gollasch, Prof. Dr. Dominik Müller and Dr. Fatimunnisa (Sayeeda) Qadri for their time and support.

I want to thank my family and my best friend Dr. Mohsen Alizadeh for their loving support and motivation.